Stochastic Control Methods for Dynamic Futures Portfolios

Yang Zhou

A dissertation
submitted in partial fulfillment of the
requirements for the degree of

Doctor of Philosophy

University of Washington

2021

Reading Committee:

Tim Leung, Chair

Matthew Lorig

Soumik Pal

Program Authorized to Offer Degree:
Department of Applied Mathematics

University of Washington

Abstract

Stochastic Control Methods for Dynamic Futures Portfolios

Yang Zhou

Chair of the Supervisory Committee:
Professor Tim Leung
Applied Mathematics

In this thesis, we discuss systematic methods to futures trading and analyze the mathematical problems that arise from trading futures. Firstly, we analyze the dynamic futures trading strategies under a general multifactor Gaussian framework. Our framework captures a number of well-known models, like the Schwartz model and Central Tendency Ornstein-Uhlenbeck (CTOU) model. We also present a new multiscale CTOU model within this framework. Secondly, we study the problem of dynamically trading futures in a general regime switching market in which the stochastic market regime is represented by a continuous-time finite-state Markov chain. As examples within our stochastic framework, we consider the Regime-Switching Geometric Brownian Motion (RS-GBM) model and Regime-Switching Exponential Ornstein-Uhlenbeck (RS-XOU) model. Thirdly, we model the stochastic spreads between the underlying spot price and associated futures prices by a multidimensional scaled Brownian bridge. In addition, the portfolio optimization problem is incorporated with constraints on the futures position. Our general setup captures the dollar neutral and market neutral constraints, which are widely used in industry. For all three problems, we apply utility maximization approaches to determine the optimal futures trading strategy. This leads to the analysis of the corresponding Hamilton-Jacobi-Bellman (HJB) equations, whose solutions are obtained explicitly or in semi-explicit form. Numerical examples are provided to illustrate the investor's certainty equivalent, optimal futures positions, and wealth process

for each problem.

TABLE OF CONTENTS

LIST OF FIGURES

LIST OF TABLES

ACKNOWLEDGMENTS

First and foremost, I would like to thank my advisor, Tim Leung. Tim taught me not only the knowledge but also how to become a good researcher. I enjoyed and appreciated the time we spent together. His enthusiasm and wisdom inspired me during my Ph.D. career. I can always learn from his guidance and personal experience. Tim values and cares about his student, and he offers tremendous help in career planning and job hunting.

I also owe my thanks to Rose Nguyen and Megan Morrison, who were my office mates in the first year. They offer great help to let me get used to the quarter system, and their enthusiasm and patience allow me to improve my language skills significantly.

I would also like to thank my friend and co-author, Xiaodong Chen. It has been a delightful time to work with Xiaodong. She is smart, hard-working, and provided great support in our project.

In the end, I would like to thank my girlfriend and my parents. Without their generous support and encouragement, I would not be able to start and complete the Ph.D. degree.

DEDICATION

I dedicate this thesis to my parents.

Chapter 1

DYNAMIC FUTURES PORTFOLIOS UNDER A MULTIFACTOR GAUSSIAN FRAMEWORK

1.1 Introduction

Futures are standardized exchange-traded bilateral contracts of agreement to buy or sell an asset at a pre-determined price at a pre-specified time in the future. At the world's largest futures exchange, the Chicago Mercantile Exchange (CME), futures trading volume averages over 15 million contracts per day.[1]

Managed futures portfolios play an integral role in hedge funds and alternative investments, with hundreds of billions under management. These investments are managed by professional investment individuals or management companies known as Commodity Trading Advisors (CTAs), and typically involve trading futures on commodities, currencies, interest rates, and other assets. Regulated and monitored by both government agencies such as the U.S. Commodity Futures Trading Commission (CFTC) and National Futures Association (NFA), this class of assets has averaged over US$300 billion annually during 2011-2020.[2]

One appeal of managed futures strategies is their advertised potential to produce uncorrelated and superior returns, as well as different risk-return profiles, compared to the equity market ([26, 22]). The classes of strategies are conceivably diverse among managed futures funds, with the popular ones being long-short strategy and momentum strategy ([31]).

In this chapter, we discuss the optimal dynamic futures trading strategies under a general Gaussian framework that the underlying asset's log-price is modeled by a multifactor diffusion process. Our framework incorporates some famous two-factor models, like the Schwartz

[1]Source: the CME Group daily exchange volume and open interest report.

[2]Source: Barclayhedge Managed Futures AUM data.

model [55] and Central Tendency Ornstein-Uhlenbeck (CTOU) model [48]. We first derive the no-arbitrage prices and historical price dynamics of the futures contracts. The optimal futures trading strategy is determined by solving a stochastic control problem, whose objective is to maximize the expected utility from trading wealth. By analyzing and solving the associated Hamilton-Jacobi-Bellman (HJB) equations, we present the value function and optimal trading strategies explicitly.

In order to quantify the value of the futures trading opportunity, we define the portfolio manager's certainty equivalent. Intuitively, it should be more beneficial to be able to trade a larger set of securities. Using certainty equivalent, we quantify the value of trading different sets of futures, and show that the highest certainty equivalent is achieved from trading all available contracts. On the other hand, it is surprising that the certainty equivalent does not depend on the current spot and futures prices. We apply our stochastic framework to the Schwartz model and CTOU model. In addition, we introduce a new multiscale CTOU model that is driven by a fast and slow mean-reverting process. We provide the numerical examples to examine model parameters for our new model.

While simpler models, like the two-factor Schwartz model and CTOU model, have the advantage of interpretability, they are often inadequate in fitting observed prices of all traded contracts, see [14]. The flexibility of multifactor models permits good fit to empirical term structure as displayed in the market. Especially in deep and liquid futures markets, such as crude oil or gold, with over ten contracts of various maturities actively traded at any given time, multifactor models are particular useful. In the literature, [19] apply a multifactor Gassian model for pricing oil futures. [18] introduce a multifactor stochastic volatility model for commodity prices to enhance calibration against observed option prices.

The continuous-time stochastic control approach for portfolio optimization dates back to [49], but much less has been done for dynamic futures portfolios. The utility maximization approach is used to derive dynamic futures trading strategies under two-factor models in [43] and [44]. A regime-switching framework for dynamic futures trading can be found in [39]. There are a few alternative mathematical approaches and applications of futures

trading. [21] study the trading and heding of bitcoin futures under mean-variance frameowrk. As an alternative approach for capturing futures and spot price dynamics, the stochastic basis model [4, 5] directly models the difference between the futures and underlying asset prices, and solve for the optimal trading strategies through utility maximization. In other applications, [8] study the Merton portfolio optimization problem under the Schwartz mean-reverting model, and [15] and [27] apply stochastic control methods to trading cointegrated securities in multifactor models.

The rest of this chapter is structured as follows. We describe the general market framework and futures dynamics in Section 1.2. The futures portfolio optimization is discussed in Section 1.3. Then, we apply our framework to Schwartz model and CTOU process in Section 1.4. In addition, we introduce the multiscale CTOU model and apply our framework in Section 1.5. Lastly, we provide numerical analysis in Section 1.6. Concluding remarks are provided in Section 1.7.

1.2 Multifactor Gaussian Model

We consider a multifactor market model. Let $\boldsymbol{X}_t$ be an N-dimensional vector $(X_t^{(1)}, \ldots, X_t^{(N)})^\top$, where $X^{(1)}$ is the log-price of the underlying asset and $(X^{(2)}, \ldots, X^{(N)})$ are observable stochastic factors. The asset's spot price is defined by

$$S_t = e^{X_t^{(1)}} . \tag{1.1}$$

Under physical measure $\mathbb{P}$, the vector of random factors $\boldsymbol{X}_t$ evolves according to

$$d\boldsymbol{X}_t = (\boldsymbol{\mu} - \boldsymbol{K}\boldsymbol{X}_t)dt + \boldsymbol{\Sigma} d\tilde{\boldsymbol{Z}}_t^{\mathbb{P}}, \tag{1.2}$$

where $\boldsymbol{\mu} = (\mu_1, \cdots, \mu_N)^\top$ is an N-dimensional column vector of constant drifts, $\boldsymbol{K}$ is an $N \times N$ matrix with constant entries k_{ij}, $\boldsymbol{\Sigma} = \text{diag}(\sigma_1, \cdots, \sigma_N)$ is an $N \times N$ diagonal matrix with constant volatility parameter σ_i, and $\tilde{\boldsymbol{Z}}_t^{\mathbb{P}} = (\tilde{Z}_t^{\mathbb{P},1}, \cdots, \tilde{Z}_t^{\mathbb{P},N})^\top$ is an N-dimensional column vector of correlated Brownian motions such that $(d\tilde{\boldsymbol{Z}}_t^{\mathbb{P}})(d\tilde{\boldsymbol{Z}}_t^{\mathbb{P}})^\top = \boldsymbol{\Omega} dt$, where the (i, j) element of the matrix $\boldsymbol{\Omega}$ is the instantaneous correlation $\rho_{ij} \in (-1, 1)$.

We assume that any Brownian motion in $\tilde{\boldsymbol{Z}}_t^{\mathbb{P}}$ could not be replicated by other $N-1$ Brownian motions, which indicates that $\boldsymbol{\Omega}$ is a symmetric positive definite matrix. Therefore, by applying Cholesky decomposition to $\boldsymbol{\Omega}$, we have $\boldsymbol{\Omega} = \boldsymbol{C}\boldsymbol{C}^\top$, where $\boldsymbol{C}$ is an invertible lower triangular matrix. Thus, we can define $d\boldsymbol{Z}_t^{\mathbb{P}} = \boldsymbol{C}^{-1} d\tilde{\boldsymbol{Z}}_t^{\mathbb{P}}$, which then is an N-dimensional column vector of independent Brownian motion increments under measure $\mathbb{P}$. Accordingly, the SDE for $\boldsymbol{X}_t$ can be written as

$$d\boldsymbol{X}_t = (\boldsymbol{\mu} - \boldsymbol{K}\boldsymbol{X}_t)dt + \boldsymbol{\Sigma}\boldsymbol{C} d\boldsymbol{Z}_t^{\mathbb{P}}. \tag{1.3}$$

Next, we denote the risk-neutral pricing measure by $\mathbb{Q}$ and the risk premium $\boldsymbol{\zeta} = (\zeta_1, \cdots, \zeta_N)^\top$. The $\mathbb{Q}$-Brownian motion is related to the $\mathbb{P}$-Brownian motion through the SDE

$$d\boldsymbol{Z}_t^{\mathbb{Q}} = d\boldsymbol{Z}_t^{\mathbb{P}} + \boldsymbol{\zeta} dt, \tag{1.4}$$

where $\boldsymbol{Z}_t^{\mathbb{Q}} = (Z_t^{\mathbb{Q},1}, \cdots, Z_t^{\mathbb{Q},N})^\top$ is the N-dimensional column vector of independent $\mathbb{Q}$-Brownian motions. Then, under measure $\mathbb{Q}$, $\boldsymbol{X}_t$ evolves according to

$$d\boldsymbol{X}_t = \Big(\boldsymbol{\mu} - \boldsymbol{\lambda} - \boldsymbol{K}\boldsymbol{X}_t\Big)dt + \boldsymbol{\Sigma}\boldsymbol{C} d\boldsymbol{Z}_t^{\mathbb{Q}}. \tag{1.5}$$

where the N-dimensional column vector $\boldsymbol{\lambda} = (\lambda_1, \cdots, \lambda_N)^\top$ is given by $\boldsymbol{\lambda} = \boldsymbol{\Sigma}\boldsymbol{C}\boldsymbol{\zeta}$.

Now we consider a futures contract of maturity T written on the underlying asset S. With the asset price defined in (1.1), the futures price at time $t \in [0, T]$ is given by

$$F(t, \boldsymbol{x}) := I\!E^{\mathbb{Q}}\big[\, \exp(X_T^{(1)}) \,|\, \boldsymbol{X}_t = \boldsymbol{x} \,\big]. \tag{1.6}$$

Define the linear differential operator

$$\mathcal{L}^{\mathbb{Q}} \cdot = \Big(\boldsymbol{\mu} - \boldsymbol{\lambda} - \boldsymbol{K}\boldsymbol{x}\Big)^\top \nabla_{\boldsymbol{x}} \cdot + \frac{1}{2} \operatorname{Tr}\Big(\boldsymbol{\Sigma}\boldsymbol{\Omega}\boldsymbol{\Sigma} \nabla_{\boldsymbol{x}\boldsymbol{x}} \cdot \Big), \tag{1.7}$$

where $\nabla_{\boldsymbol{x}} \cdot = (\partial_{x_1} \cdot, \cdots, \partial_{x_N} \cdot)^\top$ is the nabla operator and Hessian operator $\nabla_{\boldsymbol{x}\boldsymbol{x}} \cdot$ satisfies

$$\nabla_{\boldsymbol{x}\boldsymbol{x}} \cdot = \begin{bmatrix} \partial_{x_1}^2 \cdot & \partial_{x_1 x_2} \cdot & \dots & \partial_{x_1 x_N} \cdot \\ \partial_{x_1 x_2} \cdot & \partial_{x_2}^2 \cdot & \dots & \partial_{x_2 x_N} \cdot \\ \vdots & \vdots & \ddots & \vdots \\ \partial_{x_1 x_N} \cdot & \partial_{x_2 x_N} \cdot & \dots & \partial_{x_N}^2 \cdot \end{bmatrix}. \tag{1.8}$$

Then, the futures price function $F(t, \boldsymbol{x})$ solves the following PDE

$$(\partial_t + \mathcal{L}^{\mathbb{Q}})F(t, \boldsymbol{x}) = 0, \tag{1.9}$$

for $(t, \boldsymbol{x}) \in [0, T) \times \mathbb{R}^N$, with the terminal condition

$$F(T, \boldsymbol{x}) = \exp(\boldsymbol{e_1}^\top \boldsymbol{x})$$

for $\boldsymbol{x} \in \mathbb{R}^N$, where $\boldsymbol{e_1} = (1, 0, \cdots, 0)^\top$.

Proposition 1. *The price function of the futures contract with maturity T is given by*

$$F(t, \boldsymbol{x}) = \exp\left(\boldsymbol{a}(t)^\top \boldsymbol{x} + \beta(t)\right), \tag{1.10}$$

for $(t, \boldsymbol{x}) \in [0, T) \times \mathbb{R}^N$, where

$$\boldsymbol{a}(t) = \exp\left(-(T-t)\boldsymbol{K}^\top\right)\boldsymbol{e_1}, \tag{1.11}$$

$$\beta(t) = \int_t^T (\boldsymbol{\mu} - \boldsymbol{\lambda})^\top \boldsymbol{a}(s) + \frac{1}{2}\,\mathrm{Tr}\left(\boldsymbol{\Sigma\Omega\Sigma a}(s)\boldsymbol{a}(s)^\top\right) ds. \tag{1.12}$$

Proof. We substitute the ansatz solution (1.10) into PDE (1.9). The t-derivative is given by

$$\partial_t F(t, \boldsymbol{x}) = \left(\left(\frac{d\boldsymbol{a}(t)}{dt}\right)^\top \boldsymbol{x} + \frac{d\beta(t)}{dt}\right) \exp\left(\boldsymbol{a}(t)^\top \boldsymbol{x} + \beta(t)\right). \tag{1.13}$$

Then, the first and second derivatives satisfy

$$\nabla_{\boldsymbol{x}} F(t, \boldsymbol{x}) = \boldsymbol{a}(t) F(t, \boldsymbol{x}), \tag{1.14}$$

$$\nabla_{\boldsymbol{xx}} F(t, \boldsymbol{x}) = \boldsymbol{a}(t)\boldsymbol{a}(t)^\top F(t, \boldsymbol{x}). \tag{1.15}$$

By substituting (1.13), (1.14), and (1.15) into PDE (1.9), we obtain

$$\frac{d\boldsymbol{a}(t)}{dt} - \boldsymbol{K}^\top \boldsymbol{a}(t) = 0, \tag{1.16}$$

and

$$\frac{d\beta(t)}{dt} + (\boldsymbol{\mu} - \boldsymbol{\lambda})^\top \boldsymbol{a}(t) + \frac{1}{2}\,\mathrm{Tr}\left(\boldsymbol{\Sigma\Omega\Sigma a}(t)\boldsymbol{a}(t)^\top\right) = 0. \tag{1.17}$$

The terminal conditions of $\boldsymbol{a}(t)$ and $\beta(t)$ are given by

$$\boldsymbol{a}(T) = \boldsymbol{e_1}, \quad \beta(T) = 0. \tag{1.18}$$

By direct substitution, the solutions to ODEs (1.16) and (1.17) are given by (1.11) and (1.12). □

Next, we consider the futures price process, denoted by F_t. Under the risk-neutral measure $\mathbb{Q}$, F_t is a martingale and satisfies the SDE

$$\frac{dF_t}{F_t} = \frac{1}{F_t}\nabla_{\boldsymbol{x}} F(t, \boldsymbol{X}_t)^\top \boldsymbol{\Sigma C} d\boldsymbol{Z}_t^{\mathbb{Q}} = \boldsymbol{a}(t)^\top \boldsymbol{\Sigma C} d\boldsymbol{Z}_t^{\mathbb{Q}}. \tag{1.19}$$

Next, using (1.4) and $\boldsymbol{\lambda} = \boldsymbol{\Sigma C \zeta}$, the $\mathbb{P}$-dynamics for F_t is given by

$$\frac{dF_t}{F_t} = \boldsymbol{a}(t)^\top \boldsymbol{\lambda} dt + \boldsymbol{a}(t)^\top \boldsymbol{\Sigma C} d\boldsymbol{Z}_t^{\mathbb{P}}. \tag{1.20}$$

We observe from (1.20) the drift term that depends on the market prices of risk $\boldsymbol{\lambda}$ and $\boldsymbol{a}(t)$, which in turn depends on coefficient matrix $\boldsymbol{K}$ and maturity T.

1.3 Optimal Dynamic Futures Portfolio

Now consider a portfolio of M contracts of different maturities available to trade under N-factor model. Since there are N sources of randomness in the model, trading N or more than N futures will result in hedging away all the risk. Henceforth, we set $M \leq N$.

We will denote by $F^{(k)}(t, \boldsymbol{x})$ as the price function of futures contract with maturity T_k, with $T_1 < \ldots < T_M$, and by $F_t^{(k)}$ as the stochastic process for this contract, for $k = 1, \ldots, M$. Recall from (1.20) that the T_k-futures price process satisfies

$$\frac{dF_t^{(k)}}{F_t^{(k)}} = \boldsymbol{a}^{(k)}(t)^\top \boldsymbol{\lambda} dt + \boldsymbol{a}^{(k)}(t)^\top \boldsymbol{\Sigma C} d\boldsymbol{Z}_t^{\mathbb{P}} \tag{1.21}$$

$$\equiv \mu_F^{(k)}(t) dt + \boldsymbol{\sigma}_F^{(k)}(t)^\top d\boldsymbol{Z}_t^{\mathbb{P}}, \tag{1.22}$$

where we have defined

$$\mu_F^{(k)}(t) \equiv \boldsymbol{a}^{(k)}(t)^\top \boldsymbol{\lambda}, \quad \boldsymbol{\sigma}_F^{(k)}(t) \equiv \boldsymbol{C}^\top \boldsymbol{\Sigma}^\top \boldsymbol{a}^{(k)}(t). \tag{1.23}$$

Then, in matrix form, the system of futures dynamics is given by the set of SDE:

$$d\boldsymbol{F}_t = \boldsymbol{\mu}_{\boldsymbol{F}}(t)dt + \boldsymbol{\Sigma}_{\boldsymbol{F}}(t)d\boldsymbol{Z}_t^{\mathbb{P}}, \tag{1.24}$$

where

$$d\boldsymbol{F}_t = \left(\frac{dF_t^{(1)}}{F_t^{(1)}}, \cdots, \frac{dF_t^{(M)}}{F_t^{(M)}}\right)^\top, \tag{1.25}$$

$$\boldsymbol{\mu}_{\boldsymbol{F}}(t) = \left(\mu_F^{(1)}(t), \cdots, \mu_F^{(M)}(t)\right)^\top, \quad \text{and} \quad \boldsymbol{\Sigma}_{\boldsymbol{F}}(t) = \left(\boldsymbol{\sigma}_F^{(1)}(t), \cdots, \boldsymbol{\sigma}_F^{(M)}(t)\right)^\top. \tag{1.26}$$

Here, we assume there be no redundant futures contract in the portfolio, which means any futures contract could not be replicated by other $M-1$ futures contracts. To that end, we require that $\text{rank}\,(\boldsymbol{\Sigma}_{\boldsymbol{F}}) = M$. Since $\text{rank}\,(\boldsymbol{\Sigma}_{\boldsymbol{F}}) \neq M$ if $M > N$, the rank condition effectively excludes the case with more contracts than stochastic factors, as desired.

Next, we consider the trading problem for the investor. Let strategy $\boldsymbol{\pi}_t = \left(\pi_t^{(1)}, \cdots, \pi_t^{(M)}\right)^\top$, where the element $\pi_t^{(k)}$ denotes the amount of money invested in k-th futures contract. In addition, we assume the interest rate be zero for simplicity. Then, for any admissible strategy $\boldsymbol{\pi}$, the wealth process is

$$\begin{aligned} dW_t^\pi &= \sum_{k=1}^{M} \pi_t^{(k)} \frac{dF_t^{(k)}}{F_t^{(k)}} \\ &= \boldsymbol{\pi}_t^\top \boldsymbol{\mu}_{\boldsymbol{F}}(t)dt + \boldsymbol{\pi}_t^\top \boldsymbol{\Sigma}_{\boldsymbol{F}}(t)d\boldsymbol{Z}_t^{\mathbb{P}}. \end{aligned} \tag{1.27}$$

We note that the wealth process is only determined by the strategy $\boldsymbol{\pi}_t$ and it is not affected by factors variable $\boldsymbol{X}$ and futures prices $\boldsymbol{F}$.

We consider a utility maximization approach to determine the optimal strategy. The investor's risk preference is described by the exponential utility

$$U(w) = -\exp(-\gamma w), \tag{1.28}$$

where $\gamma > 0$ is the risk aversion parameter. The investor fixes a finite trading horizon $0 < \widetilde{T} \leq T_1$, which means that $\widetilde{T}$ has to be less than or equal to the maturity of the earliest expiring contract.

A strategy $\boldsymbol{\pi}$ is said to be admissible if $\boldsymbol{\pi}$ is real-valued progressively measurable and satisfies the Novikov condition [50],

$$\mathbb{E}^{\mathbb{P}}\left[\exp\left(\int_t^{\widetilde{T}} \frac{\gamma^2}{2}\boldsymbol{\pi}_s^\top \boldsymbol{\Sigma}_{\boldsymbol{F}}(s)\boldsymbol{\Sigma}_{\boldsymbol{F}}^\top(s)\boldsymbol{\pi}_s ds\right)\right] < \infty. \tag{1.29}$$

The investor seeks to maximize the expected utility of wealth at $\widetilde{T}$ by solving the stochastic control problem

$$V(t,w) = \sup_{\boldsymbol{\pi}\in\mathcal{A}_t} \mathbb{E}^{\mathbb{P}}[U(W_{\widetilde{T}}^{\boldsymbol{\pi}})|W_t = w], \tag{1.30}$$

where $\mathcal{A}_t$ denotes the set of admissible controls at the initial time t. Since the wealth SDE (1.27) does not depend on the factors variable $\boldsymbol{X}$ and futures prices $\boldsymbol{F}$, the value function does not depend on them either.

Following the standard verification approach to dynamic programming ([24, 53, 51]), we let $C^{1,2}$ denote the set of all continuous functions $f(t,x)$ that are continuously differentiable in t and twice continuously differentiable in x. Then, we assume the existence of a sufficiently smooth candidate solution $u(t,w) \in C^{1,2}$, which will later be shown to be equal to the value function V in (1.30). To facilitate presentation, we define

$$\mathcal{L}^{\boldsymbol{\pi}}\cdot = \boldsymbol{\pi}_t^\top \boldsymbol{\mu}_{\boldsymbol{F}}(t)\partial_w \cdot + \frac{1}{2}\boldsymbol{\pi}_t^\top \boldsymbol{\Sigma}_{\boldsymbol{F}}(t)\boldsymbol{\Sigma}_{\boldsymbol{F}}^\top(t)\boldsymbol{\pi}_t \partial_{ww}\cdot. \tag{1.31}$$

Then, the candidate value function $u(t,w)$ and optimal trading strategy π^* is found from the Hamilton-Jacobi-Bellman (HJB) equation

$$\partial_t u + \sup_{\boldsymbol{\pi}} \mathcal{L}^{\boldsymbol{\pi}} u = 0, \tag{1.32}$$

for $(t,w) \in [0,\widetilde{T}) \times \mathbb{R}$, along with the terminal condition

$$u(T,w) = -e^{-\gamma w}, \quad \text{for } w \in \mathbb{R}.$$

Theorem 1. *1. Define*

$$\Lambda^2(t) = \boldsymbol{\mu}_{\boldsymbol{F}}(t)^\top \left(\boldsymbol{\Sigma}_{\boldsymbol{F}}(t)\boldsymbol{\Sigma}_{\boldsymbol{F}}(t)^\top\right)^{-1} \boldsymbol{\mu}_{\boldsymbol{F}}(t)\,. \tag{1.33}$$

The unique solution to the HJB equation (1.32) *is*

$$u(t,w) = -\exp\left(-\gamma w - \frac{1}{2}\int_t^{\widetilde{T}} \Lambda^2(s)ds\right). \tag{1.34}$$

2. The optimal strategy is given by

$$\boldsymbol{\pi}^*(t) = \frac{1}{\gamma}\left(\boldsymbol{\Sigma}_{\boldsymbol{F}}(t)\boldsymbol{\Sigma}_{\boldsymbol{F}}^\top(t)\right)^{-1} \boldsymbol{\mu}_{\boldsymbol{F}}(t). \tag{1.35}$$

Proof. We will first use the ansatz

$$u(t,w) = -e^{-\gamma w}h(t), \tag{1.36}$$

to factor out w. Using the relations

$$\partial_t u = -e^{-\gamma w}\partial_t h(t), \quad \partial_w u = \gamma e^{-\gamma w}h(t), \quad \partial_{ww} u = -\gamma^2 e^{-\gamma w}h(t), \tag{1.37}$$

the PDE (1.32) becomes

$$-\frac{d}{dt}h(t) + \sup_{\boldsymbol{\pi}_t}\left[\gamma \boldsymbol{\pi}_t^\top \boldsymbol{\mu}_{\boldsymbol{F}}(t)h - \frac{1}{2}\gamma^2 \boldsymbol{\pi}_t^\top \boldsymbol{\Sigma}_{\boldsymbol{F}}(t)\boldsymbol{\Sigma}_{\boldsymbol{F}}^\top(t)\boldsymbol{\pi}_t h\right] = 0, \tag{1.38}$$

with terminal condition $h(\widetilde{T}) = 1$. From the first-order condition, which is obtained from differentiating the terms inside the supremum with respect to $\boldsymbol{\pi}_t$ and setting the equation to zero, we have

$$\gamma \boldsymbol{\mu}_{\boldsymbol{F}}(t) - \gamma^2 \boldsymbol{\Sigma}_{\boldsymbol{F}}(t)\boldsymbol{\Sigma}_{\boldsymbol{F}}^\top(t)\boldsymbol{\pi}_t = 0, \tag{1.39}$$

Recall that $\text{rank}(\boldsymbol{\Sigma}_{\boldsymbol{F}}(t)) = M$. Then, $\boldsymbol{\Sigma}_{\boldsymbol{F}}(t)\boldsymbol{\Sigma}_{\boldsymbol{F}}^\top(t)$ is an $M \times M$ invertible matrix. Accordingly, we have the optimal strategy (1.35). Given the fact that $A^\top A$ is the positive semidefinite matrix for any matrix A, the time-dependent component $\Lambda^2(t) = \boldsymbol{\mu}_{\boldsymbol{F}}(t)^\top(\boldsymbol{\Sigma}_{\boldsymbol{F}}(t)\boldsymbol{\Sigma}_{\boldsymbol{F}}(t)^\top)^{-1}\boldsymbol{\mu}_{\boldsymbol{F}}(t)$ is always non-negative.

Substituting $\boldsymbol{\pi}^*$ back, the equation (1.38) becomes

$$-\frac{d}{dt}h(t) + \frac{1}{2}\Lambda^2(t)h(t) = 0. \tag{1.40}$$

Accordingly, we have

$$h(t) = \exp\bigg(-\frac{1}{2}\int_t^{\widetilde{T}} \Lambda^2(s)ds \bigg). \tag{1.41}$$

□

Then, for a given wealth w, the candidate solution u is a non-increasing function with respect to the time t. The solution to the HJB equation is not sufficient if a verification theorem is not proven. The verification theorem connects the HJB equation (1.32) to the control problem of maximizing the expected utility at the terminal time defined in (1.30). Next, we provide the verification theorem for our problem:

Theorem 2. *Let $u(t,w)$ be given by* (1.34)*. Then,*

1. *$u(t,w) \geq V(t,w)$ for all $t \in [0,\widetilde{T}]$ and $w \in \mathbb{R}$,*

2. *the maximizer $\boldsymbol{\pi}^*$ given by* (1.35) *is admissible. Therefore, $u(t,w) = V(t,w)$ for all $t \in [0,\widetilde{T}]$ and $w \in \mathbb{R}$, and $\boldsymbol{\pi}^*$ is an optimal strategy.*

Proof. We need to show that for any admissible $\boldsymbol{\pi}$ such that $\partial_t u + \mathcal{L}^{\boldsymbol{\pi}} u \leq 0$, the expected utility of terminal wealth will be less than or equal to what the value function would indicate, namely,

$$I\!E^{\mathbb{P}}[U(W_{\widetilde{T}}^{\boldsymbol{\pi}})|\mathcal{F}_t] \leq u(t,W_t), \tag{1.42}$$

and that the equality holds when the wealth process is controlled optimally by $\boldsymbol{\pi}^*$; that is,

$$V(t,W_t^{\boldsymbol{\pi}^*}) \equiv \sup_{\boldsymbol{\pi}\in\mathcal{A}_t} I\!E^{\mathbb{P}}[U(W_{\widetilde{T}}^{\boldsymbol{\pi}})|\mathcal{F}_t] = I\!E^{\mathbb{P}}[U(W_{\widetilde{T}}^{\boldsymbol{\pi}^*})|\mathcal{F}_t] = u(t,W_t^{\boldsymbol{\pi}^*}). \tag{1.43}$$

Using Ito's formula, we obtain

$$du(t,W_t^{\boldsymbol{\pi}}) = (\partial_t + \mathcal{L}^{\boldsymbol{\pi}})u(t,W_t^{\boldsymbol{\pi}})dt + \partial_w u(t,W_t^{\boldsymbol{\pi}})\boldsymbol{\pi}_t^\top \boldsymbol{\Sigma}_{\boldsymbol{F}}(t)d\boldsymbol{Z}_t^{\mathbb{P}}. \tag{1.44}$$

Since $u < 0$ and $\partial_w u = -\gamma u$, we have

$$\begin{aligned} & d\log(-u(t, W_t^{\boldsymbol{\pi}})) \\ =& \left(-\frac{\gamma^2}{2} \boldsymbol{\pi}_t^\top \boldsymbol{\Sigma}_{\boldsymbol{F}}(t) \boldsymbol{\Sigma}_{\boldsymbol{F}}(t)^\top \boldsymbol{\pi}_t + \frac{(\partial_t + \mathcal{L}^{\boldsymbol{\pi}}) u(t, W_t^{\boldsymbol{\pi}})}{u(t, W_t^{\boldsymbol{\pi}})} \right) dt - \gamma \boldsymbol{\pi}_t^\top \boldsymbol{\Sigma}_{\boldsymbol{F}}(t) d\boldsymbol{Z}_t^{\mathbb{P}} \qquad (1.45) \\ \geq & -\frac{\gamma^2}{2} \boldsymbol{\pi}_t^\top \boldsymbol{\Sigma}_{\boldsymbol{F}}(t) \boldsymbol{\Sigma}_{\boldsymbol{F}}(t)^\top \boldsymbol{\pi}_t dt - \gamma \boldsymbol{\pi}_t^\top \boldsymbol{\Sigma}_{\boldsymbol{F}}(t) d\boldsymbol{Z}_t^{\mathbb{P}}. \qquad (1.46) \end{aligned}$$

The last inequality holds due to the fact that $(\partial_t + \mathcal{L}^{\boldsymbol{\pi}}) u \leq 0$. Then, with the admissible strategy satisfying the Novikov condition (1.29), we obtain

$$\begin{aligned} & \mathbb{E}^{\mathbb{P}} \left[U(W_{\widetilde{T}}^{\boldsymbol{\pi}}) \middle| \mathcal{F}_t \right] = \mathbb{E}^{\mathbb{P}} \left[u(\widetilde{T}, W_{\widetilde{T}}^{\boldsymbol{\pi}}) \middle| \mathcal{F}_t \right] \\ \leq & u(t, W_t^{\boldsymbol{\pi}}) \mathcal{E} \left(\int_t^{\widetilde{T}} -\gamma \boldsymbol{\pi}_s^\top \boldsymbol{\Sigma}_{\boldsymbol{F}}(s) d\boldsymbol{Z}_s^{\mathbb{P}} \right) = u(t, W_t^{\boldsymbol{\pi}}), \end{aligned} \qquad (1.47)$$

where $\mathcal{E}(\cdot)$ denotes Doléans-Dade exponential. The equality holds if $\partial_t u + \mathcal{L}^{\boldsymbol{\pi}} u = 0$. Finally, since $\boldsymbol{\pi}^*$ is a time-deterministic function, it is also admissible. Therefore, $u(t, w)$ is indeed the solution of our control problem. □

We insert the optimal strategy (1.35) into the wealth process (1.27) to derive the SDE for the optimal wealth process

$$dW_t^* = \frac{1}{\gamma} \Lambda^2(t) dt + \frac{1}{\gamma} \boldsymbol{\mu}_{\boldsymbol{F}}(t)^\top (\boldsymbol{\Sigma}_{\boldsymbol{F}}(t) \boldsymbol{\Sigma}_{\boldsymbol{F}}(t)^\top)^{-1} \boldsymbol{\Sigma}_{\boldsymbol{F}}(t) d\boldsymbol{Z}_t^{\mathbb{P}}. \qquad (1.48)$$

From this, we see that the drift of the optimal wealth process is always positive. It is proportional to $\Lambda^2(t)$ defined in (1.33). Both the drift and volatility terms are inversely proportional to risk aversion γ.

In order to quantify the value of trading futures to the investor, we define the investor's certainty equivalent associated with the utility maximization problem. The certainty equivalent is the guaranteed cash amount that would yield the same utility as that from dynamically trading futures according to (1.30). This amounts to applying the inverse of the utility function to the value function in (1.34). Precisely, we define

$$CE(t, w) = w + \frac{1}{2\gamma} \int_t^{\widetilde{T}} \Lambda^2(s) ds. \qquad (1.49)$$

Therefore, the certainty equivalent is the sum of the investor's wealth w and a non-negative time-dependent component $\frac{1}{2\gamma}\int_t^{\widetilde{T}} \Lambda^2(s)ds$. The certainty equivalent is also inversely proportional to the risk aversion parameter γ. This means that, all else being equal, a more risk averse investor values the futures trading opportunity less. From (1.11), (1.23), (1.26) and (1.33), we know the certainty equivalent depends on the coefficient matrix $\boldsymbol{K}$, volatility matrix $\boldsymbol{\Sigma}$, correlation matrix $\boldsymbol{C}$ and market prices of risk $\boldsymbol{\lambda}$. Nevertheless, the certainty equivalent does not depend on the current values of the spot price and factors represented by $\boldsymbol{X}_t$.

1.4 Two-Factor Models

In this section, we discuss the application of our framework to two well-known two-factor models: the Schwartz model and Central Tendency Ornstein-Uhlenbeck (CTOU) model. In both cases, Theorem 1 can be applied directly, and we state the optimal strategies explicitly using (1.35).

1.4.1 Schwartz Model

The Schwartz model is introduced by [55] that takes into account the stochastic convenience yield in commodity prices. The Schwartz model belongs to our multifactor framework. Indeed, this amounts to setting the coefficients in SDE (1.19) and (1.20) to be

$$\boldsymbol{\mu} = \begin{bmatrix} \mu_1 - \sigma_1^2/2 \\ \kappa\alpha \end{bmatrix}, \quad \boldsymbol{K} = \begin{bmatrix} 0 & 1 \\ 0 & \kappa \end{bmatrix}, \quad \boldsymbol{\Sigma} = \begin{bmatrix} \sigma_1 & 0 \\ 0 & \sigma_2 \end{bmatrix}, \quad \boldsymbol{C} = \begin{bmatrix} 1 & 0 \\ \rho & \sqrt{1-\rho^2} \end{bmatrix}, \tag{1.50}$$

and

$$\boldsymbol{\lambda} = (\mu_1 - r, \lambda_2)^\top. \tag{1.51}$$

where the means μ_1, α, speed of mean reversion κ, interest rate r, the volatility parameters σ_1, σ_2 and market price of convenience yield risk λ_2 are constants and the instantaneous correlation ρ lies in $(-1, 1)$.

Let's consider two futures contracts $F^{(1)}$ and $F^{(2)}$, written on this commodity, whose maturity are T_1 and T_2 respectively. The futures price $F^{(k)}(t,\boldsymbol{x})$ of maturity T_k is first obtained by [55]. In our framework, we apply the Proposition 1 and obtain:

$$F^{(k)}(t,\boldsymbol{x}) = \exp\left(\boldsymbol{a}^{(k)}(t)^\top \boldsymbol{x} + \beta^{(k)}(t)\right), \tag{1.52}$$

where $\boldsymbol{a}^{(k)}(t)$ satisfies

$$\boldsymbol{a}^{(k)}(t) = \left(1, \frac{e^{-(T_k-t)\kappa}-1}{\kappa}\right)^\top, \tag{1.53}$$

and $\beta^{(k)}(t)$ follows,

$$\begin{aligned}\beta^{(k)}(t) = &\left(r - \hat{\alpha} - \frac{\rho\sigma_1\sigma_2}{\kappa} + \frac{\sigma_2^2}{2\kappa^2}\right)(T_k - t) \\ &+ \left(\kappa\hat{\alpha} + \rho\sigma_1\sigma_2 - \frac{\sigma_2^2}{\kappa}\right)\frac{1-e^{-(T_k-t)\kappa}}{\kappa^2} + \frac{\sigma_2^2}{2}\frac{1-e^{-2(T_k-t)\kappa}}{2\kappa^3}.\end{aligned} \tag{1.54}$$

Next, we consider the trading problem that investor can choose to trade one futures contract or two different futures contracts. In our framework, we directly apply the Theorem 1. For the portfolio with T_1-futures only, we apply (1.23) and (1.26) to get the coefficients for the futures price SDE:

$$\boldsymbol{\mu_F}(t) = \mu_1 - r + \frac{e^{-(T_1-t)\kappa}-1}{\kappa}\lambda_2, \tag{1.55}$$

and

$$\boldsymbol{\Sigma_F}(t) = \left(\sigma_1 + \rho\sigma_2\frac{e^{-(T_1-t)\kappa}-1}{\kappa}, \quad \sigma_2\sqrt{1-\rho^2}\frac{e^{-(T_1-t)\kappa}-1}{\kappa}\right). \tag{1.56}$$

Applying these to formula (1.35), the optimal strategy is given by

$$\pi^{(1)*}(t) = \frac{1}{\gamma}\frac{\boldsymbol{\mu_F}(t)}{\boldsymbol{\Sigma_F}(t)\boldsymbol{\Sigma_F}^\top(t)} = \frac{1}{\gamma}\frac{\kappa^2(\mu_1-r) + \kappa(e^{-(T_1-t)\kappa}-1)\lambda_2}{\kappa^2\sigma_1^2 + 2\rho\sigma_1\sigma_2\kappa(e^{-(T_1-t)\kappa}-1) + \sigma_2^2\left(e^{-(T_1-t)\kappa}-1\right)^2}. \tag{1.57}$$

As for the portfolio of both two futures, T_1-futures and T_2-futures, according to (1.26), we have

$$\boldsymbol{\mu_F}(t) = \left(\mu_1 - r + \frac{e^{-(T_1-t)\kappa}-1}{\kappa}\lambda_2, \quad \mu_1 - r + \frac{e^{-(T_2-t)\kappa}-1}{\kappa}\lambda_2\right)^\top, \tag{1.58}$$

and

$$\boldsymbol{\Sigma_F}(t) = \begin{bmatrix} \sigma_1 + \rho\sigma_2 \frac{e^{-(T_1-t)\kappa}-1}{\kappa} & \sigma_2\sqrt{1-\rho^2}\frac{e^{-(T_1-t)\kappa}-1}{\kappa} \\ \sigma_1 + \rho\sigma_2 \frac{e^{-(T_2-t)\kappa}-1}{\kappa} & \sigma_2\sqrt{1-\rho^2}\frac{e^{-(T_2-t)\kappa}-1}{\kappa} \end{bmatrix}. \tag{1.59}$$

Then, applying (1.35) yields the optimal strategies

$$\begin{aligned} \pi^{(1)*}(t) = &- e^{\kappa(T_1-t)}\Big(\left(e^{\kappa t} - e^{\kappa T_2}\right)(r-\mu_1)\sigma_2^2 \\ &+ \left(e^{\kappa t}\lambda_2 + e^{\kappa T_2}(r\kappa - \lambda_2 - \kappa\mu_1)\right)\rho\sigma_1\sigma_2 + e^{\kappa T_2}\kappa\lambda_2\sigma_1^2\Big)/ \\ &\left(\gamma\left(e^{\kappa T_1} - e^{\kappa T_2}\right)(1-\rho^2)\sigma_1^2\sigma_2^2\right), \end{aligned} \tag{1.60}$$

$$\begin{aligned} \pi^{(2)*}(t) = &e^{\kappa(T_2-t)}\Big(\left(e^{\kappa t} - e^{\kappa T_1}\right)(r-\mu_1)\sigma_2^2 \\ &+ \left(e^{\kappa t}\lambda_2 + e^{\kappa T_1}(r\kappa - \lambda_2 - \kappa\mu_1)\right)\rho\sigma_1\sigma_2 + e^{\kappa T_1}\kappa\lambda_2\sigma_1^2\Big)/ \\ &\left(\gamma\left(e^{\kappa T_1} - e^{\kappa T_2}\right)(1-\rho^2)\sigma_1^2\sigma_2^2\right). \end{aligned} \tag{1.61}$$

The results above are also obtained by [44] using a different method.

1.4.2 CTOU Process

This model is called the Central Tendency Ornstein Uhlenbeck (CTOU), studied by [48] for pricing VIX futures. Later, [43] analyze the futures portfolio optimization problem under this model. The CTOU process also belongs to our multifactor framework. Indeed, this amounts to setting the coefficients in SDE (1.3) and (1.5):

$$\boldsymbol{\mu} = \begin{bmatrix} \lambda_1 \\ \kappa_2\theta + \lambda_2 \end{bmatrix}, \quad \boldsymbol{K} = \begin{bmatrix} \kappa_1 & -\kappa_1 \\ 0 & \kappa_2 \end{bmatrix}, \quad \boldsymbol{\Sigma} = \begin{bmatrix} \sigma_1 & 0 \\ 0 & \sigma_2 \end{bmatrix}, \quad \boldsymbol{C} = \begin{bmatrix} 1 & 0 \\ \rho & \sqrt{1-\rho^2} \end{bmatrix}, \tag{1.62}$$

and

$$\boldsymbol{\lambda} = (\lambda_1, \lambda_2)^\top, \tag{1.63}$$

where the mean θ, speeds of mean reversion $\{\kappa_1, \kappa_2\}$, the volatility parameters $\{\sigma_1, \sigma_2\}$, and adjusted market prices of risk $\{\lambda_1, \lambda_2\}$ are all constants. We note that in [48] and [43], the instantaneous correlation ρ is set to be 0.

Then, consider two futures contracts $F^{(1)}$ and $F^{(2)}$, written on this underlying, whose maturity are T_1 and T_2 respectively. Applying the Proposition 1, the futures price $F^{(k)}(t, \boldsymbol{x})$ of maturity T_k satisfies

$$F^{(k)}(t, \boldsymbol{x}) = \exp\left(\boldsymbol{a}^{(k)}(t)^\top \boldsymbol{x} + \beta^{(k)}(t)\right), \tag{1.64}$$

where $\boldsymbol{a}^{(k)}(t)$ satisfies

$$\boldsymbol{a}^{(k)}(t) = \left(e^{-(T_k-t)\kappa_1}, \frac{\kappa_1}{\kappa_1-\kappa_2}\left(e^{-(T_k-t)\kappa_2} - e^{-(T_k-t)\kappa_1}\right)\right)^\top, \tag{1.65}$$

and $\beta^{(k)}(t)$ follows,

$$\begin{aligned}
\beta^{(k)}(t) &= \theta - D_1(T_k-t)\theta + \frac{\sigma_1^2}{4\kappa_1}\left(1 - e^{-2\kappa_1(T_k-t)}\right) \\
&+ \rho\sigma_1\sigma_2\frac{\kappa_1}{\kappa_1-\kappa_2}\left(\frac{1-e^{-(\kappa_1+\kappa_2)(T_k-t)}}{\kappa_1+\kappa_2} - \frac{1-e^{-2\kappa_1(T_k-t)}}{2\kappa_1}\right) \\
&+ \frac{\sigma_2^2}{2}\left(\frac{\kappa_1}{\kappa_1-\kappa_2}\right)^2\left(\frac{1-e^{-2\kappa_2(T_k-t)}}{2\kappa_2} + \frac{1-e^{-2\kappa_1(T_k-t)}}{2\kappa_1} - 2\frac{1-e^{-(\kappa_1+\kappa_2)(T_k-t)}}{\kappa_1+\kappa_2}\right),
\end{aligned} \tag{1.66}$$

with

$$D_1(\tau) = \frac{\kappa_1}{\kappa_1-\kappa_2}e^{-\kappa_2\tau} - \frac{\kappa_2}{\kappa_1-\kappa_2}e^{-\kappa_1\tau}. \tag{1.67}$$

When we set $\rho = 0$, the result is consistent with [48] and [43].

Next, we consider the trading problem for the investor. The investor can choose to trade one futures contract or two different futures contracts. We apply the Theorem 1 directly.

If only futures contract $F^{(1)}$ is included in the portfolio, then according to (1.23) and (1.26), we have $\boldsymbol{\mu_F}(t) \equiv \mu_F(t)$, where

$$\mu_F(t) = e^{-(T_1-t)\kappa_1}\lambda_1 + D_2(T_1-t)\lambda_2 \tag{1.68}$$

is a scalar, and

$$\boldsymbol{\Sigma_F}(t) = \left(e^{-(T_1-t)\kappa_1}\sigma_1 + \rho D_2(T_1-t)\sigma_2, \quad \sqrt{1-\rho^2}D_2(T_1-t)\sigma_2\right), \tag{1.69}$$

with

$$D_2(\tau) = \frac{\kappa_1}{\kappa_1-\kappa_2}\left(e^{-\tau\kappa_2} - e^{-\tau\kappa_1}\right). \tag{1.70}$$

Then, the optimal strategy (1.35) becomes

$$\pi^{(1)*}(t) = \frac{1}{\gamma}\frac{\mu_F(t)}{\boldsymbol{\Sigma_F}(t)\boldsymbol{\Sigma_F}^{\top}(t)} \tag{1.71}$$

$$= \frac{1}{\gamma}\frac{e^{-(T_1-t)\kappa_1}\lambda_1 + D_2(T_1-t)\lambda_2}{e^{-2(T_1-t)\kappa_1}\sigma_1^2 + D_2^2(T_1-t)\sigma_2^2 + 2\rho e^{-(T_1-t)\kappa_1}D_2(T_1-t)\sigma_1\sigma_2}. \tag{1.72}$$

By Theorem 1, we can also get

$$\Lambda_1^2(t) = \gamma\pi^{(1)*}(t)\mu_F(t) \tag{1.73}$$

$$= \frac{\left(e^{-(T_1-t)\kappa_1}\lambda_1 + D_2(T_1-t)\lambda_2\right)^2}{e^{-2(T_1-t)\kappa_1}\sigma_1^2 + D_2^2(T_1-t)\sigma_2^2 + 2\rho e^{-(T_1-t)\kappa_1}D_2(T_1-t)\sigma_1\sigma_2}, \tag{1.74}$$

and certainty equivalent

$$CE_1(t,w) = w + \frac{1}{2\gamma}\int_t^{\tilde{T}} \Lambda_1^2(s)ds. \tag{1.75}$$

As for trading two futures contracts $F^{(1)}$ and $F^{(2)}$, according to (1.26), we have

$$\boldsymbol{\mu_F}(t) = \begin{bmatrix} e^{-(T_1-t)\kappa_1}\lambda_1 + D_2(T_1-t)\lambda_2 \\ e^{-(T_2-t)\kappa_1}\lambda_1 + D_2(T_2-t)\lambda_2 \end{bmatrix}, \tag{1.76}$$

and

$$\boldsymbol{\Sigma_F}(t) = \begin{bmatrix} e^{-(T_1-t)\kappa_1}\sigma_1 + \rho D_2(T_1-t)\sigma_2 & \sqrt{1-\rho^2}D_2(T_1-t)\sigma_2 \\ e^{-(T_2-t)\kappa_1}\sigma_1 + \rho D_2(T_2-t)\sigma_2 & \sqrt{1-\rho^2}D_2(T_2-t)\sigma_2 \end{bmatrix}. \tag{1.77}$$

Then, applying formula (1.35), we obtain the optimal strategies

$$\begin{aligned}\pi_1^*(t) =& \Big(\kappa_1\left(e^{-(T_2-t)\kappa_2} - e^{-(T_2-t)\kappa_1}\right)(\sigma_2^2\lambda_1 - \rho\sigma_1\sigma_2\lambda_2) \\ &+ (\kappa_1-\kappa_2)e^{-(T_2-t)\kappa_1}(\rho\sigma_1\sigma_2\lambda_1 - \sigma_1^2\lambda_2)\Big)/ \\ &\left(\gamma\kappa_1(1-\rho^2)\left(e^{-(T_1-t)\kappa_1-(T_2-t)\kappa_2} - e^{-(T_1-t)\kappa_2-(T_2-t)\kappa_1}\right)\sigma_1^2\sigma_2^2\right),\end{aligned} \tag{1.78}$$

$$\begin{aligned}\pi_2^*(t) =& -\Big(\kappa_1\left(e^{-(T_1-t)\kappa_2} - e^{-(T_1-t)\kappa_1}\right)(\sigma_2^2\lambda_1 - \rho\sigma_1\sigma_2\lambda_2) \\ &+ (\kappa_1-\kappa_2)e^{-(T_1-t)\kappa_1}(\rho\sigma_1\sigma_2\lambda_1 - \sigma_1^2\lambda_2)\Big)/ \\ &\left(\gamma\kappa_1(1-\rho^2)\left(e^{-(T_1-t)\kappa_1-(T_2-t)\kappa_2} - e^{-(T_1-t)\kappa_2-(T_2-t)\kappa_1}\right)\sigma_1^2\sigma_2^2\right).\end{aligned} \tag{1.79}$$

As a check, when we set $\rho = 0$ in (1.71), (1.78) and (1.79), we recover the optimal strategies provided in [43].

We note that by substituting (1.76) and (1.77) in (1.33) and (1.34), we obtain

$$\Lambda_2^2(t) = \frac{\lambda_2^2\sigma_1^2 - 2\rho\lambda_1\lambda_2\sigma_1\sigma_2 + \lambda_1^2\sigma_2^2}{(1-\rho^2)\sigma_1^2\sigma_2^2}. \tag{1.80}$$

and the value function:

$$u_2(t,w) = -\exp\left(-\gamma w - \frac{1}{2}\frac{\lambda_2^2\sigma_1^2 - 2\rho\lambda_1\lambda_2\sigma_1\sigma_2 + \lambda_1^2\sigma_2^2}{(1-\rho^2)\sigma_1^2\sigma_2^2}(\widetilde{T}-t)\right), \tag{1.81}$$

which is surprisingly independent of the speeds of mean reversion κ_1 and κ_2. Furthermore, if we represent the value function using the risk premia $\boldsymbol{\zeta} = (\zeta_1, \zeta_2)^\top$, where $\boldsymbol{\zeta}$ satisfies $\boldsymbol{\zeta} = \boldsymbol{C}^{-1}\boldsymbol{\Sigma}^{-1}\boldsymbol{\lambda}$, then the value function is simplified as

$$u_2(t,w) = -\exp\left(-\gamma w - \frac{\zeta_1^2 + \zeta_2^2}{2}(\widetilde{T}-t)\right), \tag{1.82}$$

which reveals that the value function depends only on the risk premia. This is an interesting contrast when compared to the case of trading only a single futures, where the certainty equivalent, $CE_1(t,w)$ in (1.75), does not admit the same kind of simplification and depends on other model parameters. This is intuitive since trading one futures exposes the investor to unhedged risk in the model, so it is reasonable that the trading strategy should depend on the model parameters.

In turn, the certainty equivalent is given by

$$CE_2(t,w) = w + \frac{1}{2\gamma}\frac{\lambda_2^2\sigma_1^2 - 2\rho\lambda_1\lambda_2\sigma_1\sigma_2 + \lambda_1^2\sigma_2^2}{(1-\rho^2)\sigma_1^2\sigma_2^2}(\widetilde{T}-t) \tag{1.83}$$

$$= w + \frac{\zeta_1^2 + \zeta_2^2}{2\gamma}(\widetilde{T}-t). \tag{1.84}$$

Therefore, the value of trading opportunity is proportional to the squared sum of the two risk premia $(\zeta_1^2 + \zeta_2^2)$ associated with the two Brownian motions in the CTOU model. In particular, this means that if the price dynamics of the spot asset under the historical measure and risk-neutral measure are identical, which corresponds to the case of zero risk premia,

then the certainty equivalent will vanish. Lastly, as expected, it is also inversely proportional to risk aversion γ.

In the following proposition, we show that it is more beneficial for the investor to trade two futures instead of one.

Proposition 2. *For any time t and wealth w, the following inequality holds:*

$$CE_2(t,w) \geq CE_1(t,w), \tag{1.85}$$

where $CE_1(t,w)$ and $CE_2(t,w)$ are given by (1.75) *and* (1.83) *respectively.*

Proof. Both certainty equivalents admit the same form given by (1.49), so it remains to prove that $\Lambda_1^2(t) \leq \Lambda_2^2(t)$ for any time $t \leq \tilde{T}$. Denote $a = \exp(-(T_1 - t)\kappa_1)$ and $b = D_2(T_1 - t)$. Then by (1.73), we have

$$\Lambda_1^2(t) = \frac{(a\lambda_1 + b\lambda_2)^2}{a^2\sigma_1^2 + b^2\sigma_2^2 + 2\rho ab\sigma_1\sigma_2}. \tag{1.86}$$

Using this and (1.80), we have

$$\Lambda_2^2(t) - \Lambda_1^2(t) = \frac{\left(\sigma_1^2\lambda_2 a - \sigma_2^2\lambda_1 b + \rho\sigma_1\sigma_2(b\lambda_2 - a\lambda_1)\right)^2}{(1-\rho^2)(a^2\sigma_1^2 + b^2\sigma_2^2 + 2\rho ab\sigma_1\sigma_2)\sigma_1^2\sigma_2^2} \geq 0, \tag{1.87}$$

as desired. □

Numerical examples of the certainty equivalents for CTOU model are presented in Section 1.6.

1.5 The Multiscale Central Tendency Ornstein-Uhlenbeck Model

In this section, we introduce the class of two-scale central tendency Ornstein-Uhlenbeck (CTOU) process. We also discuss the futures pricing and futures trading problem under this model.

1.5.1 Model Formulation

Following the change of measure procedure described in Section 1.2, we donote the log-price of the underlying asset by $X_t^{(1)}$ and its evolution under the physical measure $\mathbb{P}$ is given by the system of stochastic differential equations:

$$dX_t^{(1)} = \kappa\left(X_t^{(2)} + X_t^{(3)} - X_t^{(1)}\right)dt + \sigma_1 dZ_t^{\mathbb{P},1}, \tag{1.88}$$

$$dX_t^{(2)} = \frac{1}{\epsilon}\left(\alpha_2 - X_t^{(2)}\right)dt + \frac{1}{\sqrt{\epsilon}}\sigma_2\left(\rho_{12}dZ_t^{\mathbb{P},1} + \sqrt{1-\rho_{12}^2}dZ_t^{\mathbb{P},2}\right), \tag{1.89}$$

$$dX_t^{(3)} = \delta\left(\alpha_3 - X_t^{(3)}\right)dt + \sqrt{\delta}\sigma_3\left(\rho_{13}dZ_t^{\mathbb{P},1} + \rho_{23}dZ_t^{\mathbb{P},2} + \sqrt{1-\rho_{13}^2-\rho_{23}^2}dZ_t^{\mathbb{P},3}\right), \tag{1.90}$$

where $Z^{\mathbb{P},1}$, $Z^{\mathbb{P},2}$ and $Z^{\mathbb{P},3}$ are independent Brownian motions under the physical measure $\mathbb{P}$.

As such, the stochastic mean of log price $X^{(1)}$ is the sum of two factors $X_t^{(2)}$ and $X_t^{(3)}$. The first factor $X_t^{(2)}$ is a fast mean reverting diffusion process. We denote by $1/\epsilon$ the rate of mean reversion of this process, with $\epsilon > 0$ being a small parameter which corresponds to the time scale of this process. It is an ergodic process and its invariant distribution is independent of ϵ. This distribution is Gaussian with mean α_2 and variance $\sigma_2^2/2$. In addition, we assume that the correlation coefficient ρ_{12} is constant and $|\rho_{12}| < 1$.

The process $X_t^{(3)}$ is slowly varying, obtained by slowing down the diffusion process with a small parameter δ. We also assume the correlation coefficient ρ_{13} and ρ_{23} are constants, which satisfy $\rho_{13}^2 + \rho_{23}^2 < 1$.

We specify the risk premium as ζ_i, for $i = 1, 2, 3$, which satisfy

$$dZ_t^{\mathbb{Q},i} = dZ_t^{\mathbb{P},i} + \zeta_i, \tag{1.91}$$

where $Z^{\mathbb{Q},1}$, $Z^{\mathbb{Q},2}$ and $Z^{\mathbb{Q},3}$ are independent Brownian motions under risk-neutral measure $\mathbb{Q}$. We introduce the combined market prices of volatility risk λ_i, for $i = 1, 2, 3$, defined by

$$\lambda_1 = \zeta_1\sigma_1, \tag{1.92}$$

$$\tag{1.93}$$

$$\lambda_2 = \frac{1}{\sqrt{\epsilon}}\sigma_2\left(\zeta_1\rho_{12} + \zeta_2\sqrt{1-\rho_{12}^2}\right), \tag{1.94}$$

$$\lambda_3 = \sqrt{\delta}\sigma_3\left(\zeta_1\rho_{13} + \zeta_2\rho_{23} + \zeta_3\sqrt{1-\rho_{13}^2-\rho_{23}^2}\right). \tag{1.95}$$

Then, we write the evolution under the risk neutral measure as:

$$dX_t^{(1)} = \kappa\left(X_t^{(2)} + X_t^{(3)} - X_t^{(1)} - \lambda_1/\kappa\right)dt + \sigma_1 dZ_t^{\mathbb{Q},1}, \tag{1.96}$$

$$dX_t^{(2)} = \frac{1}{\epsilon}\left(\alpha_2 - X_t^{(2)} - \epsilon\lambda_2\right)dt + \frac{1}{\sqrt{\epsilon}}\sigma_2\left(\rho_{12}dZ_t^{\mathbb{Q},1} + \sqrt{1-\rho_{12}^2}dZ_t^{\mathbb{Q},2}\right), \tag{1.97}$$

$$\begin{aligned} dX_t^{(3)} = {} & \delta\left(\alpha_3 - X_t^{(3)} - \lambda_3/\delta\right)dt \\ & + \sqrt{\delta}\sigma_3\left(\rho_{13}dZ_t^{\mathbb{Q},1} + \rho_{23}dZ_t^{\mathbb{Q},2} + \sqrt{1-\rho_{13}^2-\rho_{23}^2}dZ_t^{\mathbb{Q},3}\right). \end{aligned} \tag{1.98}$$

This two-scale central tendency Ornstein-Uhlenbeck model belongs to our multifactor model framework discussed in the previous sections. Indeed, this amounts to setting the coefficients in SDE (1.3) and (1.5) to be

$$\boldsymbol{\mu} = (0, \alpha_2/\epsilon, \delta\alpha_3)^\top, \quad \boldsymbol{\lambda} = (\lambda_1, \lambda_2, \lambda_3)^\top, \tag{1.99}$$

$$\boldsymbol{K} = \begin{bmatrix} \kappa & -\kappa & -\kappa \\ 0 & 1/\epsilon & 0 \\ 0 & 0 & \delta \end{bmatrix}, \quad \boldsymbol{\Sigma} = \begin{bmatrix} \sigma_1 & 0 & 0 \\ 0 & \sigma_2/\sqrt{\epsilon} & 0 \\ 0 & 0 & \sqrt{\delta}\sigma_3 \end{bmatrix}, \tag{1.100}$$

and

$$\boldsymbol{C} = \begin{bmatrix} 1 & 0 & 0 \\ \rho_{12} & \sqrt{1-\rho_{12}^2} & 0 \\ \rho_{13} & \rho_{23} & \sqrt{1-\rho_{13}^2-\rho_{23}^2} \end{bmatrix}. \tag{1.101}$$

Remark 1. *We remark that if the stochastic mean of log price $X^{(1)}$ is only modeled by $X^{(2)}$ or $X^{(3)}$, instead of their sum, it will reduce to the CTOU model, which is discussed in the Section 1.4.2. For example, if the log price $X^{(1)}$ evolves according to*

$$dX_t^{(1)} = \kappa\left(X_t^{(2)} - X_t^{(1)}\right)dt + \sigma_1 dZ_t^{\mathbb{P},1}, \tag{1.102}$$

where $X_t^{(2)}$ *admits the process* (1.89)*, we can just apply the theory in Section 1.4.2 by setting*

$$\boldsymbol{\mu} = \begin{bmatrix} 0 \\ \alpha_2/\epsilon \end{bmatrix}, \quad \boldsymbol{K} = \begin{bmatrix} \kappa & -\kappa \\ 0 & 1/\epsilon \end{bmatrix}, \tag{1.103}$$

$$\boldsymbol{\Sigma} = \begin{bmatrix} \sigma_1 & 0 \\ 0 & \sigma_2/\sqrt{\epsilon} \end{bmatrix}, \quad \boldsymbol{C} = \begin{bmatrix} 1 & 0 \\ \rho_{12} & \sqrt{1-\rho_{12}^2} \end{bmatrix}, \tag{1.104}$$

and

$$\boldsymbol{\lambda} = (\lambda_1, \lambda_2)^\top, \tag{1.105}$$

in (1.62) *and* (1.63)*.*

1.5.2 Futures Pricing and Futures Trading

First, we consider three futures contracts $F^{(1)}$, $F^{(2)}$ and $F^{(3)}$, written on this underlying, whose maturity are T_1, T_2 and T_3 respectively. For convenience, we define the following functions:

$$\begin{aligned} f_k(p,t) &:= e^{-(T_k-t)p}, \\ g_k(p,t) &:= \frac{1-e^{-(T_k-t)p}}{p}. \end{aligned}$$

Then, applying the Proposition 1, the futures price $F^{(k)}(t,\boldsymbol{x})$ of maturity T_k under this multiscale CTOU model satisfies

$$F^{(k)}(t,\boldsymbol{x}) = \exp\left(\boldsymbol{a}^{(k)}(t)^\top \boldsymbol{x} + \beta^{(k)}(t)\right), \tag{1.106}$$

where $\boldsymbol{a}^{(k)}(t)$ satisfies

$$\boldsymbol{a}^{(k)}(t) = \left(f_k(\kappa,t),\ \frac{\epsilon\kappa}{1-\epsilon\kappa}\left(f_k(\kappa,t) - f_k(1/\epsilon,t)\right),\ \frac{\kappa}{\delta-\kappa}\left(f_k(\kappa,t) - f_k(\delta,t)\right)\right)^\top, \tag{1.107}$$

and $\beta^{(k)}(t)$ is given by

$$\begin{aligned}
\beta^{(k)}(t) &= \int_t^{T_k} (\boldsymbol{\mu}-\boldsymbol{\lambda})^\top \boldsymbol{a}^{(k)}(s) + \frac{1}{2}\,\mathrm{Tr}\left(\boldsymbol{\Sigma}\boldsymbol{\Omega}\boldsymbol{\Sigma}\boldsymbol{a}^{(k)}(s)\boldsymbol{a}^{(k)}(s)^\top\right) ds \\
&= \left(-\lambda_1 + \frac{\epsilon\kappa}{1-\epsilon\kappa}(\alpha_2/\epsilon - \lambda_2) + \frac{\kappa}{\delta-\kappa}(\delta\alpha_3 - \lambda_3)\right) g_k(\kappa, s) \\
&\quad - \frac{\epsilon\kappa(\alpha_2/\epsilon - \lambda_2)}{1-\epsilon\kappa} g_k(1/\epsilon, s) - \frac{\kappa(\delta\alpha_3 - \lambda_3)}{\delta-\kappa} g_k(\delta, s) \\
&\quad + \frac{1}{2}\Bigg(1 + \left(\frac{\epsilon\kappa}{1-\epsilon\kappa}\right)^2 + \left(\frac{\kappa}{\delta-\kappa}\right)^2 + \frac{2\rho_{12}\epsilon\kappa}{1-\epsilon\kappa} + \frac{2\rho_{13}\kappa}{\delta-\kappa} \\
&\qquad + \frac{2\left(\rho_{12}\rho_{13} + \rho_{23}\sqrt{1-\rho_{12}^2}\right)\epsilon\kappa^2}{(1-\epsilon\kappa)(\delta-\kappa)}\Bigg) g_k(2\kappa, t) \\
&\quad + \frac{1}{2}\left(\frac{\epsilon\kappa}{1-\epsilon\kappa}\right)^2 g_k(2/\epsilon, s) + \frac{1}{2}\left(\frac{\kappa}{\delta-\kappa}\right)^2 g_k(2\delta, s) \\
&\quad - \Bigg(\left(\frac{\epsilon\kappa}{1-\epsilon\kappa}\right)^2 + \rho_{12}\frac{\epsilon\kappa}{1-\epsilon\kappa} + \left(\rho_{12}\rho_{13} + \rho_{23}\sqrt{1-\rho_{12}^2}\right) \\
&\qquad \frac{\epsilon\kappa^2}{(1-\epsilon\kappa)(\delta-\kappa)}\Bigg) g_k(1/\epsilon + \kappa, s) \\
&\quad - \Bigg(\left(\frac{\kappa}{\delta-\kappa}\right)^2 + \rho_{13}\frac{\kappa}{\delta-\kappa} + \left(\rho_{12}\rho_{13} + \rho_{23}\sqrt{1-\rho_{12}^2}\right) \\
&\qquad \frac{\epsilon\kappa^2}{(1-\epsilon\kappa)(\delta-\kappa)}\Bigg) g_k(\delta + \kappa, s) \\
&\quad + \left(\rho_{12}\rho_{13} + \rho_{23}\sqrt{1-\rho_{12}^2}\right) \frac{\epsilon\kappa^2}{(1-\epsilon\kappa)(\delta-\kappa)} g_k(1/\epsilon + \delta, s). \qquad (1.108)
\end{aligned}$$

Next, we analyze the trading problem for the investor. According to (1.20), (1.23) and (1.106), the stochastic process $F_t^{(k)}$ for k-th futures contract admits the $\mathbb{P}$-dynamics:

$$\frac{dF_t^{(k)}}{F_t^{(k)}} = \mu_F^{(k)}(t)dt + \boldsymbol{\sigma}_F^{(k)}(t)^\top d\boldsymbol{Z}_t^{\mathbb{P}}, \qquad (1.109)$$

where

$$\mu_F^{(k)}(t) = f_k(\kappa, t)\lambda_1 + \frac{\epsilon\kappa}{1-\epsilon\kappa}\left(f_k(\kappa, t) - f_k(1/\epsilon, t)\right)\lambda_2 + \frac{\kappa}{\delta-\kappa}\left(f_k(\kappa, t) - f_k(\delta, t)\right)\lambda_3, \quad (1.110)$$

and

$$\begin{aligned}
&\boldsymbol{\sigma}_F^{(k)}(t) \\
&= \begin{bmatrix} f_k(\kappa,t)\sigma_1 + \rho_{12}\frac{\epsilon\kappa}{1-\epsilon\kappa}\left(f_k(\kappa,t) - f_k(1/\epsilon,t)\right)\sigma_2 + \rho_{13}\frac{\kappa}{\delta-\kappa}\left(f_k(\kappa,t) - f_k(\delta,t)\right)\sigma_3 \\ \sqrt{1-\rho_{12}^2}\frac{\epsilon\kappa}{1-\epsilon\kappa}\left(f_k(\kappa,t) - f_k(1/\epsilon,t)\right)\sigma_2 + \rho_{23}\frac{\kappa}{\delta-\kappa}\left(f_k(\kappa,t) - f_k(\delta,t)\right)\sigma_3 \\ \sqrt{1-\rho_{13}^2-\rho_{23}^2}\frac{\kappa}{\delta-\kappa}\left(f_k(\kappa,t) - f_k(\delta,t)\right)\sigma_3 \end{bmatrix}.
\end{aligned} \tag{1.111}$$

As discussed in the Section 1.3, there are three options for the investor: trade one futures contract, trade two different futures contracts and trade three different futures contracts.

If there is only one futures contract $F^{(1)}$ available in the market. Then by (1.26), we have

$$\boldsymbol{\mu_F}(t) = \mu_F^{(1)}(t), \quad \boldsymbol{\Sigma_F} = \boldsymbol{\sigma}_F^{(1)}(t)^\top. \tag{1.112}$$

Then, the optimal strategy (1.35) becomes

$$\pi^{(1)*}(t) = \frac{1}{\gamma}\frac{\boldsymbol{\mu_F}(t)}{\boldsymbol{\Sigma_F}(t)\boldsymbol{\Sigma_F}^\top(t)} = \frac{1}{\gamma}\frac{\mu_F^{(1)}(t)}{\boldsymbol{\sigma}_F^{(1)}(t)^\top\boldsymbol{\sigma}_F^{(1)}(t)}. \tag{1.113}$$

where $\mu_F^{(1)}(t)$ is shown as (1.110) and $\boldsymbol{\sigma}_F^{(1)}(t)$ is shown as (1.111).

If the investor trade two futures $F^{(1)}$ and $F^{(2)}$, then by (1.26), we have

$$\boldsymbol{\mu_F}(t) = \left(\mu_F^{(1)}(t), \mu_F^{(2)}(t)\right)^\top, \quad \boldsymbol{\Sigma_F}(t) = \left(\boldsymbol{\sigma}_F^{(1)}(t), \boldsymbol{\sigma}_F^{(2)}(t)\right)^\top. \tag{1.114}$$

Then, according to (1.35), we have the optimal strategy

$$\begin{aligned}
\pi^{(1)*}(t) &= \frac{\boldsymbol{\sigma}_F^{(2)}(t)^\top\boldsymbol{\sigma}_F^{(2)}(t)\mu_F^{(1)}(t) - \boldsymbol{\sigma}_F^{(1)}(t)^\top\boldsymbol{\sigma}_F^{(2)}(t)\mu_F^{(2)}(t)}{\gamma\left(\boldsymbol{\sigma}_F^{(1)}(t)^\top\boldsymbol{\sigma}_F^{(1)}(t)\boldsymbol{\sigma}_F^{(2)}(t)^\top\boldsymbol{\sigma}_F^{(2)}(t) - \left(\boldsymbol{\sigma}_F^{(1)}(t)^\top\boldsymbol{\sigma}_F^{(2)}(t)\right)^2\right)}, \\
\pi^{(2)*}(t) &= \frac{\boldsymbol{\sigma}_F^{(1)}(t)^\top\boldsymbol{\sigma}_F^{(1)}(t)\mu_F^{(2)}(t) - \boldsymbol{\sigma}_F^{(1)}(t)^\top\boldsymbol{\sigma}_F^{(2)}(t)\mu_F^{(1)}(t)}{\gamma\left(\boldsymbol{\sigma}_F^{(1)}(t)^\top\boldsymbol{\sigma}_F^{(1)}(t)\boldsymbol{\sigma}_F^{(2)}(t)^\top\boldsymbol{\sigma}_F^{(2)}(t) - \left(\boldsymbol{\sigma}_F^{(1)}(t)^\top\boldsymbol{\sigma}_F^{(2)}(t)\right)^2\right)}.
\end{aligned} \tag{1.115}$$

If the investor trades three futures $F^{(1)}$, $F^{(2)}$ and $F^{(3)}$, then by (1.26), we have

$$\boldsymbol{\mu_F}(t) = \left(\mu_F^{(1)}(t), \mu_F^{(2)}(t), \mu_F^{(3)}(t)\right)^\top, \quad \boldsymbol{\Sigma_F}(t) = \left(\boldsymbol{\sigma}_F^{(1)}(t), \boldsymbol{\sigma}_F^{(2)}(t), \boldsymbol{\sigma}_F^{(3)}(t)\right)^\top. \tag{1.116}$$

Then, according to (1.35), we have the optimal strategy

$$\begin{bmatrix} \pi^{(1)*}(t) \\ \pi^{(2)*}(t) \\ \pi^{(3)*}(t) \end{bmatrix} = \frac{1}{\gamma} \begin{bmatrix} \boldsymbol{\sigma}_F^{(1)}(t)^\top \boldsymbol{\sigma}_F^{(1)}(t), & \boldsymbol{\sigma}_F^{(1)}(t)^\top \boldsymbol{\sigma}_F^{(2)}(t), & \boldsymbol{\sigma}_F^{(1)}(t)^\top \boldsymbol{\sigma}_F^{(3)}(t) \\ \boldsymbol{\sigma}_F^{(2)}(t)^\top \boldsymbol{\sigma}_F^{(1)}(t), & \boldsymbol{\sigma}_F^{(2)}(t)^\top \boldsymbol{\sigma}_F^{(2)}(t), & \boldsymbol{\sigma}_F^{(2)}(t)^\top \boldsymbol{\sigma}_F^{(3)}(t) \\ \boldsymbol{\sigma}_F^{(3)}(t)^\top \boldsymbol{\sigma}_F^{(1)}(t), & \boldsymbol{\sigma}_F^{(3)}(t)^\top \boldsymbol{\sigma}_F^{(2)}(t), & \boldsymbol{\sigma}_F^{(3)}(t)^\top \boldsymbol{\sigma}_F^{(3)}(t) \end{bmatrix}^{-1} \boldsymbol{\mu_F}(t). \quad (1.117)$$

1.6 Numerical Illustration

We begin with numerical examples for the multiscale CTOU model discussed in the Section 1.5. With the closed-form expressions obtained in the Section 1.5.2, we now implement the futures prices, optimal strategies and wealth processes numerically, using the parameters in Table 1.1. Primarily, we let ϵ and δ be small parameters and we consider trading three futures with maturities $T_1 = 1/12$ year, $T_2 = 2/12$ year and $T_3 = 3/12$ year. Then, our trading horizon will be $\widetilde{T} = 1/12$ year, no greater than the futures maturities. We use 'trading day' as the x axis in some figures. We assume there be 252 trading days in a year and 21 trading days for a month. Therefore, our trading horizon is 21 trading days in total.

$X_0^{(1)}$	$X_0^{(2)}$	$X_0^{(3)}$	α_2	α_3	κ	ϵ	δ	σ_1	σ_2	σ_3
1	0.5	0.5	0.5	0.5	5	0.05	0.01	0.8	0.02	0.3
ρ_{12}	ρ_{13}	ρ_{23}	λ_1	λ_2	λ_3	T_1	T_2	T_3	$\widetilde{T}$	γ
0	0	0	0.02	0.02	0.02	1/12	2/12	3/12	1/12	1

Table 1.1: Parameters for multiscale CTOU model.

In Figure 1.1, we generate the term structure of futures prices with different log-prices. In the left figure, the log-price $X^{(1)} = 0.85$, 0.9 and 0.95, which is smaller than the instantaneous stochastic mean $X^{(2)} + X^{(3)} = 1$. Then the asset's spot price is in contango and it will lead to that the futures price increases for the time to maturity. In the right figure, where $X^{(1)} > X^{(2)} + X^{(3)}$, the asset's spot price is in backwardation and the futures price decreases for the time to maturity.

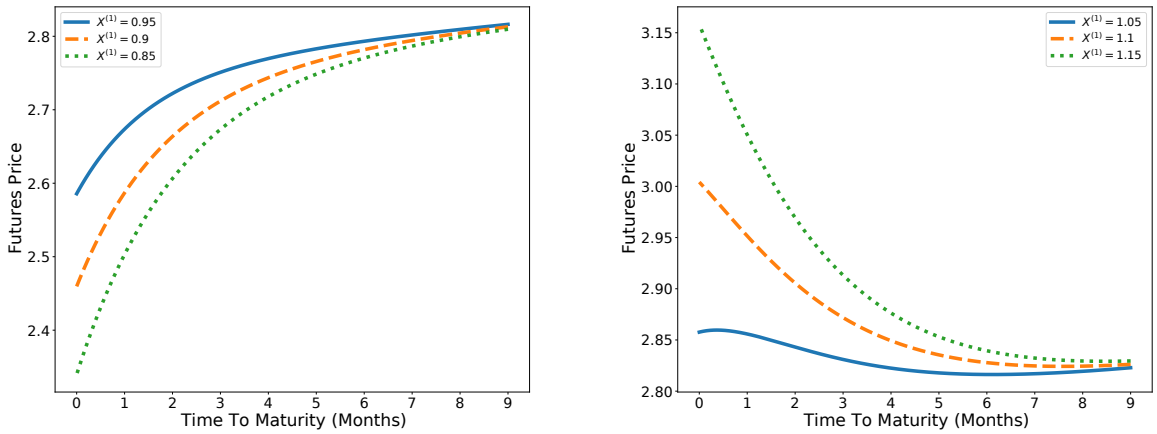

Figure 1.1: Left: the term structure of futures price in contango with $X^{(1)} = 0.95$, 0.90 and 0.85. Right: the term structure of futures price in backwardation with $X^{(1)} = 1.15$, 1.10 and 1.05. Other parameters are shown in Table 1.1.

In Figure 1.2, we plot the simulated paths and 95% confidence intervals for three factors in the top figure and middle figure. As shown in the middle figure, the 95% confidence interval of the slow-varying factor $X^{(3)}$ is much narrower than the one for fast-varying factor $X^{(2)}$. At the bottom, we plot the spot price in the solid lines and futures prices in the dashed lines. We observe that three paths for the futures prices are highly correlated and T_1-futures price is equal to the asset's spot price at its maturity date T_1, which is the 21st trading day.

In Figure 1.3, we plot the optimal positions (in dollars) as functions of time for different portfolios. We illustrate the optimal strategies for one-contract portfolio, two-contract portfolio and three-contract portfolio respectively. Solid lines represent the optimal investment on T_1-futures. Dashed lines represent the optimal investment on T_2-futures. Dotted lines represent optimal investment on T_3-futures. The formula for optimal strategies are given in (1.113)–(1.117). As it turns out, the optimal positions in cash amount are deterministic functions for time, but the units of futures in the portfolios still depend directly on asset's spot price and futures prices.

When trading one futures, the investor faces significant risks exposure. Therefore, the

position is relatively small due to risk aversion. Moreover, the investor takes significantly larger position in three-contract portfolio since he can hedge all the risks. From a computational perspective, this is related to the large condition number of the matrix in 1.117 where the optimal positions are calculated. Nevertheless, the net exposure is significantly reduced by the opposite (long/short) positions. As shown in Figure 1.4, the net optimal positions across all three portfolios are of the same order of magnitude and very close to zero.

Next, the wealth processes for three portfolios are shown in Figure 1.5. On the left, we plot wealth processes as functions of time for one-contract portfolio and two-contract portfolio. We observe that the wealth paths for these two portfolios are pretty close, and they both seem to mostly follow the spot price process, which is also trending downward in a similar manner. However, on the right, the wealth process for the three-contract portfolio exhibits very different path behavior compared to those on the left. In particular, this wealth process does not seem to follow the spot price.

We plot certainty equivalent for different portfolios on Figure 1.6. First, we observe that the certainty equivalent increases with respect to the trading horizon $\widetilde{T}$. As the trading horizon reduces to zero, the certainty equivalent converges to the initial wealth w, which is set to be 0 in this example. It is consistent with equation (1.49). Second, with more contracts to trade, the investor has a higher certainty equivalent, but different futures combinations lead to varying values. In this example, trading the short-term futures, T_1 and T_2 futures, yields the highest certainty equivalent. On the right, we see that risk aversion reduces the certainty equivalent for any trading horizon $\widetilde{T}$.

In Table 1.2, we present the certainty equivalents for all possible futures combinations and different correlation parameters ρ_{12} and ρ_{13}. It also shows that the certainty equivalent is much higher when there are more contracts to trade. In addition, if there is only one futures contract to trade, the certainty equivalent is increasing with respect to its maturity, see first three columns. In addition, the certainly equivalents depend on the correlation parameters ρ_{12} and ρ_{13}.

Lastly, we return to the CTOU model presented in 1.4.2. In Table 1.3, we present

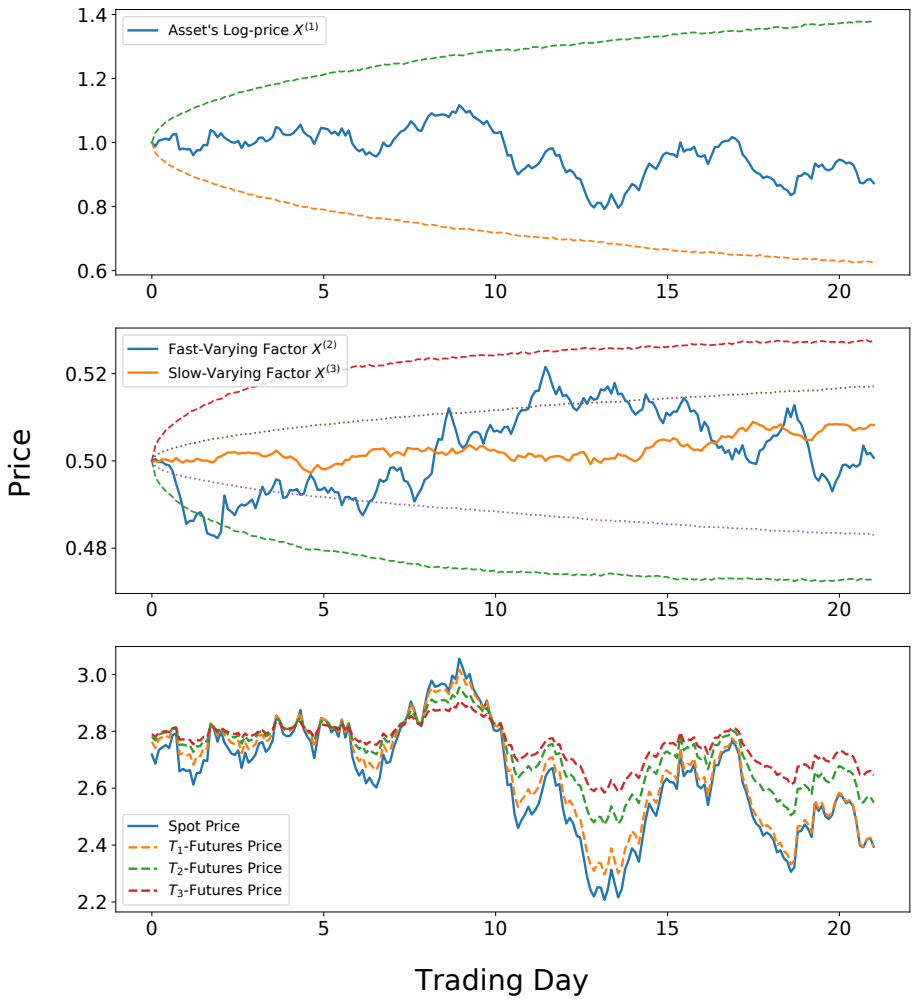

Figure 1.2: Top: simulated paths for asset's log-price $X^{(1)}$. Dashed curves represent 95% confidence intervals. Middle: simulated path for the fast-varying factor $X^{(2)}$ and slow-varying factor $X^{(2)}$. Dashed curves represent 95% confidence intervals for $X^{(2)}$ and dotted curves represent 95% confidence intervals for $X^{(3)}$. Bottom: simulated paths for asset's spot price and futures prices. Parameters are shown in Table 1.1.

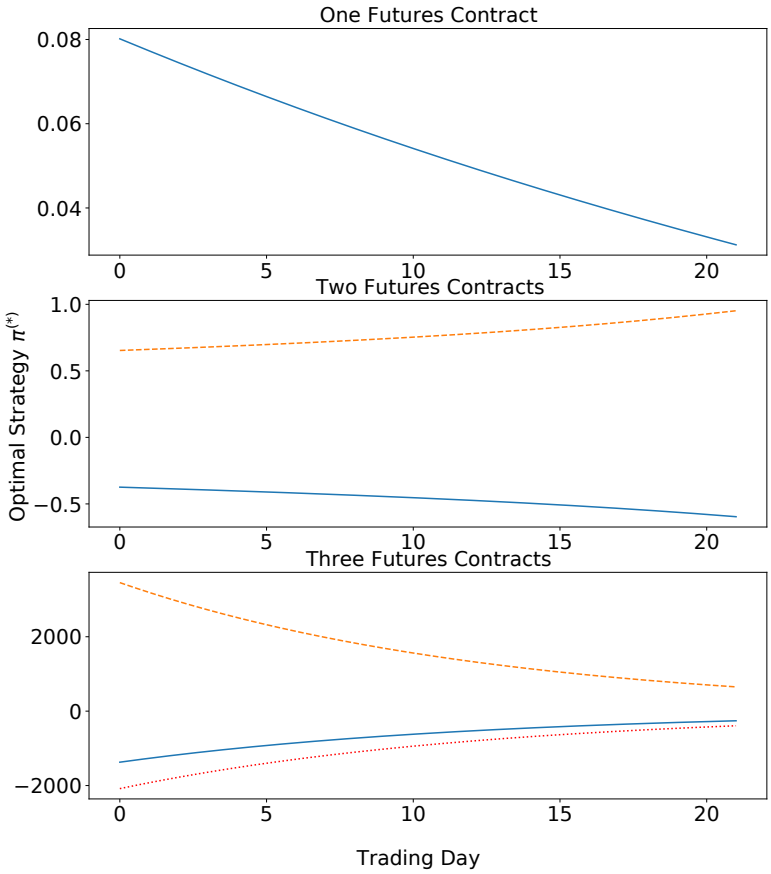

Figure 1.3: The optimal strategy $\pi^{(*)}$ as a function of time for different futures portfolios. In each plot when applicable, the solid line is the optimal investment on T_1-futures, dashed line is the optimal investment on T_2-futures, and dotted line is the optimal investment on T_3-futures. Parameters are shown in Table 1.1.

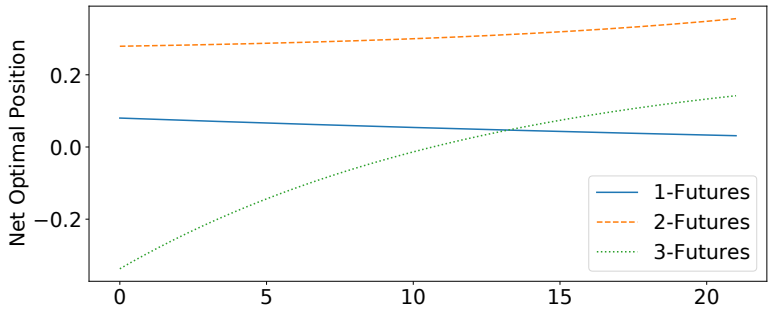

Figure 1.4: The net optimal positions for portfolios with different numbers of futures. The maximum and minimum net optimal positions for the one-futures portfolio (solid line) are 0.08 and 0.03 respectively. The maximum and minimum net optimal positions for the two-futures portfolio (dashed line) are 0.36 and 0.28 respectively. The maximum and minimum net optimal positions for the three-futures portfolio (dotted line) are 0.14 and -0.34 respectively.

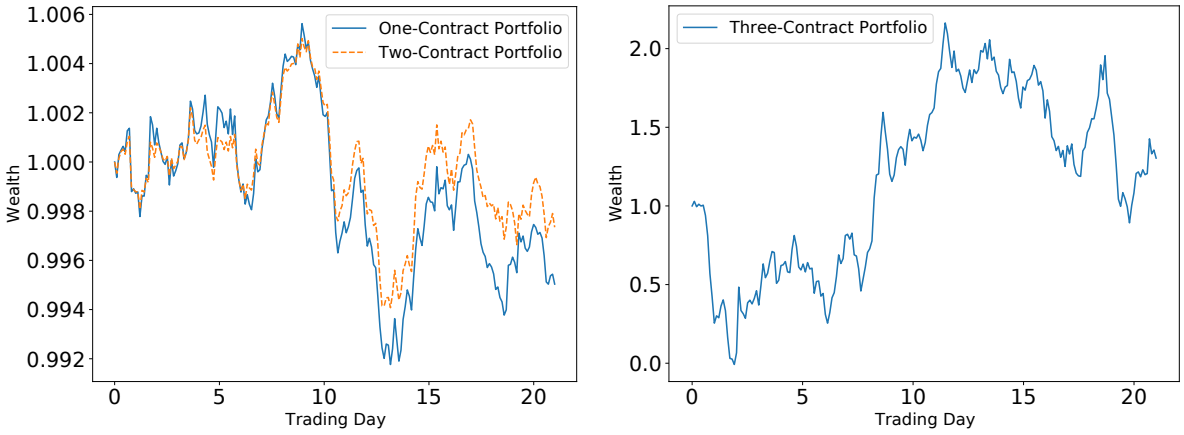

Figure 1.5: Left: wealth processes as functions of time for one-contract portfolio and two-contract portfolio. Right: wealth process as function of time for three contract-portfolio. Parameters are shown in the Table 1.1.

the certainty equivalents corresponding to different values of the speed of reversion κ_1 and correlation ρ. We use the estimated parameters from the "full sample" in Table 4 of [48] and Table 1 of [43]. It shows that higher speed of mean reversion κ_1 leads to higher certainty equivalent. However, when two futures contracts are traded, the dependence of certainty equivalents on κ_1 and correlation parameter ρ disappears, which has been already shown by value function (1.82). This phenomenon is also pointed out by [43] that the certainty equivalent only depends on market prices of risk ζ_1 and ζ_2 when two futures are traded.

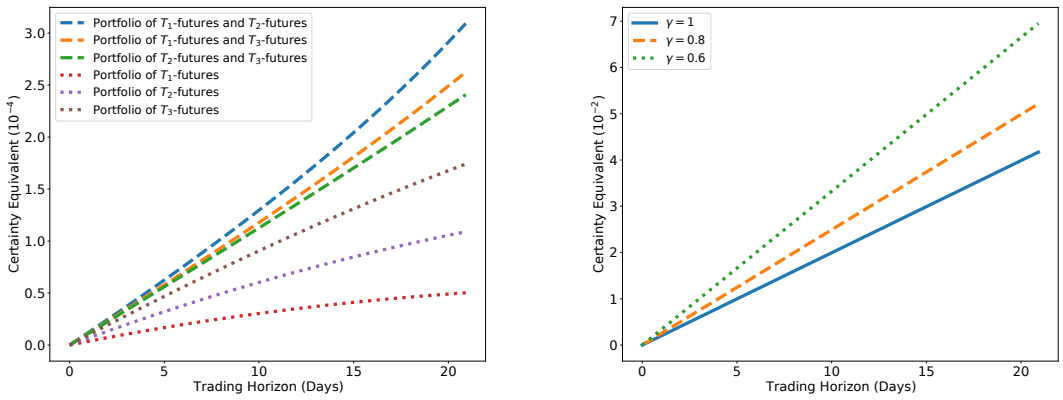

Figure 1.6: Left: certainty equivalents as functions of trading horizon $\widetilde{T}$ for one-contract portfolios and two-contract portfolios. Right: certainty equivalents as functions of trading horizon $\widetilde{T}$ for three-contract portfolio with different risk-aversion parameter γ. Other parameters are shown in Table 1.1.

1.7 Conclusion

We have extended the study of optimal trading in commodity futures market under two-factor models to a multifactor model. Closed-form expressions for the optimal controls and for the value function are obtained. Using these, we illustrated the optimal strategies. Intuitively, it should be more valuable to the investor to access a larger set of securities, and this intuition

Parameters		Futures Combinations (Maturity)						
		T_1	T_2	T_3	$\{T_1, T_2\}$	$\{T_1, T_3\}$	$\{T_2, T_3\}$	$\{T_1, T_2, T_3\}$
$\rho_{12} = 0$	$\rho_{13} = -0.5$	0.563	1.58	3.25	5.36	4.65	4.41	419
	$\rho_{13} = 0$	0.502	1.09	1.74	3.09	2.62	2.41	417
	$\rho_{13} = 0.5$	0.456	0.837	1.19	2.88	2.35	2.01	417
$\rho_{12} = 0.5$	$\rho_{13} = -0.5$	0.561	1.56	3.23	5.34	4.64	4.40	543
	$\rho_{13} = 0$	0.500	1.08	1.73	3.08	2.62	2.40	542
	$\rho_{13} = 0.5$	0.454	0.833	1.18	2.87	2.34	2.01	541
$\rho_{12} = -0.5$	$\rho_{13} = -0.5$	0.565	1.59	3.27	5.39	4.66	4.42	571
	$\rho_{13} = 0$	0.504	1.10	1.75	3.11	2.63	2.41	569
	$\rho_{13} = 0.5$	0.457	0.842	1.20	2.90	2.36	2.02	569

Table 1.2: The certainty equivalents ($\times 10^{-4}$) for all possible futures combinations and different correlation parameters ρ_{12} and ρ_{13}. Other parameters are shown in the Table 1.1.

Parameters		Futures Combinations (Maturity)		
		T_1	T_2	$\{T_1, T_2\}$
$\kappa_1 = 5.827$	$\rho = -0.5$	3.66	45.6	209
	$\rho = 0$	3.96	36.3	209
	$\rho = 0.5$	2.48	19.4	209
$\kappa_1 = 0.827$	$\rho = -0.5$	0.0281	0.290	209
	$\rho = 0$	0.0393	0.377	209
	$\rho = 0.5$	0.0264	0.259	209

Table 1.3: The certainty equivalents ($\times 10^{-3}$) for all possible futures combinations, different speed of reversion κ_1 and correlation parameters ρ in CTOU model. Other parameters: $\kappa_2 = 0.3$, $\sigma_1 = 1.037$, $\sigma_2 = 0.446$, $\zeta_1 = -0.010$, $\zeta_2 = 2.242$, $T_1 = 1/12$, $T_2 = 2/12$ and $\widetilde{T} = 1/12$.

is confirmed quantitatively through the certainty equivalents associated with the optimal futures portfolios.

In the presence of market frictions, trading more contracts might not necessarily be more beneficial. Therefore, it is practically important to determine the right number of contracts and rebalancing strategies accounting for transaction costs. Such an extension to our model would be interesting for future research.

Another direction is model estimation. In fact, one advantage of the multifactor model, as argued by [19], is the ease of estimation via Kalman filter. In other related studies ([55, 29, 60]), Kalman filtering and other calibration methodologies can handle multifactor models with hidden state variables and measurement errors. Inclusion of measurement errors is necessary since the number of available market prices is generally higher than the number of state variables that need to be estimated.

Chapter 2

DYNAMIC FUTURES PORTFOLIO IN A REGIME-SWITCHING MARKET FRAMEWORK

2.1 Introduction

Asset prices are often seen as being dependent on the market conditions. Market regimes may change suddenly and persist for a period of time. The unpredictability of the timing of regime changes also means that associated risks are almost impossible to hedge. In order to capture these crucial properties of market dynamics, one major approach is to represent stochastic market regimes by a finite-state Markov chain. In most cases, the Markov chain is an exogenous random process and is not directly tradable. The effects of the Markov chain are reflected in the asset price dynamics. In particular, the asset's expected return and volatility may vary across regimes.

Regime switching models date back to [30], who introduced a regime switching time series model to capture the movements of the stock prices and showed that the regime switching model represents the stock returns better than the model with deterministic coefficients. Thereafter, regime switching has been applied to many problems in economics and finance, including derivatives pricing ([13], [23], and [2], among many others), and portfolio selection ([62, 54, 36, 17, 57]).

In this chapter, we present a stochastic control approach to generate dynamic futures trading strategies. We consider a general regime-switching framework in which the stochastic market regime is represented by a continuous-time finite-state Markov chain. The underlying asset's spot price is modeled by a Markov-modulated diffusion process. Then, we derive the no-arbitrage price dynamics for the futures contracts and determine the optimal futures trading strategy by solving a utility maximization problem. By analyzing and solving the

associated Hamilton-Jacobi-Bellman (HJB) equations, we derive the investor's value function and optimal trading strategies.

In comparison to related studies on portfolio optimization with regime switching, we investigate the dynamic trading of futures, rather than stocks, in a general regime-switching market framework that can be applied to an array of regime-switching models. This different setup leads to the interaction between the historical measure and risk-neutral pricing measure, and how they affect the evolution of futures prices and portfolio wealth. In particular, the regime-switching feature also leads to jumps in the futures prices and the investor's wealth process, even though the underlying asset price has continuous paths. Moreover, under our regime-switching framework, the certainty equivalent is the same across different underlying models as long as the market price of risk stays the same.

Among our findings, we show that the investor's value function admits a separable form under a general regime-switching market framework, and the original HJB equations are reduced to a system of linear ODEs. In addition, we also define the investor's certainty equivalent to quantify the value of the futures trading opportunity to the investor. Surprisingly both the value function and certainty equivalent do not depend on the current spot and futures prices, and admits a universal form across different model specifications. Nevertheless, the risk premia associated with the regime-switching model play a crucial role, not only in the value function and certainty equivalent, but also in the optimal strategy. In addition, we show two applications of our model, regime-switching Geometric Brownian Motion (RS-GBM) and regime-switching Exponential Ornstein-Uhlenbeck (RS-XOU) model. Exponential Ornstein-Uhlenbeck model is one of the mean reversion models used to analyze futures market.

The rest of this chapter is structured as follows. We describe the general market framework in Section 2.2. The dynamic futures portfolio optimization is discussed in Section 2.3. We apply our framework to the RS-GBM model and RS-XOU model in Sections 2.4 and 2.5, respectively. Concluding remarks are provided in Section 2.6.

2.2 Futures Price Dynamics

We fix a probability space $(\Omega, \mathcal{G}, \mathbb{Q})$, where $\mathbb{Q}$ is the risk-neutral pricing measure $\mathbb{Q}$. Let ξ be a continuous-time irreducible finite-state Markov chain with state space $E = \{1, 2, \ldots, M\}$. The generator matrix of ξ, denoted by $\tilde{\boldsymbol{Q}}$, has entries $\tilde{\boldsymbol{Q}}(i,j) = \tilde{q}(i,j)$ such that $\tilde{q}(i,j) \geq 0$ for $i \neq j$ and $\sum_{j \in E} \tilde{q}(i,j) = 0$ for $i \in E$. This Markov chain represents the changing market regime and influences the underlying asset's price dynamics.

We can use a stochastic integral with respect to a Poisson random measure to represent Markov chain ξ. For $i, j \in E$ with $i \neq j$, let $\Delta(i,j)$ be the consecutive left-closed, right-open intervals of the real line, each having length $\tilde{q}(i,j)$. Define a function $h : E \times \mathbb{R} \to \mathbb{R}$ by

$$h(i,z) = \sum_{j \in E \setminus \{i\}} (j-i) I_{\{z \in \Delta(i,j)\}}. \tag{2.1}$$

Then, under measure $\mathbb{Q}$, the Markov chain ξ_t evolves according to

$$d\xi_t = \int_{\mathbb{R}} h(\xi_t, z) N(dt, dz), \tag{2.2}$$

where $N(dt, dz)$ is the Poisson random measure with intensity $dt \times \tilde{\mu}(dz)$ and $\tilde{\mu}$ is the Lebesgue measure satisfying

$$\int_{\mathbb{R}} I_{\{z \in \Delta(i,j)\}} \tilde{\mu}(dz) = |\Delta(i,j)| = \tilde{q}(i,j), \tag{2.3}$$

with $|\Delta(i,j)|$ being the length of $\Delta(i,j)$. We can also express SDE (2.2) as

$$d\xi_t = \sum_{j \in E \setminus \{\xi_t\}} \tilde{q}(\xi_t, j)(j - \xi_t) dt + \int_{\mathbb{R}} h(\xi_t, z) M^{\mathbb{Q}}(dt, dz), \tag{2.4}$$

using the compensated Poisson process under measure $\mathbb{Q}$ defined by

$$M^{\mathbb{Q}}(dt, dz) = N(dt, dz) - dt \times \tilde{\mu}(dz). \tag{2.5}$$

The underlying asset's spot price is denoted by S_t. Its log-price, $X_t = \log(S_t)$, evolves according to

$$dX_t = \tilde{a}(t, X_t, \xi_t) dt + b(t, X_t, \xi_t) dZ_t^{\mathbb{Q}}, \tag{2.6}$$

where $Z^{\mathbb{Q}}$ is the standard Brownian motion under the measure $\mathbb{Q}$ and independent of ξ. The drift and volatility functions $\tilde{a}(\cdot,\cdot,\cdot)$ and $b(\cdot,\cdot,\cdot)$ are assumed to satisfy the conditions such that SDE (2.6) has a strong solution.

Consider a futures contract on the underlying asset S with maturity T. Like (1.6) in Chapter 1, the no-arbitrage price of this futures at time $t \leq T$ is given by the conditional expectation under the risk-neutral pricing measure $\mathbb{Q}$:

$$F_i(t,x) = I\!E^{\mathbb{Q}}[\exp(X_T)|X_t = x, \xi_t = i]. \tag{2.7}$$

The futures price function $F_i(t,x)$ is determined from the following system of PDEs

$$\partial_t F_i + \mathcal{L}_i^{\mathbb{Q}} F_i + \sum_{j \in E\setminus\{i\}} \tilde{q}(i,j)(F_j - F_i) = 0, \tag{2.8}$$

for $(t,x) \in [0,T) \times \mathbb{R}$ and $i = 1, \ldots, M$, where

$$\mathcal{L}_i^{\mathbb{Q}} \cdot := \tilde{a}(t,x,i)\partial_x \cdot + \frac{b^2(t,x,i)}{2}\partial_{xx} \cdot \ . \tag{2.9}$$

To facilitate presentation, we have dropped the variables from different functions in (2.8) and will do the same in PDEs that follow when no ambiguity arises.

For the futures trading problem, asset and futures prices are observed under the physical measure $\mathbb{P}$. Under measure $\mathbb{P}$, the Markov chain ξ has generator matrix $\boldsymbol{Q}$ with entries $\boldsymbol{Q}(i,j) = q(i,j)$, where $i,j \in E$. Since $\mathbb{P}$ and $\mathbb{Q}$ are equivalent measures, we have $q(i,j) = 0$ iff $\widetilde{q}(i,j) = 0$. To relate the Poisson random measures under measures $\mathbb{P}$ and $\mathbb{Q}$, we denote by $\mu(dz)$ the intensity measure of $N(dt,dz)$ under measure $\mathbb{P}$ such that

$$\mu(dz) = \begin{cases} \dfrac{q(i,j)}{\widetilde{q}(i,j)}\widetilde{\mu}(dz), & \text{for } z \in \Delta(i,j), \\ \widetilde{\mu}(dz), & \text{others}, \end{cases} \tag{2.10}$$

under the convention that $0/0 = 1$. Then, the compensated Poisson process under measure $\mathbb{P}$ is

$$M^{\mathbb{P}}(dt,dz) = M^{\mathbb{Q}}(dt,dz) - \sum_{i,j \in E, i \neq j} \frac{q(i,j) - \widetilde{q}(i,j)}{\widetilde{q}(i,j)} I_{\{z \in \Delta(i,j)\}} dt \times \widetilde{\mu}(dz). \tag{2.11}$$

Accordingly, the Markov chain ξ_t satisfies

$$d\xi_t = \sum_{j \in E \setminus \{\xi_t\}} q(\xi_t, j)(j - \xi_t)dt + \int_{\mathbb{R}} h(\xi_t, z) M^{\mathbb{P}}(dt, dz). \tag{2.12}$$

To relate the Brownian motions under measures $\mathbb{P}$ and $\mathbb{Q}$, we denote by $\zeta(\xi_t)$ the risk premium associated with the Brownian motion such that

$$dZ_t^{\mathbb{Q}} = dZ_t^{\mathbb{P}} + \zeta(\xi_t)dt. \tag{2.13}$$

In turn, the log spot price satisfies

$$dX_t = a(t, X_t, \xi_t)dt + b(t, X_t, \xi_t)dZ_t^{\mathbb{P}}, \tag{2.14}$$

whose drift is given by

$$a(t, x, i) := \widetilde{a}(t, x, i) + \zeta(i)b(t, x, i).$$

Here, $Z^{\mathbb{P}}$ is the standard Brownian motion under $\mathbb{P}$ and is independent of ξ.

Applying Itô's lemma, the futures price F_t satisfies the stochastic differential equation (SDE),

$$dF_t = \eta(t, X_t, \xi_t)dZ_t^{\mathbb{Q}} + \int_{\mathbb{R}} \sum_{j \in E \setminus \{\xi_t\}} \Delta_F(t, X_t, \xi_t, j) I_{\{z \in \Delta(\xi_t, j)\}} M^{\mathbb{Q}}(dt, dz), \tag{2.15}$$

where we have defined

$$\eta(t, x, i) = b(t, x, i)\partial_x F_i(t, x), \tag{2.16}$$

$$\Delta_F(t, x, i, j) = F_j(t, x) - F_i(t, x), \tag{2.17}$$

for $i, j \in E$. In particular, $\Delta_F(t, x, i, i) = 0$ by definition. We note that F_t is a $\mathbb{Q}$-martingale. Applying (2.13), the futures price F_t admits the $\mathbb{P}$-dynamics:

$$\begin{aligned} dF_t = &\left(\eta(t, X_t, \xi_t)\zeta(\xi_t) + \sum_{j \in E \setminus \{\xi_t\}} (q(\xi_t, j) - \widetilde{q}(\xi_t, j))\Delta_F(t, X_t, \xi_t, j) \right) dt \\ &+ \eta(t, X_t, \xi_t)dZ_t^{\mathbb{P}} + \int_{\mathbb{R}} \sum_{j \in E \setminus \{\xi_t\}} \Delta_F(t, X_t, \xi_t, j) I_{\{z \in \Delta(\xi_t, j)\}} M^{\mathbb{P}}(dt, dz). \end{aligned} \tag{2.18}$$

A key feature of this regime-switching framework is that the futures price process is a jump-diffusion even though the spot price process has continuous paths. The jumps in the futures prices will have direct impact on the strategies in dynamic futures portfolio.

2.3 Futures Portfolio Optimization

We now consider the problem of dynamic trading futures contracts. Consider M futures $\boldsymbol{F} = (F^{(1)}, \ldots, F^{(M)})$ written on the same asset S with different maturities, denoted by $T_1 < T_2 < \ldots < T_M$ without loss of generality. We define $M \times M$ *coefficient matrix* by

$$\boldsymbol{\Gamma}(t,x,i) = \begin{bmatrix} \eta^{(1)}(t,x,i) & \eta^{(2)}(t,x,i) & \cdots & \eta^{(M)}(t,x,i) \\ \Delta_F^{(1)}(t,x,i,1) & \Delta_F^{(2)}(t,x,i,1) & \cdots & \Delta_F^{(M)}(t,x,i,1) \\ \vdots & \vdots & \vdots & \vdots \\ \Delta_F^{(1)}(t,x,i,i-1) & \Delta_F^{(2)}(t,x,i,i-1) & \cdots & \Delta_F^{(M)}(t,x,i,i-1) \\ \Delta_F^{(1)}(t,x,i,i+1) & \Delta_F^{(2)}(t,x,i,i+1) & \cdots & \Delta_F^{(M)}(t,x,i,i+1) \\ \vdots & \vdots & \ddots & \vdots \\ \Delta_F^{(1)}(t,x,i,M) & \Delta_F^{(2)}(t,x,i,M) & \cdots & \Delta_F^{(M)}(t,x,i,M) \end{bmatrix}. \tag{2.19}$$

The intuition here is that the coefficient matrix gives a link between the traded futures and sources of randomness:

$$\begin{bmatrix} dF_t^{(1)} \\ dF_t^{(2)} \\ \cdots \\ dF_t^{(M)} \end{bmatrix} \longleftrightarrow \begin{bmatrix} dZ_t^{\mathbb{Q}} \\ \int_{\mathbb{R}} I_{\{z \in \Delta(\xi_t, j)\}} M^{\mathbb{Q}}(dt, dz) \\ \cdots \\ \int_{\mathbb{R}} I_{\{z \in \Delta(\xi_t, \xi_t - 1)\}} M^{\mathbb{Q}}(dt, dz) \\ \int_{\mathbb{R}} I_{\{z \in \Delta(\xi_t, \xi_t + 1)\}} M^{\mathbb{Q}}(dt, dz) \\ \cdots \\ \int_{\mathbb{R}} I_{\{z \in \Delta(\xi_t, M)\}} M^{\mathbb{Q}}(dt, dz) \end{bmatrix}.$$

It follows from (2.15) that if this $M \times M$ matrix $\boldsymbol{\Gamma}$ is invertible, then it is sufficient to these M futures to fully replicate any other futures on S with a different maturity, up to the shortest maturity. To see this, for a futures with an arbitrary maturity T, its price is connected with

the prices of the M futures as follows:

$$dF_t = \begin{bmatrix} dF_t^{(1)} & dF_t^{(2)} & \cdots & dF_t^{(M)} \end{bmatrix} \mathbf{\Gamma}(t, X_t, \xi_t)^{-1} \begin{bmatrix} \eta(t, X_t, \xi_t) \\ \Delta_F(t, X_t, \xi_t, 1) \\ \vdots \\ \Delta_F(t, X_t, \xi_t, \xi_t - 1) \\ \Delta_F(t, X_t, \xi_t, \xi_t + 1) \\ \vdots \\ \Delta_F(t, X_t, \xi_t, M) \end{bmatrix},$$

for $0 \leq t \leq T \wedge T_1$. In other words, the T-futures is redundant in this market with M regimes.

2.3.1 Utility Maximization

We consider a portfolio of M futures with different maturities $T_1 < T_2 < \ldots < T_M$. We assume that these futures are not redundant, and the interest rate is zero. We fix the trading horizon $\widetilde{T}$, which must not exceed the shortest maturities of the futures in the portfolio. Hence, we require that $\widetilde{T} \leq T_1$.

Like (1.27) in Chapter 1, we let strategy $\boldsymbol{\pi}_t = \left(\pi_t^{(1)}, \cdots, \pi_t^{(M)}\right)^\top$, where the element $\pi_t^{(k)}$ denotes the amount of money invested in k-th futures contract. Then, the wealth process is given by

$$dW_t^{\varpi} = \sum_{k=1}^{M} \pi_t^{(k)} \frac{dF_t^{(k)}}{F_t^{(k)}} \tag{2.20}$$

$$= \sum_{k=1}^{M} \varpi_t^{(k)} \, dF_t^{(k)}, \tag{2.21}$$

where $\varpi_t^{(k)} = \pi_t^{(k)} / F_t^{(k)}$ represents the units of futures $F^{(k)}$ in the portfolio.

We now reorganize terms in wealth process (2.21). To that end, we define the transformed

strategies by

$$\widetilde{\varpi}_t^{(0)} = \sum_{k=1}^{M} \varpi_t^{(k)} \eta^{(k)}(t, X_t, \xi_t), \tag{2.22}$$

$$\widetilde{\varpi}_t^{(j)} = \sum_{k=1}^{M} \varpi_t^{(k)} \Delta_F^{(k)}(t, X_t, \xi_t, j), \quad \text{for} \quad j \in E. \tag{2.23}$$

In particular, since $\Delta_F^{(k)}(t, x, i, i) = 0$, for $\forall k = 1, \ldots, M$ and $\forall i \in E$, according to (2.17), it follows that

$$\widetilde{\varpi}_t^{(\xi_t)} = \sum_{k=1}^{M} \varpi_t^{(k)} \Delta_F^{(k)}(t, X_t, \xi_t, \xi_t) = 0.$$

In matrix form, we have

$$\widetilde{\boldsymbol{\varpi}}_{\boldsymbol{t}} = \mathbf{\Gamma}(t, X_t, \xi_t) \boldsymbol{\varpi}_{\boldsymbol{t}}, \tag{2.24}$$

where $\widetilde{\boldsymbol{\varpi}}_{\boldsymbol{t}} = (\widetilde{\varpi}_t^{(0)}, \widetilde{\varpi}_t^{(1)}, \cdots, \widetilde{\varpi}_t^{(\xi_t - 1)}, \widetilde{\varpi}_t^{(\xi_t + 1)}, \cdots, \widetilde{\varpi}_t^{(M)})^\top$. Applying (2.15), (2.22), and (2.23) to (2.21), the wealth process becomes

$$\begin{aligned} dW_t^{\varpi} = & \left(\zeta(\xi_t) \widetilde{\varpi}_t^{(0)} + \sum_{j \in E \setminus \{\xi_t\}} (q(\xi_t, j) - \widetilde{q}(\xi_t, j)) \widetilde{\varpi}_t^{(j)} \right) dt \\ & + \widetilde{\varpi}_t^{(0)} dZ_t^{\mathbb{P}} + \int_{\mathbb{R}} \sum_{j \in E \setminus \{\xi_t\}} \widetilde{\varpi}_t^{(j)} I_{\{z \in \Delta(\xi_t, j)\}} M^{\mathbb{P}}(dt, dz). \end{aligned} \tag{2.25}$$

Notice that the wealth process is subject to jumps whenever the market regime switches states.

We consider a utility maximization approach to determine the optimal futures trading strategy. The investor seeks to maximize the expected utility by dynamically trading the futures continuously over time. We assume the associated coefficient matrix $\mathbf{\Gamma}(t, X_t, \xi_t)$ be invertible, and it would act as a bijection mapping between $\boldsymbol{\varpi}_{\boldsymbol{t}}$ and $\widetilde{\boldsymbol{\varpi}}_{\boldsymbol{t}}$. This allows us to solve the portfolio optimization problem by maximizing over $\widetilde{\boldsymbol{\varpi}}_{\boldsymbol{t}}$. Notice the wealth process (2.25) does not explicitly depend on X_t. The investor solves the following utility maximization problem

$$u_i(t, w) = \sup_{\widetilde{\boldsymbol{\varpi}}} I\!E^{\mathbb{P}} \big[U(W_T^{\boldsymbol{\varpi}}) | W_t = w, \xi_t = i \big], \tag{2.26}$$

where $U(w) = -e^{-\gamma w}$ is exponential utility function with a constant risk aversion parameter $\gamma > 0$.

The investor's value function $u_i(t, w)$ is determined from a system of Hamilton-Jacobi-Bellman (HJB) equations. Precisely, we have

$$\begin{aligned} &\partial_t u_i + \max_{\widetilde{\boldsymbol{\varpi}}_t} \left\{ \left(\zeta_i \widetilde{\varpi}_t^{(0)} - \sum_{j \in E \setminus \{i\}} \widetilde{q}_{ij} \widetilde{\varpi}_t^{(j)} \right) \partial_w u_i + \frac{(\widetilde{\varpi}_t^{(0)})^2}{2} \partial_{ww} u_i \right. \\ &\left. + \sum_{j \in E \setminus \{i\}} q_{ij} \left(u_j(t, w + \widetilde{\varpi}_t^{(j)}) - u_i(t, w) \right) \right\} = 0, \end{aligned} \tag{2.27}$$

for $i \in E$ and $t \in [0, \widetilde{T})$. The terminal condition is $u_i(\widetilde{T}, w) = -e^{-\gamma w}$, for $i \in E$. We have used the shorthand notations: $\widetilde{q}_{ij} \equiv \widetilde{q}(i, j)$, $q_{ij} \equiv q(i, j)$ and $\zeta_i \equiv \zeta(i)$.

Performing the optimization in the HJB equation (2.27) and assuming that $\partial_{ww} u_i \leq 0$ (which will be verified later), we obtain the first-order conditions for the optimal strategy:

$$\begin{cases} \widetilde{\varpi}^{(0)*}(t, w, i) = -\zeta_i \dfrac{\partial_w u_i(t, w)}{\partial_{ww} u_i(t, w)}, \\ \partial_w u_j(t, w + \widetilde{\varpi}^{(j)*}(t, w, i)) = \dfrac{\widetilde{q}_{ij}}{q_{ij}} \partial_w u_i(t, w), \end{cases} \tag{2.28}$$

for $i \in E$ and $j \in E \setminus \{i\}$. Plugging this into (2.27), the HJB equations become

$$\partial_t u_i - \frac{(\zeta_i \partial_w u_i)^2}{2 \partial_{ww} u_i} - \sum_{j \in E \setminus \{i\}} \widetilde{q}_{ij} \widetilde{\varpi}_i^{(j)*} \partial_w u_i + \sum_{j \in E \setminus \{i\}} q_{ij} \left(u_j(t, w + \widetilde{\varpi}_i^{(j)*}) - u_i(t, w) \right) = 0, \tag{2.29}$$

for $i \in E$, where we have denoted $\widetilde{\varpi}_i^{(j)*} \equiv \widetilde{\varpi}^{(j)*}(t, w, i)$.

We now consider the transformation for the value function

$$u_i(t, w) = -e^{-\gamma w + \varphi_i(t)}. \tag{2.30}$$

Applying this to the first-order conditions (2.28) and HJB equation (2.29), the optimal strategy can be written explicitly

$$\begin{cases} \widetilde{\varpi}_i^{(0)*} = \dfrac{\zeta_i}{\gamma}, \\ \widetilde{\varpi}_i^{(j)*}(t) = -\dfrac{1}{\gamma} \left(\log \dfrac{\widetilde{q}_{ij}}{q_{ij}} + \varphi_i(t) - \varphi_j(t) \right), \end{cases} \tag{2.31}$$

for $i \in E$ and $j \in E \setminus \{i\}$. We note that both $\widetilde{\varpi}_i^{(0)*}$ and $\widetilde{\varpi}_i^{(j)*}(t)$ do not depend on wealth w.

Substituting the transformation (2.30) and optimal strategy (2.31) into (2.29), we obtain a system of ODEs for $\varphi_i(t)$:

$$\varphi_i^\top(t) - \sum_{j \in E\setminus\{i\}} \widetilde{q}_{ij}\Big(\varphi_i(t) - \varphi_j(t)\Big) - \alpha_i = 0, \tag{2.32}$$

where

$$\alpha_i = \frac{\zeta_i^2}{2} + \sum_{j \in E\setminus\{i\}} \widetilde{q}_{ij} \log \frac{\widetilde{q}_{ij}}{q_{ij}} - \widetilde{q}_{ij} + q_{ij}, \tag{2.33}$$

for $i \in E$ and $t \in [0, \widetilde{T})$. The terminal condition is $\varphi_i(\widetilde{T}) = 0$ for $i \in E$. This ODE system admits the solution

$$\boldsymbol{\varphi}(t) = -\int_t^{\widetilde{T}} \exp\Big(\widetilde{\boldsymbol{Q}}(\widetilde{T} - s)\Big)\, \boldsymbol{\alpha}\, ds\,, \tag{2.34}$$

where $\widetilde{\boldsymbol{Q}}$ is the generator matrix for ξ_t under measure $\mathbb{Q}$, $\boldsymbol{\varphi}(t) = (\varphi_1(t), \cdots, \varphi_M(t))^\top$ and $\boldsymbol{\alpha} = (\alpha_1(t), \cdots, \alpha_M(t))^\top$.

With this solution, along with transformation (2.30), direction calculations now show that the second-order condition $\partial_{ww} u_i = \gamma^2 u_i \leq 0$ is satisfied. Therefore, the solution to the HJB system (2.27) is indeed given by (2.30). In addition, the optimal strategy $\boldsymbol{\varpi}^*$ can be recovered from (2.24).

The ODE system (2.32) implies a probabilistic representation for $\varphi_i(t)$, given by

$$\varphi_i(t) = I\!E^{\mathbb{Q}}\bigg[-\int_t^{\widetilde{T}} \alpha(\xi_s) ds \bigg| \xi_t = i \bigg], \tag{2.35}$$

where $\alpha(i) = \alpha_i$ is given by (2.33). Given that $x \log x - x + 1 \geq 0$, $\forall x > 0$, it follows that $\alpha(i) \geq 0$ and $\varphi_i(t) \leq 0$. Intuitively, $\exp(\varphi_i(t))$ acts like a discounting factor that depends directly on the regime-switching market price of risk. Since the exponential utility is negative and $\varphi_i(t) \leq 0$, this implies that $u_i(t, w) \geq -e^{-\gamma w}$, which means that the investor achieves a higher expected utility by dynamically trading the futures, as compared to only holding the same constant cash amount w.

Next, by putting the optimal strategy $\widetilde{\varpi}_i^{(0)*}$ and $\widetilde{\varpi}_i^{(j)*}(t)$ in (2.25), we obtain the optimal wealth process

$$\begin{aligned} dW_t^* &= \frac{1}{\gamma}\Bigg(\zeta^2(\xi_t) - \sum_{j\in E\setminus\{\xi_t\}}\Big(q(\xi_t,j)-\widetilde{q}(\xi_t,j)\Big)\Bigg(\log\frac{\widetilde{q}(\xi_t,j)}{q(\xi_t,j)}+\varphi(t,\xi_t)-\varphi(t,j)\Bigg)\Bigg)dt \\ &+ \frac{\zeta(\xi_t)}{\gamma}dZ_t^{\mathbb{P}} - \frac{1}{\gamma}\int_{\mathbb{R}}\sum_{j\in E\setminus\{\xi_t\}}\Bigg(\log\frac{\widetilde{q}(\xi_t,j)}{q(\xi_t,j)}+\varphi(t,\xi_t)-\varphi(t,j)\Bigg)I_{\{z\in\Delta(\xi_t,j)\}}M^{\mathbb{P}}(dt,dz), \end{aligned} \tag{2.36}$$

where we have denoted $\varphi(t,i)=\varphi_i(t)$, for $i\in E$. The coefficients of the optimal wealth process in (2.36) do not depend on the spot price X_t but are modulated by the continuous-time Markov chain ξ_t. The optimal wealth is connected with the risk-neutral pricing measure and futures prices through the market price of risk $\zeta(\xi_t)$. The investor's risk aversion parameter γ also affects the optimal wealth. In particular, a higher γ will reduce the magnitude of the drift and volatility of the optimal wealth process.

Remark 2. *When $M=2$, the ODE system* (2.32) *admits an explicit solution*

$$\varphi_i(t) = -\frac{1}{\widetilde{\lambda}_1+\widetilde{\lambda}_2}\Bigg((\widetilde{\lambda}_2\alpha_1+\widetilde{\lambda}_1\alpha_2)(\widetilde{T}-t)+\widetilde{\lambda}_i(\alpha_i-\alpha_j)\frac{1-e^{-(\widetilde{\lambda}_1+\widetilde{\lambda}_2)(\widetilde{T}-t)}}{\widetilde{\lambda}_1+\widetilde{\lambda}_2}\Bigg), \tag{2.37}$$

where $\widetilde{\lambda}_i=\widetilde{q}_{ij}$, for $(i,j)\in\{(1,2),(2,1)\}$ and $t\in[0,\widetilde{T}]$. In turn, the optimal strategy is given by

$$\begin{aligned} &\begin{bmatrix} \varpi_i^{(1)*}(t,x) \\ \varpi_i^{(2)*}(t,x) \end{bmatrix} = \\ &-\frac{1}{\gamma b(t,x,i)((F_j^{(2)}(t,x)-F_i^{(2)}(t,x))\partial_x F_i^{(1)}(t,x)-(F_j^{(1)}(t,x)-F_i^{(1)}(t,x))\partial_x F_i^{(2)}(t,x))} \\ &\begin{bmatrix} -\zeta_i(F_j^{(2)}(t,x)-F_i^{(2)}(t,x))-b(t,x,i)\partial_x F_j^{(2)}(t,x)(\log\frac{\widetilde{\lambda}_i}{\lambda_i}+\varphi_i(t)-\varphi_j(t)) \\ \zeta_i(F_j^{(1)}(t,x)-F_i^{(1)}(t,x))+b(t,x,i)\partial_x F_j^{(1)}(t,x)(\log\frac{\widetilde{\lambda}_i}{\lambda_i}+\varphi_i(t)-\varphi_j(t)) \end{bmatrix}, \end{aligned} \tag{2.38}$$

where $\lambda_i=q_{ij}$, for $(i,j)\in\{(1,2),(2,1)\}$ and $(t,x)\in[0,\widetilde{T}]\times\mathbb{R}$.

2.3.2 Certainty Equivalent

In order to quantify the value of trading futures to the investor, we define the investor's certainty equivalent associated with the utility maximization problem. The certainty equivalent

is the guaranteed cash amount that would yield the same utility as that from dynamically trading futures according to (2.26). This amounts to applying the inverse of the utility function to the value function in (2.30), that is,

$$CE_i(t,w) := U^{-1}(u_i(t,w)) = w - \frac{\varphi_i(t)}{\gamma}. \tag{2.39}$$

Therefore, the certainty equivalent is the sum of the investor's wealth w and a time-dependent component $-\frac{\varphi_i(t)}{\gamma}$. From the probabilistic representation in (2.35), we know that $\varphi_i(t)$ is negative. The certainty equivalent is also inversely proportional to the risk aversion parameter γ, which means that a more risk averse investor has a lower certainty equivalent, valuing the futures trading opportunity less.

Under our regime-switching framework, the certainty equivalent is the same across different underlying models as long as the market prices of risk stay the same. Therefore, without picking a specific model, we can still compute the certainty equivalent. Figure 2.1 illustrates the certainty equivalents under two risk aversion levels under two regimes in a two-regime market. Under each regime, the less risk averse investor ($\gamma = 0.5$) has a higher certainty equivalent than the more risk averse investor ($\gamma = 2$). According to the parameters for the two regimes, Regime 2 has a higher market price of risk than regime 1, which explains that the investor's certainty equivalent is higher in regime 2 than in regime 1. All else being equal, the certainty equivalent is higher when there is more time to trade. Hence, as the trading horizon reduces to zero, the certainty equivalent converges to the initial wealth w, which is set to be 1 in this example. This means that the second term in (2.39) converges to zero since $\varphi_i(t) \to 0$ as $t \to \widetilde{T}$.

In the next two sections, we consider two model specifications and provide numerical examples.

2.4 Regime-Switching Geometric Brownian Motion

Suppose the log-price of the underlying asset follows the SDE

$$dX_t = \mu(\xi_t)dt + \sigma(\xi_t)dZ_t^{\mathbb{Q}}, \tag{2.40}$$

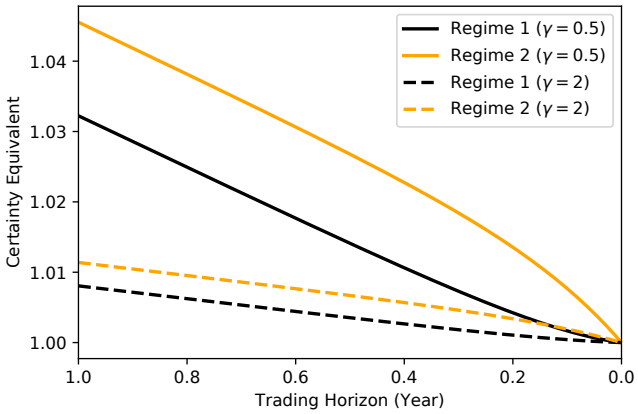

Figure 2.1: The certainty equivalents corresponding to two different risk aversion levels in a two-regime market. They are plotted as functions of the trading horizon, for $\gamma = 0.5$ (solid lines) and $\gamma = 2$ (dashed lines) in regime 1 (dark color) and regime 2 (light color). Common parameters are $\widetilde{q}_{12} = q_{12} = 0.8$, $\widetilde{q}_{21} = q_{21} = 0.6$, $w = 1$, $\zeta_1 = 0.1$ and $\zeta_2 = 0.3$.

under the risk-neutral measure $\mathbb{Q}$. We call this model the regime-switching Geometric Brownian Motion (RS-GBM) because without ξ the spot price S is simply a GBM. This model belongs to our regime-switching framework discussed in the previous section. Indeed, this amounts to setting the coefficients in SDE (2.6) to be

$$\widetilde{a}(t, X_t, \xi_t) = \mu(\xi_t), \quad \text{and} \quad b(t, X_t, \xi_t) = \sigma(\xi_t). \tag{2.41}$$

Substituting (2.41) into (2.8), we obtain the PDE system for the futures price function under this model. Precisely, for $i \in E$, we have

$$\partial_t F_i + \mu_i \partial_x F_i + \frac{\sigma_i^2}{2} \partial_{xx} F_i + \sum_{j \in E \setminus \{i\}} \widetilde{q}(i,j)(F_j - F_i) = 0, \tag{2.42}$$

with $\mu_i = \mu(i)$ and $\sigma_i = \sigma(i)$. The terminal condition is $F_i(T, x) = e^x$, $x \in \mathbb{R}$.

Under this model, the futures price admits the separation of variables:

$$F_i(t, x) = e^x \, g_i(t), \tag{2.43}$$

where $(g_i(t))_{i=1,\dots,M}$ solve the system of ODEs:

$$\frac{dg_i(t)}{dt} + (\mu_i + \frac{\sigma_i^2}{2})g_i(t) + \sum_{j\in E\setminus\{i\}} \widetilde{q}(i,j)(g_j(t) - g_i(t)) = 0, \tag{2.44}$$

for $t \in [0,T)$, with the terminal condition $g_i(T) = 1$, for $i = 1,\dots,M$. Defining $\boldsymbol{g}(t) = (g_1(t),\dots,g_M(t))^\top$, we can write the solution as

$$\boldsymbol{g}(t) = \exp\Big((\boldsymbol{G} + \widetilde{\boldsymbol{Q}})(T-t)\Big)\mathbf{1}, \tag{2.45}$$

where $\widetilde{\boldsymbol{Q}}$ is the generator matrix under the measure $\mathbb{Q}$ and

$$\boldsymbol{G} = \mathrm{diag}(\frac{2\mu_1+\sigma_1^2}{2}, \frac{2\mu_2+\sigma_2^2}{2}, \dots, \frac{2\mu_M+\sigma_M^2}{2}). \tag{2.46}$$

In addition, the ODE system (2.44) implies a probabilistic representation for $g_i(t)$:

$$g_i(t) = \mathbb{E}^{\mathbb{Q}}\left[\exp\left(\int_t^T \mu(\xi_s) + \frac{\sigma^2(\xi_s)}{2}ds\right)\Big|\xi_t = i\right]. \tag{2.47}$$

To sum up, the futures price in regime i is given by

$$F_i(t,x) = \exp(x)\Big(\exp\Big((\boldsymbol{G} + \widetilde{\boldsymbol{Q}})(T-t)\Big)\mathbf{1}\Big)_i, \tag{2.48}$$

where the subscript i denotes the ith entry of the vector.

In turn, using (2.15), the futures price satisfies the SDE

$$\begin{aligned} dF_t = &\Big(\sigma(\xi_t)F(t,X_t,\xi_t)\zeta(\xi_t) + \sum_{j\in E\setminus\{\xi_t\}}(q(\xi_t,j) - \widetilde{q}(\xi_t,j))\Big(F(t,X_t,j) - F(t,X_t,\xi_t)\Big)\Big)dt \\ &+ \sigma(\xi_t)F(t,X_t,\xi_t)dZ_t^{\mathbb{P}} + \int_{\mathbb{R}}\sum_{j\in E\setminus\{\xi_t\}}\Big(F(t,X_t,j) - F(t,X_t,\xi_t)\Big)I_{\{z\in\Delta(\xi_t,j)\}}M^{\mathbb{P}}(dt,dz). \end{aligned} \tag{2.49}$$

Next, we consider a portfolio of futures with M different maturities $T_1 < T_2 < \cdots < T_M$. If the associated coefficient matrix $\boldsymbol{\Gamma}$ is invertible, we can apply results in the Section 2.3. To that end, we have following proposition for coefficient matrix $\boldsymbol{\Gamma}$.

Proposition 3. *If $\mathbf{\Gamma}(t_0, x, i)$ is invertible for some specific time $t_0 \leq T_1$, then $\mathbf{\Gamma}(t, x, i)$ is invertible for any time $t \leq T_1$.*

Proof. By (2.19), the coefficient matrix is given by

$$\mathbf{\Gamma}(t,x,i) = e^x \begin{bmatrix} \sigma_i g_i^{(1)}(t) & \sigma_i g_i^{(2)}(t) & \cdots & \sigma_i g_i^{(M)}(t) \\ g_1^{(1)}(t) - g_i^{(1)}(t) & g_1^{(2)}(t) - g_i^{(2)}(t) & \cdots & g_1^{(M)}(t) - g_i^{(M)}(t) \\ \vdots & \vdots & \vdots & \vdots \\ g_{i-1}^{(1)}(t) - g_i^{(1)}(t) & g_{i-1}^{(2)}(t) - g_i^{(2)}(t) & \cdots & g_{i-1}^{(M)}(t) - g_i^{(M)}(t) \\ g_{i+1}^{(1)}(t) - g_i^{(1)}(t) & g_{i+1}^{(2)}(t) - g_i^{(2)}(t) & \cdots & g_{i+1}^{(M)}(t) - g_i^{(M)}(t) \\ \vdots & \vdots & \ddots & \vdots \\ g_M^{(1)}(t) - g_i^{(1)}(t) & g_M^{(2)}(t) - g_i^{(2)}(t) & \cdots & g_M^{(M)}(t) - g_i^{(M)}(t) \end{bmatrix}, \tag{2.50}$$

for $i \in E$. The determinant of coefficient matrix $\mathbf{\Gamma}$ is denoted by

$$\Phi_i(t,x) = \det \mathbf{\Gamma}(t,x,i), \qquad i \in E. \tag{2.51}$$

We define the matrix $\widetilde{\mathbf{\Gamma}}$ by adding $1/\sigma_i$ of the first row to other rows in matrix $\mathbf{\Gamma}$. Then, we define the matrix $\boldsymbol{H_k}$ by taking t-derivative in the k-th row of matrix $\widetilde{\mathbf{\Gamma}}$. For example,

$$\boldsymbol{H_1}(t,x,i) = e^x \begin{bmatrix} \sigma_i \frac{d}{dt} g_i^{(1)}(t) & \sigma_i \frac{d}{dt} g_i^{(2)}(t) & \cdots & \sigma_i \frac{d}{dt} g_i^{(M)}(t) \\ g_1^{(1)}(t) & g_1^{(2)}(t) & \cdots & g_1^{(M)}(t) \\ \vdots & \vdots & \vdots & \vdots \\ g_{i-1}^{(1)}(t) & g_{i-1}^{(2)}(t) & \cdots & g_{i-1}^{(M)}(t) \\ g_{i+1}^{(1)}(t) & g_{i+1}^{(2)}(t) & \cdots & g_{i+1}^{(M)}(t) \\ \vdots & \vdots & \ddots & \vdots \\ g_M^{(1)}(t) & g_M^{(2)}(t) & \cdots & g_M^{(M)}(t) \end{bmatrix}. \tag{2.52}$$

Then, holding the log-price x fixed, we differentiate to get

$$\frac{d}{dt}\Phi_i(t,x) = \frac{d}{dt} \det \widetilde{\mathbf{\Gamma}}(t,x,i) = \sum_{k=1}^{M} \det \boldsymbol{H_k}(t,x,i). \tag{2.53}$$

Applying (2.44) and $\sum_{j \in E \setminus \{i\}} \widetilde{q}(i,j) = -\widetilde{q}(i,i)$, we get

$$\sum_{k=1}^{M} \det \boldsymbol{H_k}(t,x,i) = \sum_{k=1}^{M} - \left(\mu_k + \frac{\sigma_k^2}{2} + \widetilde{q}(k,k) \right) \Phi_i(t,x), \tag{2.54}$$

for $i \in E$.

Combining (2.53) and (2.54), we have

$$\frac{d}{dt}\Phi_i(t,x) + \sum_{k=1}^{M}\left(\mu_k + \frac{\sigma_k^2}{2} + \widetilde{q}(k,k)\right)\Phi_i(t,x) = 0. \tag{2.55}$$

Then, for any $t_0, t \le T_1$, $\Phi_i(t,x)$ satisfies

$$\Phi_i(t,x) = \exp\left(-\sum_{k=1}^{M}\left(\mu_k + \frac{\sigma_k^2}{2} + \widetilde{q}(k,k)\right)(t-t_0)\right)\Phi_i(t_0,x). \tag{2.56}$$

Thus, if $\mathbf{\Gamma}(t_0,x,i)$ is invertible for some specific time $t_0 \le T_1$, then $\mathbf{\Gamma}(t,x,i)$ is invertible for any time $t \le T_1$. □

Example 1. *Market with Two Regimes Assume a market with two regimes, i.e.* $E = \{1,2\}$. *The coefficient matrix* $\mathbf{\Gamma}$ *for futures pair* $(F^{(1)}, F^{(2)})$ *is given explicitly by*

$$\mathbf{\Gamma}(t,x,i) = e^x \begin{bmatrix} \sigma_i g_i^{(1)}(t) & \sigma_i g_i^{(2)}(t) \\ g_j^{(1)}(t) - g_i^{(1)}(t) & g_j^{(2)}(t) - g_i^{(2)}(t) \end{bmatrix}, \tag{2.57}$$

for $(i,j) \in \{(1,2),(2,1)\}$. *Then, the matrix determinant* $\Phi_i(t,x)$ *is also explicit:*

$$\Phi_i(t,x) = e^{2x}\sigma_i(g_i^{(1)}(t)g_j^{(2)}(t) - g_j^{(1)}(t)g_i^{(2)}(t)), \tag{2.58}$$

for $(i,j) \in \{(1,2),(2,1)\}$.

Applying Proposition 3, the coefficient matrix $\mathbf{\Gamma}$ *is invertible for any time* $t \le T_2$, *if and only if* $\Phi_i(T_2,x) = e^{2x}\sigma_i(g_j^{(2)}(T_2) - g_i^{(2)}(T_2)) \neq 0$, *which is equivalent to* $\mu_1 + \sigma_1^2/2 \neq \mu_2 + \sigma_2^2/2$ *accorinding to the probabilistic representation* (2.47).

If $\mu_1 + \sigma_1^2/2 \neq \mu_2 + \sigma_2^2/2$, *we can apply the results in Section 2.3. The value function* $u_i(t,w)$ *satisfies*

$$u_i(t,w) = -e^{-\gamma w + \varphi_i(t)}, \tag{2.59}$$

where $\varphi_i(t)$ *is given by* (2.37). *Applying* (2.38), *we immediately obtain the optimal strategy*

$$\begin{aligned}\begin{bmatrix} \varpi_i^{(1)*}(t,x) \\ \varpi_i^{(2)*}(t,x) \end{bmatrix} = &-\frac{e^{-x}}{\gamma\sigma_i(g_i^{(1)}(t)g_j^{(2)}(t) - g_j^{(1)}(t)g_i^{(2)}(t))} \\ &\begin{bmatrix} -\zeta_i(g_j^{(2)}(t) - g_i^{(2)}(t)) - \sigma_i g_i^{(2)}(t)\left(\log\frac{\widetilde{\lambda}_i}{\lambda_i} + \varphi_i(t) - \varphi_j(t)\right) \\ \zeta_i(g_j^{(1)}(t) - g_i^{(1)}(t)) + \sigma_i g_i^{(1)}(t)\left(\log\frac{\widetilde{\lambda}_i}{\lambda_i} + \varphi_i(t) - \varphi_j(t)\right) \end{bmatrix},\end{aligned} \tag{2.60}$$

for $(i,j) \in \{(1,2),(2,1)\}$ *and* $(t,x) \in [0,\widetilde{T}] \times \mathbb{R}$.

If $\mu_1 + \sigma_1^2/2 = \mu_2 + \sigma_2^2/2$*, the futures prices will be the same in two states according to* (2.47)*. Therefore, the futures price SDE becomes*

$$dF_t = \sigma(\xi_t)F(t, X_t, \xi_t)\zeta(\xi_t)dt + \sigma(\xi_t)F(t, X_t, \xi_t)dZ_t^{\mathbb{P}}, \tag{2.61}$$

which, in contrast to (2.49)*, has continuous paths.*

To illustrate the futures trading problem under this model, we simulate the sample paths for spot price, futures price, optimal investment, and optimal wealth process. The regime switching between two states, with transition probabilities $q_{12} = 2$ and $q_{21} = 4$ which are entries of generator matrix $\boldsymbol{Q}$. The trading horizon $\widetilde{T} = 0.6$ which is no greater than the maturity of the futures contract $T_1 = 0.6$ and $T_2 = 0.8$. All parameters are summarized in the Table 2.1.

$\widetilde{q}_{12} = q_{12}$	$\widetilde{q}_{21} = q_{21}$	$\zeta(1)$	$\zeta(2)$	γ	$\widetilde{T}$
2	4	0.1	0.3	1	0.6
μ_1	μ_2	σ_1	σ_2	T_1	T_2
-0.2	0.2	0.2	0.3	0.6	0.8

Table 2.1: Parameters for the RS-GBM model for Figures 2.2–2.5.

As shown in Figure 2.2, the market starts in regime 2, then switches to regime 1 at time t_1 before returning to regime 2 at time t_2. Under RS-GBM model, the futures price (see (2.48)) tends to amplify the spot price. Thus, the futures price is volatile relative to the spot price. Moreover, each regime switch can cause an instant jump in the futures price but not in the spot price. Since the trading horizon coincides with the maturity of the T_1-futures, the corresponding futures price converges to the spot price towards the end.

In Figure 2.3, we illustrate the sample paths of the optimal positions in the two futures over the trading horizon. As we can see, the optimal positions are of opposite signs, meaning

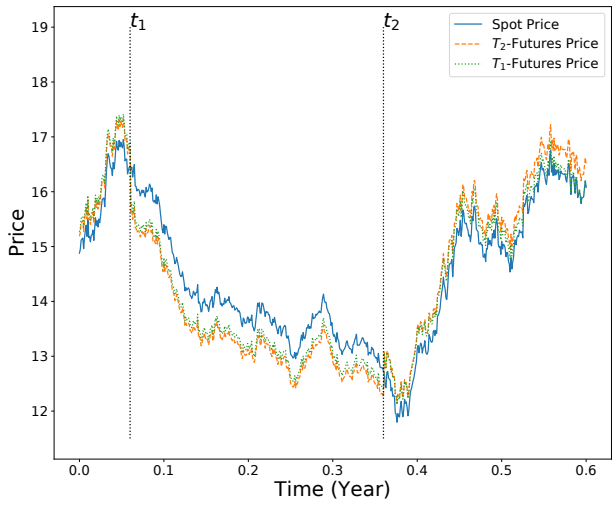

Figure 2.2: Sample paths of the spot price, T_1-futures price, and T_2-futures price over the trading horizon under the RS-GBM model. The market starts in regime 2, then switches to regime 1 at time t_1, before switching back to regime 2 at time t_2.

that the investor will go long on the T_1-Futures and short on the T_2-Futures. Long-short strategies are very common in futures trading, and they can help mitigate the effect of regime switching. As the market switches from regime 2 to regime 1 at time t_1, the magnitude of the futures position is reduced immediately. The investor then take larger long-short positions when the market returns to regime 2 from regime 1 at time t_2. According to the sample paths, the optimal positions tend to decay in time during each regime, meaning that the investor gradually reduces investments towards the end of the trading horizon.

Figure 2.4 shows the wealth process corresponding to the optimal trading strategy in Figure 2.3. The long-short strategy tends to reduce the shock in portfolio vlaue due to regime switching. Therefore, no sizable jumps in the wealth process are observed at the regime-swtiching times t_1 and t_2. As we can see, the wealth process decreases slightly in regime 1. This is intuitive since regime 1 has lower risk premium than in regime 2. The wealth increases sharply in regime 2 towards the end of the trading horizon, even though the

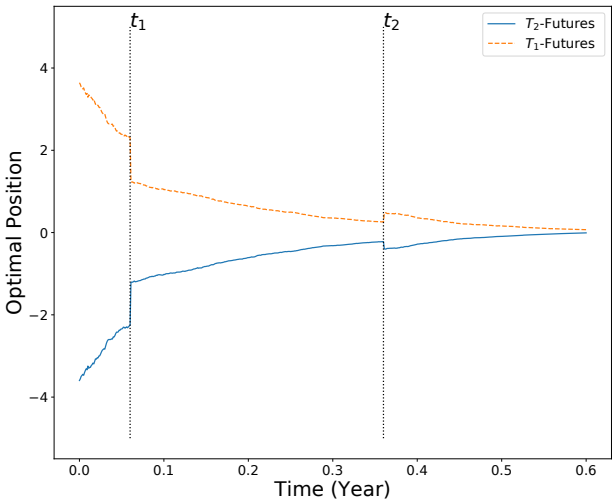

Figure 2.3: Sample paths of the optimal positions $(\varpi^{(1)}, \varpi^{(2)})$ in the T_1-futures and T_2-futures respectively under the RS-GBM model. The futures positions tend to decrease over time and approaches zero near the end of the trading horizon. Jumps in both positions occur at the regiem-switching times t_1 and t_2.

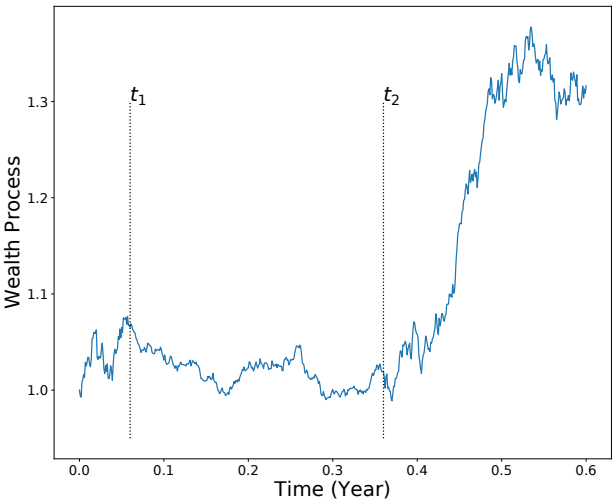

Figure 2.4: Sample path of the optimal wealth process over the trading horizon under the RS-GBM model.

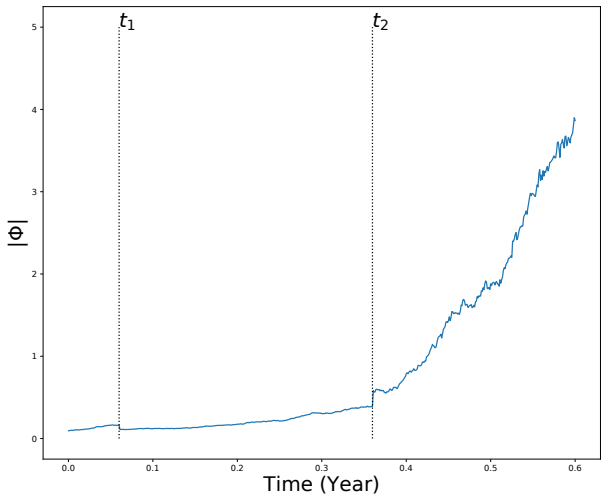

Figure 2.5: Sample path of the absolute value of the determinant Φ for the coefficient matrix Γ under the RS-GBM model.

positions are gradually reduced over time.

In Figure 2.5, we plot the sample path for the absolute value of coefficient matrix determinant $|\Phi|$ corresponding to the sample paths of the spot and futures prices. Recall from (2.56), $|\Phi|$ is exponentially increasing or decreasing overtime. Moreover, in our numerical settings, the term $\widetilde{q}(i,i) = -\widetilde{q}(i,j)$ dominates the term $\mu_i + \sigma_i^2/2$. Therefore, $|\Phi|$ appears to be exponentially increasing in time. Since $|\Phi|$ is not equal to 0, Γ is invertible and we are able to apply the results in the Section 2.3 for the RS-GBM model.

2.5 Regime-Switching Exponential Ornstein-Uhlenbeck Model

As is well known, the Exponential Ornstein-Uhlenbeck process and its variations are widely used to model commodity prices. We now consider the regime-switching Exponential Ornstein-Uhlenbeck (RS-XOU) model and illustrate the optimal trading strategies under this model. In the RS-XOU model, the log spot price evolves according to

$$dX_t = \kappa(\xi_t)(\theta(\xi_t) - X_t)dt + \sigma(\xi_t)dZ_t^{\mathbb{Q}}, \tag{2.62}$$

where $\kappa(\xi_t)$, $\theta(\xi_t)$ and $\sigma(\xi_t)$ are the functions of regimes. This amounts to setting $\widetilde{a}(t, X_t, \xi_t) = \kappa(\xi_t)(\theta(\xi_t) - X_t)$ and $b(t, X_t, \xi_t) = \sigma(\xi_t)$ in (2.6).

2.5.1 Futures Dynamics and Utility Maximization

The futures price function $F_i(t, x)$ satisfies PDE (2.8). Substituting (2.62) into (2.15), we obtain the $\mathbb{Q}$-dynamics for futures price F_t:

$$dF_t = \eta(t, X_t, \xi_t) dZ_t^{\mathbb{Q}} + \int_{\mathbb{R}} \sum_{j \in E \setminus \{\xi_t\}} \Big(F(t, X_t, j) - F(t, X_t, \xi_t) \Big) I_{\{z \in \Delta(\xi_t, j)\}} M^{\mathbb{Q}}(dt, dz), \tag{2.63}$$

where the volatility term is given by

$$\eta(t, x, i) = \sigma_i \partial_x F_i(t, x). \tag{2.64}$$

In addition, under the measure $\mathbb{P}$,

$$\begin{aligned} dF_t = &\Bigg(\zeta(\xi_t)\eta(t, X_t, \xi_t) + \sum_{j \in E \setminus \{\xi_t\}} (q(\xi_t, j) - \widetilde{q}(\xi_t, j)) \Big(F(t, X_t, j) - F(t, X_t, \xi_t) \Big) \Bigg) dt \\ &+ \eta(t, X_t, \xi_t) dZ_t^{\mathbb{P}} + \int_{\mathbb{R}} \sum_{j \in E \setminus \{\xi_t\}} \Big(F(t, X_t, j) - F(t, X_t, \xi_t) \Big) I_{\{z \in \Delta(\xi_t, j)\}} M^{\mathbb{P}}(dt, dz). \end{aligned} \tag{2.65}$$

Example 2. *Market with Two Regimes We consider a portfolio of futures with two different maturities T_1 and T_2 in a two-state market, i.e. $E = \{1, 2\}$. The associated coefficient matrix is given by*

$$\mathbf{\Gamma}(t, x, i) = \begin{bmatrix} \sigma_i \partial_x F_i^{(1)}(t, x) & \sigma_i \partial_x F_i^{(2)}(t, x) \\ F_j^{(1)}(t, x) - F_i^{(1)}(t, x) & F_j^{(2)}(t, x) - F_i^{(2)}(t, x) \end{bmatrix}, \tag{2.66}$$

for $(i, j) \in \{(1, 2), (2, 1)\}$. Moreover, we assume $\mathbf{\Gamma}(t, x, i)$ be invertible. Under this assumption, we can apply the result in Section 2.3. The value function $u_i(t, w) = -e^{-\gamma w + \varphi_i(t)}$, where $\varphi_i(t)$ is given by (2.37)*, holds.*

Applying (2.38)*, we immediately obtain the optimal strategy*

$$\begin{aligned}
&\begin{bmatrix} \varpi_i^{(1)*}(t,x) \\ \varpi_i^{(2)*}(t,x) \end{bmatrix} \\
&= -\frac{1}{\gamma\sigma_i((F_j^{(2)}(t,x)-F_i^{(2)}(t,x))\partial_x F_i^{(1)}(t,x)-(F_j^{(1)}(t,x)-F_i^{(1)}(t,x))\partial_x F_i^{(2)}(t,x))} \\
&\begin{bmatrix} -\zeta_i(F_j^{(2)}(t,x)-F_i^{(2)}(t,x))-\sigma_i\partial_x F_j^{(2)}(t,x)(\log\frac{\widetilde{\lambda}_i}{\lambda_i}+\varphi_i(t)-\varphi_j(t)) \\ \zeta_i(F_j^{(1)}(t,x)-F_i^{(1)}(t,x))+\sigma_i\partial_x F_j^{(1)}(t,x)(\log\frac{\widetilde{\lambda}_i}{\lambda_i}+\varphi_i(t)-\varphi_j(t)) \end{bmatrix},
\end{aligned} \tag{2.67}$$

for $(i,j)\in\{(1,2),(2,1)\}$ *and* $(t,x)\in[0,\widetilde{T}]\times\mathbb{R}$.

Remark 3. *If the speed of mean reversion is identical in all regimes, i.e.* $\kappa_i=\kappa\ \forall i$*, then the futures price admits the following form*

$$F_i(t,x)=\exp\left(e^{-\kappa(T-t)}x\right)h_i(t), \tag{2.68}$$

where $(h_i(t))_{i=1,\dots,M}$ *solves the ODE system*

$$\frac{h_i(t)}{dt}+\left(\kappa\theta_i e^{-\kappa(T-t)}+\frac{\sigma_i^2}{2}e^{-2\kappa(T-t)}\right)h_i(t)+\sum_{j\in E\setminus\{i\}}\widetilde{q}(i,j)(h_j(t)-h_i(t))=0, \tag{2.69}$$

with the terminal condition $h_i(T)=1$*, for* $i=1,\dots,M$.

The price formula (2.68) *means that* $\eta(t,x,i)=\sigma_i e^{-\kappa(T-t)}F_i(t,x)$ *in (2.15). As a result, the futures price satisfies the SDE*

$$\begin{aligned}
dF_t &= \sigma(\xi_t)e^{-\kappa(T-t)}\exp\left(e^{-\kappa(T-t)}X_t\right)h(t,\xi_t)dZ_t^{\mathbb{Q}} \\
&\quad+\exp\left(e^{-\kappa(T-t)}X_t\right)\int_{\mathbb{R}}\sum_{j\in E\setminus\{\xi_t\}}\Big(h(t,j)-h(t,\xi_t)\Big)I_{\{z\in\Delta(\xi_t,j)\}}M^{\mathbb{Q}}(dt,dz),
\end{aligned} \tag{2.70}$$

where we have denoted $h(t,i)\equiv h_i(t)$.

2.5.2 Numerical Implementation & Examples

We now discuss the numerical procedure to compute the futures price under the RS-XOU model in this section. We have computed and checked our prices using the finite difference method (FDM) and fast Fourier transform (FFT).

To apply the finite difference method, we first re-write futures price PDE (2.8) in terms of $s = e^x$ to get

$$\partial_t F_i + \left(\kappa_i(\theta_i - \ln s) + \frac{\sigma_i^2}{2}\right) s\partial_s F_i + \frac{\sigma_i^2 s^2}{2}\partial_{ss} F_i + \sum_{j \in E\setminus\{i\}} \widetilde{q}(i,j)(F_j - F_i) = 0, \tag{2.71}$$

for $(t, s) \in [0, T) \times \mathbb{R}_+$, with the terminal condition $F_i(T, s) = s$. Then we can apply the Crank-Nicolson method to equation (2.71) directly with Dirichlet boundary conditions. The method is standard, so we omit the details here.

Next, we discuss the Fourier time-stepping method. begin first by discretizing the continuous-time Markov chain ξ_t with time step of size δt, and we keep ξ_t constant on each time interval $(t_n, t_{n+1}]$ $(t_n = n\delta t)$, for $n = 0, \ldots, T/\delta t - 1$, with transition probabilities

$$P_{kl} := \begin{cases} 1 + \widetilde{q}_{ll}\delta t, & k = l, \\ \widetilde{q}_{kl}\delta t, & otherwise. \end{cases} \tag{2.72}$$

In turn, the futures price satisfies the recursive relation

$$F_i(t_n, x) = \sum_{j=1,\ldots,M} P_{ij} F_j(t_{n+}, x), \tag{2.73}$$

where $F_j(t_{n+}, x) = \lim_{t \downarrow t_n} F_j(t, x)$.

Since we assume Markov chain ξ_t stay constant on time intervals $(t_n, t_{n+1}]$, the martingale property of futures price implies that

$$F_i(t_{n+}, x) = I\!E^{\mathbb{Q}}[F_i(t_{n+1}, X_{t_{n+1}})|X_{t_n} = x], \tag{2.74}$$

for $i = 1, \ldots, M$, and $n = 0, \ldots, T/\delta t - 1$. Therefore, we have following PDE for the futures price within each time interval $(t_n, t_{n+1}]$ and regime i,

$$\partial_t F_i + \kappa_i(\theta_i - x)\partial_x F_i + \frac{\sigma_i^2}{2}\partial_{xx} F_i = 0. \tag{2.75}$$

Next, we apply Fourier transform to PDE (2.75). To that end, we define

$$\mathcal{F}[f](\omega) = \int_{-\infty}^{\infty} f(x) \exp(-j\omega x) dx, \tag{2.76}$$

where j denotes the imaginary identity and ω denotes the frequency. Then, we obtain a first-order PDE for $\hat{F} := \mathcal{F}[F]$:

$$\partial_t \hat{F}_i + \kappa_i \omega \partial_\omega \hat{F}_i + \left(\kappa_i \theta_i j\omega + \kappa_i - \frac{\omega^2 \sigma_i^2}{2} \right) \hat{F}_i = 0, \tag{2.77}$$

for $(t, \omega) \in [0, T) \times \mathbb{R}$, where $\hat{F}(t, \omega) \equiv \mathcal{F}[F](t, \omega)$. Noted that we use the following property of the Fourier transform to derive PDE (2.77),

$$\mathcal{F}[x f_x] = -\mathcal{F}[f] - \omega \mathcal{F}_\omega[f]. \tag{2.78}$$

To solve PDE (2.77) we employ the method of characteristics to get

$$\hat{F}_i(t_n+, \omega) = \phi_i(\delta t, \omega) \hat{F}_i(t_{n+1}, e^{\kappa_i \delta t} \omega), \tag{2.79}$$

with

$$\phi_i(\delta t, \omega) = \exp\left(\kappa_i \delta t - \theta_i j\omega (1 - e^{\kappa_i \delta t}) + \frac{\sigma_i^2 \omega^2}{4\kappa_i} (1 - e^{2\kappa_i \delta t}) \right).$$

Combining equation (2.73) and (2.79), we have following backward equation in the frequency space,

$$\hat{F}_i(t_n, \omega) = \sum_{j=1,\ldots,M} P_{ij} \phi_j(\delta t, \omega) \hat{F}_j(t_{n+1}, e^{\kappa_j \delta t} \omega), \tag{2.80}$$

for $i = 1, \ldots, M$, and $n = 0, \ldots, T/\delta t - 1$. We then apply backward induction via (2.80) to calculate $\hat{F}_i(t, \omega)$. To recover the original futures price function, we apply inverse Fourier transform. For the numerical implementation of Fourier transform and inverse Fourier transform, we utilize the standard fast Fourier transform algorithm. This FST method has been applied more broadly by [33] to solve partial-integro differential equations (PIDEs) that arise in options pricing problems. For more details and other applications of this numerical approach, we refer to [58] and [33], and references therein.

We simulate the sample paths for spot price, futures prices, optimal investment, and optimal wealth process. The regime switching between two states, with transition probabilities $q_{12} = 2$ and $q_{21} = 4$ which are entries of generator matrix $\boldsymbol{Q}$. The trading horizon $\widetilde{T} = 0.6$, and the two futures contracts have maturities $T_1 = 0.6$ and $T_2 = 0.8$. All parameters are

summarized in the Table 2.2.

$\widetilde{q}_{12} = q_{12}$	$\widetilde{q}_{21} = q_{21}$	$\zeta(1)$	$\zeta(2)$	κ_1	κ_2	γ
2	4	0.1	0.3	1	2	1
θ_1	θ_2	σ_1	σ_2	T_1	T_2	$\widetilde{T}$
2.5	2.7	0.2	0.3	0.6	0.8	0.6

Table 2.2: Parameters for the RS-XOU model for Figures 2.6–2.9.

For the sample paths shown in Figure 2.6, the market starts in regime 2, then switches to regime 1 at time t_1) before returning to regime 2 at time t_2. The two price levels $\exp(\theta_1)$ and $\exp(\theta_2)$ are the long-run means of the spot price in regimes 1 and 2 respectively. In each regime, the spot price tends to move towards the corresponding mean level. The spot and futures prices tend to move in tandem. Nevertheless, like in Figure 2.2, each regime switch can cause an instant jump in the futures price but not in the spot price.

Figure 2.7 shows the sample path of the optimal positions in the two futures over the trading horizon. The optimal strategy is to long T_1-Futures and short T_2-Futures. The long-short positions help reduce the effect of regime switching. As the market switches from regime 2 to regime 1 at time t_1, the magnitude of the futures position is immediately reduced. The investor then take larger positions when the market returns to regime 2 from regime 1 at time t_2. According to the sample paths, the optimal positions tend to decay in time during each regime, meaning that the investor gradually reduces investments towards the end of the trading horizon.

Figure 2.8 shows the optimal wealth process over time. By placing opposite position in two futures, we reduce the shock in portfolio vlaue due to regime switching. Therefore, we do not observe sizable jumps in the wealth process at the regime-swtiching times t_1 and t_2. Just like the futures and spot prices, the wealth process tends to decrease in regime 1 and

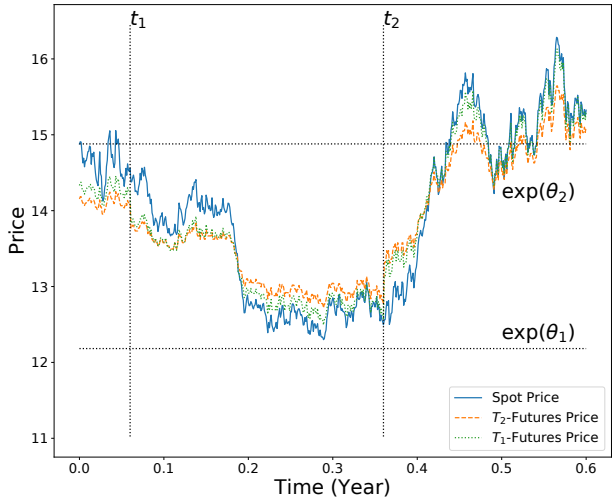

Figure 2.6: Sample paths of the spot price, T_1-futures price, and T_2-futures price over the trading horizon under the RS-XOU model. The market starts in regime 2, then switches to regime 1 at time t_1, before switching back to regime 2 at time t_2.

increase in regime 2 (towards the end of the trading horizon).

Lastly in Figure 2.9, we plot the sample path for $|\Phi|$, which is the absolute value of coefficient matrix determinant Γ. The strict positivity of $|\Phi|$ informs us that Γ is invertible and thus the results in Section 2.3 can be applied. Like in Figure 2.5, $|\Phi|$ tends to increase exponentially in time.

2.6 Conclusion

We have analyzed the problem of dynamically trading a portfolio of futures in a regime-switching market. Under a general market framework, the portfolio optimization problem leads to the analytical and numerical studies of a system of HJB equations, which are solved explicitly. The optimal trading strategies and optimal wealth process are also given analytically and illustrated numerically. Our methodology has been applied to the RS-GBM and RS-XOU models, but it can also be used for other model specifications within the framework

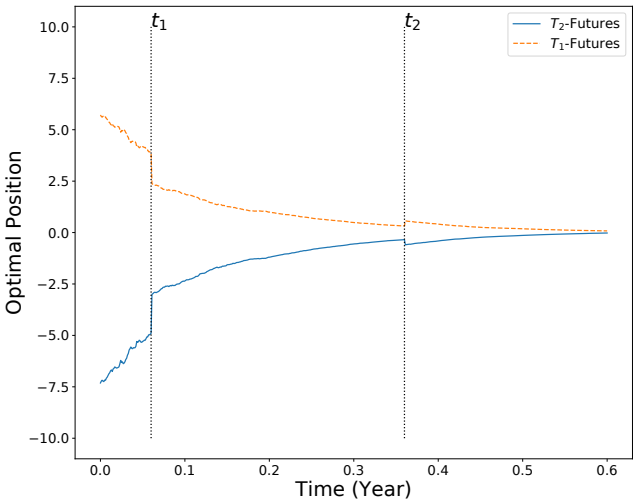

Figure 2.7: Sample paths of the optimal positions $(\varpi^{(1)}, \varpi^{(2)})$ in the T_1-futures and T_2-futures respectively under the RS-XOU model. The futures positions tend to decrease over time and approaches zero near the end of the trading horizon. Jumps in both positions occur at the regiem-switching times t_1 and t_2.

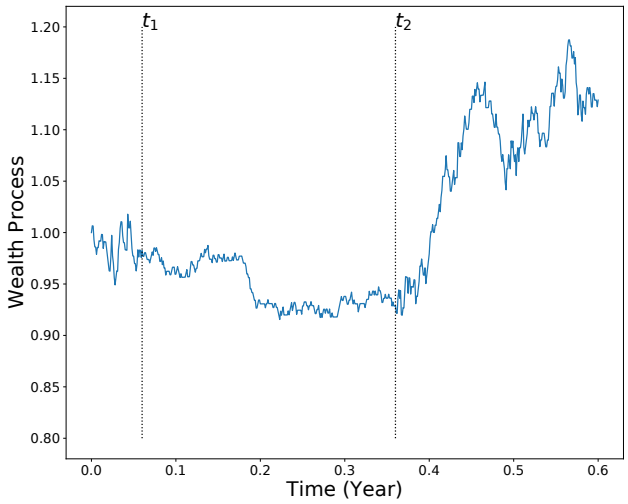

Figure 2.8: Sample path of the optimal wealth process over the trading horizon under the RS-XOU model.

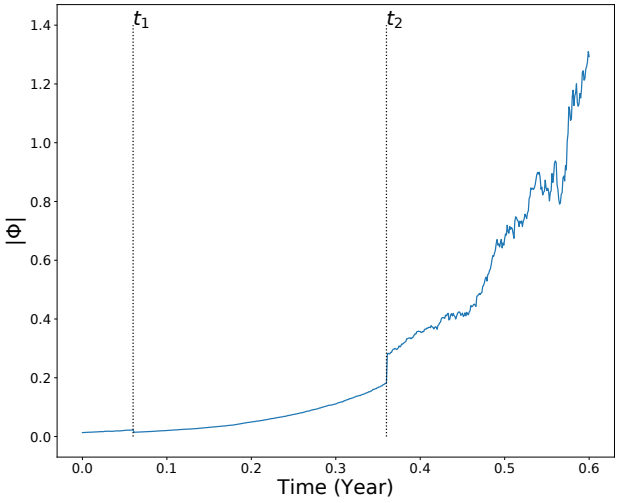

Figure 2.9: Sample path of the absolute value of the determinant Φ for the coefficient matrix Γ under the RS-XOU model.

or adapted to study models with additional factors.

Moreover, one can also utilize our framework to examine other classes of trading strategies, such as rolling and timing strategies. We refer to [41] and [37] for such strategies under mean-reverting models without regime switching. Another major application of futures portfolios is for tracking or gaining exposure to a commodity or index (see e.g. [42] and references therein). It would be of practical interest to examine the effect of regime switching on the strategies and tracking errors. Other than futures portfolio, it is also useful to study the dynamic trading of other derivatives, such as options and swaps, in a regime-switching market.

Chapter 3

DYNAMIC FUTURES PORTFOLIOS WITH CONSTRAINTS

3.1 Introduction

In the previous chapters, the futures portfolios consist of multiple futures contracts written on the same underlying asset. A natural extension is to include futures of different underlying assets. This will drastically expand the set of trading instruments and increase the diversity of exposure. As a result, the portfolio manager has access to various assets within the same asset class (e.g. gold, silver, copper) as well as across asset classes (e.g. precious metals, agricultural commodities, oil and gas, equity, and volatility).

Such a portfolio expansion also come with some new challenges. With more different underlying assets and futures, the dimension of the portfolio optimization problem is significantly increased. Furthermore, one must address the dependency structure among the underlying assets and their futures, even if the underlying assets are not traded. This calls for a stochastic model that can capture the correlation among all the futures and underlying assets while maintaining analytical tractability, numerically efficiency, and interpretability.

Motivated by these observations, we introduce in this chapter an alternative way to model the joint price dynamics of the underlying assets and associated futures. The key idea is as follows. In practice, market frictions and inefficiencies may render the futures price different from the spot price prior to maturity. For each futures contract, the spread between the two prices is called the *basis*. By no-arbitrage theory, futures prices must converge to the spot price at expiry, so the basis process is expected to converge to zero as the associated futures contract expires as well. This price behavior leads us to (i) express each futures price process through the associated basis, and (ii) model the random basis using a Brownian bridge. With multiple futures contracts, we apply a *multidimensional* Brownian bridge,

where each component converges to zero at the respective maturity. The model is presented in Section 3.2.

In Section 3.3, we analyze the problem of dynamically trading futures with different underlying assets under the stochastic basis model. Compared to the previous chapters, another new element of our utility maximization problem is the incorporation of portfolio constraints on the futures positions. Our general setup captures the dollar neutral and market neutral constraints, which are widely used in industry. The optimal strategies for both unconstrained and constrained cases are derived. This is achieved by solving the associated Hamilton-Jacobi-Bellman (HJB) equations. We also provide verification theorem that confirms the solution to value function is indeed the solution to the associated HJB equation. Moreover, we show that the original HJB equations are reduced to a system of linear ODEs and the investor's value function admits a separable form under our stochastic basis framework.

In Section 3.4, we define the certainty equivalents corresponding to portfolios with different constraints. This allows us to quantify the impact of portfolio constraints on the value of futures trading. In addition, we solve for the optimal constraint that maximizes the certainty equivalent for the risk-averse portfolio manager. Numerical examples are provided in Section 3.5 to illustrate how certainty equivalent depend on number of traded futures and different portfolio constraints.

In the literature, evidence of futures basis has motivated several studies on related trading strategies. [56] examine the VIX (volatility index) futures basis and discuss trading strategies involving VIX futures and S&P index futures. [12] present a link between the option market frictions to changes in the VIX futures basis and find that market information embedded in illiquid S&P options is reflected in the VIX but not in VIX futures.

Several studies have modeled the stochastic basis for trading purposes. For example, [9, 10] assume that the basis of an index futures follows a Brownian bridge. Using an optimal stopping approach, they compute the value of the timing option to trade the basis, along with the optimal trading boundaries. Also under a standard Brownian bridge model, [20] provide

an alternative trading strategy and specification of transaction costs. Another related work by [46] assume that the basis follows a scaled Brownian bridge and the investor is subject to a collateral constraint, and derive the strategy that maximizes the expected logarithmic utility of terminal wealth. Our stochastic basis model is closest to that introduced by [4, 5], but in contrast the portfolio optimization problem herein involves multiple different underlying assets that are not traded, and the portfolio is subject to constraints.

In a number of companion papers [43, 44, 39], the utility maximization approach is used to derive dynamic futures trading strategies under various stochastic models without portfolio constraints. Market neutral constraint is taken into consideration to determine optimal pair trading in [47] and [3], while [61] propose a mean-reverting portfolio design with an investment budget constraint. Most recently, [45] analyze the optimal portfolio for multiple co-integrated assets with a general linear constraint. Compared to these studies, our model is a multidimensional stochastic basis framework for futures trading with portfolio constraints. Our analysis show how optimal strategies and value function depend on the stochastic basis and different portfolio constraints.

3.2 Model Formulation

We fix a physical probability space $(\Omega, \mathcal{F}, \mathbb{P})$, where $\mathbb{P}$ is the physical probability measure. The market consists of M risky underlying assets $S_{t,i}$ for $i \in \{1, \ldots, M\}$, along with a positive constant rate $r \geq 0$. The asset's spot prices $S_{t,i}$ evolve according to a multidimensional geometric Brownian motion:

$$dS_{t,i} = S_{t,i} \left(\mu_{i,S} dt + \sum_{k=1}^{i} \sigma_{i,k,S} dZ_{t,k} \right), \quad i \in \{1, \ldots, M\}, \tag{3.1}$$

where $\mu_{i,S}$ is the constant drift, $\sigma_{i,k,S}$, for $1 \leq k \leq i$, are constant volatility parameters, and $(Z_{t,1}, \ldots, Z_{t,M})^\top$ is a standard M-dimensional Brownian motion under the measure $\mathbb{P}$. We assume that this underlying asset or index is not continuously traded, which is typical in many futures markets. As studied by [6] for the VIX futures market, the futures contract and underlying are not linked by a no-arbitrage condition. Therefore, unlike Chapters 1 and 2 where the futures price is defined as a condition expectation of the future spot price, in this chapter the prices of the futures and underlying assets are linked through a multidimensional stochastic basis process.

For each underlying asset $S_{t,i}$, there are N_i futures contracts $F_{t,i,j}$ written on this asset with expiration dates $T_{i,j}$, for $j \in \{1, \ldots, N_i\}$. For counting and indexing, we define the order numbers

$$P_{i,j} = \sum_{k=1}^{i-1} N_k + j, \quad i \in \{1, \ldots, M\}, \quad j \in \{1, \ldots, N_i\}, \tag{3.2}$$

and total number

$$N = \sum_{k=1}^{M} N_k = P_{M,N_M}. \tag{3.3}$$

Then, we can line up all N futures one by one, where the futures $F_{t,i,j}$ is the $P_{i,j}$-th contract.

Next, we derive the futures price dynamics via the random basis process. To that end, we define the log-value of the random basis for the futures contract $F_{t,i,j}$ by

$$Y_{t,i,j} := \log \left(\frac{F_{t,i,j}}{S_{t,i}} \right) - r(T_{i,j} - t); \quad 0 \leq t \leq T_{i,j}, \quad i \in \{1, \ldots, M\}, \quad j \in \{1, \ldots, N_i\}. \tag{3.4}$$

Then, we assume the log-basis $Y_{t,i,j}$ evolve according to multidimensional Brownian bridge:

$$dY_{t,i,j} = \left(m_{i,j} - \frac{\kappa_{i,j} Y_{t,i,j}}{T_{i,j} - t} \right) dt + \sum_{k=1}^{P_{i,j}+M} \sigma_{P_{i,j},k,Y} dZ_{t,k}, \tag{3.5}$$

for $i \in \{1, \ldots, M\}, \quad j \in \{1, \ldots, N_i\}$, where drift $m_{i,j}$, coefficient $\kappa_{i,j}$ and volatility parameter $\sigma_{P_{i,j},k,Y}$ are constants for $1 \leq k \leq P_{i,j} + M$, and $(Z_{t,1}, \ldots, Z_{t,N+M})^\top$ is a standard $N + M$ dimensional Brownian motion under the measure $\mathbb{P}$. We define the filtration $\mathbb{F} = (\mathcal{F}_t)_{t \geq 0}$ being the augmented σ-algebra generated by $\{(Z_{u,1}, \ldots, Z_{u,N+M}); 0 \leq u \leq t\}$ and satisfies the usual conditions. By construction, each log-basis $Y_{t,i,j}$ converges to 0 at the corresponding futures maturity $T_{i,j}$.

From the basis process, we derive the futures price dynamics using Ito's lemma. Precisely, each futures price satisfies the stochastic differential equation (SDE)

$$dF_{t,i,j} = F_{t,i,j} \left[\left(\theta_{i,j} - \frac{\kappa_{i,j} Y_{t,i,j}}{T_{i,j} - t} \right) dt + \sum_{k=1}^{P_{i,j}+M} \sigma_{P_{i,j},k,F} dZ_{t,k} \right], \tag{3.6}$$

where the drift parameter $\theta_{i,j}$ is given by

$$\theta_{i,j} = -r + m_{i,j} + \mu_{i,S} + \frac{1}{2} \left(2 \sum_{k=1}^{i} \sigma_{i,k,S} \sigma_{P_{i,j},k,Y} + \sum_{k=1}^{P_{i,j}+M} \sigma_{P_{i,j},k,Y}^2 \right), \tag{3.7}$$

and volatility parameter $\sigma_{P_{i,j},k,F}$ satisfies

$$\sigma_{P_{i,j},k,F} = \begin{cases} \sigma_{i,k,S} + \sigma_{P_{i,j},k,Y}, & 1 \leq k \leq i, \\ \sigma_{P_{i,j},k,Y}, & i < k \leq P_{i,j} + M, \end{cases} \tag{3.8}$$

for $i \in \{1, \ldots, M\}$ and $j \in \{1, \ldots, N_i\}$.

In order to rewrite SDEs (3.1), (3.5) and (3.6) in the matrix form, we define the vector of assets $\mathbf{S}_t \in \mathbb{R}^M$, the vector of log-basis process $\mathbf{Y}_t \in \mathbb{R}^N$ and the vector of futures prices $\mathbf{F}_t \in \mathbb{R}^N$ as

$$\begin{aligned} \mathbf{S}_t &:= (S_{t,1}, \ldots, S_{t,M})^\top, \\ \mathbf{Y}_t &:= (Y_{t,1,1}, \ldots, Y_{t,1,N_1}, Y_{t,2,1}, \ldots, Y_{t,M,N_M})^\top, \\ \mathbf{F}_t &:= (F_{t,1,1}, \ldots, F_{t,1,N_1}, F_{t,2,1}, \ldots, F_{t,M,N_M})^\top. \end{aligned} \tag{3.9}$$

We also define coefficients vectors and standard Brownian motions by

$$\begin{aligned}
\boldsymbol{\mu} &:= (\mu_{1,S}, \ldots, \mu_{M,S})^\top \in \mathbb{R}^M, \\
\boldsymbol{\theta} &:= (\theta_{1,1}, \ldots, \theta_{1,N_1}, \theta_{2,1}, \ldots, \theta_{M,N_M})^\top \in \mathbb{R}^N, \\
\mathbf{m} &:= (m_{t,1,1}, \ldots, m_{t,1,N_1}, m_{t,2,1}, \ldots, m_{t,M,N_M})^\top \in \mathbb{R}^N, \\
\boldsymbol{K}(t) &:= \operatorname{diag}\left(\frac{\kappa_{1,1}}{T_{1,1}-t}, \ldots, \frac{\kappa_{1,N_1}}{T_{1,N_1}-t}, \frac{\kappa_{2,1}}{T_{2,1}-t}, \ldots, \frac{\kappa_{M,N_M}}{T_{M,N_M}-t}\right) \in \mathbb{R}^{N\times N}, \\
\mathbf{Z}_{t,1} &:= (Z_{t,1}, \ldots, Z_{t,M})^\top \in \mathbb{R}^M, \\
\mathbf{Z}_{t,2} &:= (Z_{t,M+1}, \ldots, Z_{t,N+M})^\top \in \mathbb{R}^N.
\end{aligned} \tag{3.10}$$

Considering M underlying assets, we denote by $\widetilde{\boldsymbol{\Sigma}}_{\boldsymbol{S}} \in \mathbb{R}^{M\times M}$ the volatility matrix associated with the spot price process; that is,

$$\widetilde{\boldsymbol{\Sigma}}_{\boldsymbol{S}} = \begin{bmatrix} \sigma_{1,1,S} & 0 & \ldots & 0 \\ \sigma_{2,1,S} & \sigma_{2,2,S} & \ldots & 0 \\ \vdots & \vdots & \ddots & \vdots \\ \sigma_{M,1,S} & \sigma_{M,2,S} & \ldots & \sigma_{M,M,S} \end{bmatrix}. \tag{3.11}$$

Also, we define the volatility parameter matrices $\widetilde{\boldsymbol{\Sigma}}_{\boldsymbol{YS}} \in \mathbb{R}^{N\times M}$, $\widetilde{\boldsymbol{\Sigma}}_{\boldsymbol{Y}} \in \mathbb{R}^{N\times N}$ for N log-bases by

$$\widetilde{\boldsymbol{\Sigma}}_{\boldsymbol{YS}} = \begin{bmatrix} \sigma_{1,1,Y} & \ldots & \sigma_{1,M,Y} \\ \sigma_{2,1,Y} & \ldots & \sigma_{2,M,Y} \\ \vdots & \ddots & \vdots \\ \sigma_{N,1,Y} & \ldots & \sigma_{N,M,Y} \end{bmatrix}, \quad \widetilde{\boldsymbol{\Sigma}}_{\boldsymbol{Y}} = \begin{bmatrix} \sigma_{1,M+1,Y} & 0 & \ldots & 0 \\ \sigma_{2,M+1,Y} & \sigma_{2,M+2,Y} & \ldots & 0 \\ \vdots & \vdots & \ddots & \vdots \\ \sigma_{N,M+1,Y} & \sigma_{N,M+2,Y} & \ldots & \sigma_{N,M+N,Y} \end{bmatrix}, \tag{3.12}$$

and the volatility parameter matrices $\widetilde{\boldsymbol{\Sigma}}_{\boldsymbol{FS}} \in \mathbb{R}^{N\times M}$, $\widetilde{\boldsymbol{\Sigma}}_{\boldsymbol{F}} \in \mathbb{R}^{N\times N}$ for N futures by

$$\widetilde{\boldsymbol{\Sigma}}_{\boldsymbol{FS}} = \begin{bmatrix} \sigma_{1,1,F} & \ldots & \sigma_{1,M,F} \\ \sigma_{2,1,F} & \ldots & \sigma_{2,M,F} \\ \vdots & \ddots & \vdots \\ \sigma_{N,1,F} & \ldots & \sigma_{N,M,F} \end{bmatrix}, \quad \widetilde{\boldsymbol{\Sigma}}_{\boldsymbol{F}} = \begin{bmatrix} \sigma_{1,M+1,F} & 0 & \ldots & 0 \\ \sigma_{2,M+1,F} & \sigma_{2,M+2,F} & \ldots & 0 \\ \vdots & \vdots & \ddots & \vdots \\ \sigma_{N,M+1,F} & \sigma_{N,M+2,F} & \ldots & \sigma_{N,M+N,F} \end{bmatrix}. \tag{3.13}$$

With these notations, the SDEs (3.1),(3.5), and (3.6) can be written in matrix form:

$$d\mathbf{S}_t = \text{diag}(\mathbf{S}_t)\left[\boldsymbol{\mu}dt + \widetilde{\boldsymbol{\Sigma}}_{\mathbf{S}}d\boldsymbol{Z}_{t,1}\right], \tag{3.14}$$

$$d\mathbf{Y}_t = (\mathbf{m} - \boldsymbol{K}(t)\mathbf{Y}_t)dt + \widetilde{\boldsymbol{\Sigma}}_{\mathbf{YS}}d\boldsymbol{Z}_{t,1} + \widetilde{\boldsymbol{\Sigma}}_{\mathbf{Y}}d\boldsymbol{Z}_{t,2}, \tag{3.15}$$

$$d\mathbf{F}_t = \text{diag}(\mathbf{F}_t)\left[(\boldsymbol{\theta} - \boldsymbol{K}(t)\mathbf{Y}_t)dt + \widetilde{\boldsymbol{\Sigma}}_{\mathbf{FS}}d\boldsymbol{Z}_{t,1} + \widetilde{\boldsymbol{\Sigma}}_{\mathbf{F}}d\boldsymbol{Z}_{t,2}\right]. \tag{3.16}$$

We note that by (3.8), we have $\widetilde{\boldsymbol{\Sigma}}_{\mathbf{Y}} = \widetilde{\boldsymbol{\Sigma}}_{\mathbf{F}}$ and

$$\widetilde{\boldsymbol{\Sigma}}_{\mathbf{FS}} - \widetilde{\boldsymbol{\Sigma}}_{\mathbf{YS}} = \underbrace{\begin{bmatrix} \sigma_{1,1,S} & 0 & \dots & 0 \\ \vdots & \vdots & \ddots & \vdots \\ \sigma_{1,1,S} & 0 & \dots & 0 \\ \sigma_{2,1,S} & \sigma_{2,2,S} & \dots & 0 \\ \vdots & \vdots & \ddots & \vdots \\ \sigma_{2,1,S} & \sigma_{2,2,S} & \dots & 0 \\ \vdots & \vdots & \ddots & \vdots \\ \sigma_{M,1,S} & \sigma_{M,2,S} & \dots & \sigma_{M,M,S} \\ \vdots & \vdots & \ddots & \vdots \\ \sigma_{M,1,S} & \sigma_{M,2,S} & \dots & \sigma_{M,M,S} \end{bmatrix}}_{M} \begin{matrix} \left.\begin{matrix} \\ \\ \\ \end{matrix}\right\} N_1 \\ \left.\begin{matrix} \\ \\ \\ \end{matrix}\right\} N_2 \\ \left.\begin{matrix} \\ \\ \\ \end{matrix}\right\} N_M \end{matrix}. \tag{3.17}$$

3.3 Portfolio Optimization

Most speculative futures trading strategies involve only the futures but not the underlying assets. Indeed, many underlying assets cannot be traded directly (e.g. volatility index) or traded with sufficient liquidity (e.g. agricultural commodities). In other cases where the underlying asset is traded or accessible via an ETF (e.g. gold and silver), futures are traded as a proxy for their underlying assets because of their attractive trading characteristics such as liquidity, leverage, and the ease of taking short positions.

Motivated by these practical applications, we formulate and solve the optimal investment problem faced by a investor who invest in the market but only trades the futures contracts.

This is an optimal investment problem in an incomplete market, since the underlying assets are not tradable.

Like (1.27) in Chapter 1 and (2.21) in Chapter 2, we denote by $W_t^{\boldsymbol{\pi}}$ the value of investor's portfolio and assume $\pi_{t,i,j}$ be the money amount invested on the futures $F_{t,i,j}$. For simplicity, we assume a zero interest rate. Then, the wealth process $W_t^{\boldsymbol{\pi}}$ evolves according to

$$dW_t^{\boldsymbol{\pi}} = \sum_{i=1}^{M} \sum_{j=1}^{N_i} \pi_{t,i,j} \frac{dF_{t,i,j}}{F_{t,i,j}} \tag{3.18}$$

$$= \boldsymbol{\pi}_t^\top \left[(\boldsymbol{\theta} - \boldsymbol{K}(t)\mathbf{Y}_t)dt + \widetilde{\boldsymbol{\Sigma}}_{\mathbf{FS}} d\boldsymbol{Z}_{t,1} + \widetilde{\boldsymbol{\Sigma}}_{\mathbf{F}} d\boldsymbol{Z}_{t,2} \right], \tag{3.19}$$

where we have defined the strategy as the vector

$$\boldsymbol{\pi}_t := (\pi_{t,1,1}, \ldots, \pi_{t,1,N_1}, \pi_{t,2,1}, \ldots, \pi_{t,M,N_M})^\top. \tag{3.20}$$

In this section, we discuss the optimal trading strategy for futures portfolio with or without constraints through utility maximization. Among our findings, the associated Hamilton-Jacobi-Bellman equation (HJB) reduces to a series of ODE equations, which could be solved numerically. In addition, we provide the verification theorem for our utility maximization problem.

Like in previous chapters, the investor's risk preferences are modeled by the exponential utility

$$U(w) = -e^{-\gamma w}, \tag{3.21}$$

where $\gamma > 0$ is the risk aversion parameter.

Let's begin with general strategies without constraints, which we use superscript 'no' to denote 'no constraints' in our presentation.

3.3.1 Futures Portfolio without Constraints

In this section, we will discuss the case that the investor puts no portfolio constraints on the strategy $\boldsymbol{\pi}$. Then, the investor seeks an admissible strategy $\boldsymbol{\pi} \in \mathcal{A}^{no}$, that maximizes the expected utility of wealth at T, where $0 < T < T_{i,j}$ for all $i \in \{1, \ldots, M\}$ and $j \in$

$\{1, \ldots, N_i\}$. It means trading stops strictly before the expiry of the futures contracts. Then, the convergence between asset's price $S_{t,i}$ and futures price $F_{t,i,j}$ is not realized in the market. This non-convergence has practical relevance since speculative futures trades are always closed out before the delivery date.

Before defining the set of admissible trading strategies, we construct an auxiliary process corresponding to any given strategy $\boldsymbol{\pi}$ by

$$\begin{aligned} A_t^{\boldsymbol{\pi}} = \int_0^t \left(-\boldsymbol{Y}_s^\top \boldsymbol{H}^{no}(t) + \boldsymbol{g}^{no}(t)^\top\right) \left(\widetilde{\boldsymbol{\Sigma}}_{\boldsymbol{YS}} d\boldsymbol{Z}_{s,1} + \widetilde{\boldsymbol{\Sigma}}_{\boldsymbol{Y}} d\boldsymbol{Z}_{s,2}\right) \\ -\gamma \boldsymbol{\pi}_s^\top \left(\widetilde{\boldsymbol{\Sigma}}_{\mathbf{FS}} d\boldsymbol{Z}_{s,1} + \widetilde{\boldsymbol{\Sigma}}_{\mathbf{F}} d\boldsymbol{Z}_{s,2}\right), \end{aligned} \tag{3.22}$$

where $\boldsymbol{H}^{no}(t), \boldsymbol{g}^{no}(t)$ are deterministic functions that depend only on the model parameters, which will appear later in Theorem 3 by solving the corresponding ODEs. Next, we define the set of admissible strategies.

Definition 1 (Admissibility)**.** *We denote $\mathcal{A}^{no}$ the set of all $\mathcal{F}_t$-adapted processes $\{\boldsymbol{\pi}_t\}_{0\le t\le T}$, such that*

(i) $\mathbb{E}^{\mathbb{P}}\left(\int_0^T |\boldsymbol{\pi}_t^\top \mathbf{Y}_t| + \|\boldsymbol{\pi}_t\|^2 dt\right) < \infty$;

(ii) $W_t^{\boldsymbol{\pi}} \in \mathcal{D}$, *P-a.s., for all* $t \in [0,T]$, *where* $\mathcal{D} = \mathbb{R}$ *and* $(W_t^{\boldsymbol{\pi}})_{0\le t\le T}$ *is given by* (3.18)*;*

(iii) $\mathbb{E}^{\mathbb{P}}\left(\exp\left(A_T^{\boldsymbol{\pi}} - \frac{1}{2}\langle A^{\boldsymbol{\pi}}\rangle_T\right)\right) = 1$.

Condition *(i)* is a general integrability condition to ensure the existence of the wealth process, condition *(ii)* is to assure that the wealth should be positive almost surely, and condition *(iii)* can be found in many places, e.g. [35], which guarantees that the stochastic exponential of $A_t^{\boldsymbol{\pi}}$ is a martingale.

Then, the value function for the investor's utility maximization problem is defined by

$$V^{no}(t, \boldsymbol{y}, w) = \sup_{\boldsymbol{\pi}\in\mathcal{A}^{no}} \mathbb{E}^{\mathbb{P}}[U(W_T^{\boldsymbol{\pi}}) | \mathbf{Y}_t = \boldsymbol{y}, W_t^{\boldsymbol{\pi}} = w]. \tag{3.23}$$

To solve the portfolio optimization problem, we define the volatility matrices $\boldsymbol{\Sigma_Y} \in \mathbb{R}^{N\times N}$, $\boldsymbol{\Sigma_{FY}} \in \mathbb{R}^{N\times N}$ and $\boldsymbol{\Sigma_F} \in \mathbb{R}^{N\times N}$ matrix, as

$$\boldsymbol{\Sigma_Y} = \widetilde{\boldsymbol{\Sigma}}_{\mathbf{YS}}\widetilde{\boldsymbol{\Sigma}}_{\mathbf{YS}}^{\top} + \widetilde{\boldsymbol{\Sigma}}_{\mathbf{Y}}\widetilde{\boldsymbol{\Sigma}}_{\mathbf{Y}}^{\top}, \tag{3.24}$$

$$\boldsymbol{\Sigma_{FY}} = \widetilde{\boldsymbol{\Sigma}}_{\mathbf{FS}}\widetilde{\boldsymbol{\Sigma}}_{\mathbf{YS}}^{\top} + \widetilde{\boldsymbol{\Sigma}}_{\mathbf{F}}\widetilde{\boldsymbol{\Sigma}}_{\mathbf{Y}}^{\top}, \tag{3.25}$$

$$\boldsymbol{\Sigma_F} = \widetilde{\boldsymbol{\Sigma}}_{\mathbf{FS}}\widetilde{\boldsymbol{\Sigma}}_{\mathbf{FS}}^{\top} + \widetilde{\boldsymbol{\Sigma}}_{\mathbf{F}}\widetilde{\boldsymbol{\Sigma}}_{\mathbf{F}}^{\top}. \tag{3.26}$$

Also to facilitate the presentation, we define the linear operator

$$\mathcal{L}\,\cdot = (\mathbf{m} - \boldsymbol{K}(t)\boldsymbol{y})^{\top}\nabla_{\boldsymbol{y}}\,\cdot + \frac{1}{2}\mathrm{Tr}(\boldsymbol{\Sigma_Y}\nabla^2_{\boldsymbol{y}}\cdot), \tag{3.27}$$

where $\nabla_{\boldsymbol{y}}\cdot = (\partial_{y_{1,1}}\cdot, \ldots, \partial_{y_{1,N_1}}\cdot, \partial_{y_{2,1}}\cdot, \ldots, \partial_{y_{M,N_M}}\cdot)^{\top}$ is the nabla operator, and the Hessian operator $\nabla^2_{\boldsymbol{y}}\cdot$ satisfies

$$\nabla^2_{\boldsymbol{y}}\cdot = \begin{bmatrix} \partial^2_{y_{1,1}}\cdot & \partial_{y_{1,1}}\partial_{y_{1,2}}\cdot & \cdots & \partial_{y_{1,1}}\partial_{y_{N,N_M}}\cdot \\ \partial_{y_{1,2}}\partial_{y_{1,1}}\cdot & \partial^2_{y_{1,2}}\cdot & \cdots & \partial_{y_{1,2}}\partial_{y_{N,N_M}}\cdot \\ \vdots & \vdots & \ddots & \vdots \\ \partial_{y_{N,N_M}}\partial_{y_{1,1}}\cdot & \partial_{y_{N,N_M}}\partial_{y_{1,2}}\cdot & \cdots & \partial^2_{y_{N,N_M}}\cdot \end{bmatrix}. \tag{3.28}$$

and column-valued-function $\boldsymbol{a}^{no}(t, \boldsymbol{y}, w)$

$$\boldsymbol{a}^{no}(t, \boldsymbol{y}, w) = (\boldsymbol{\theta} - \boldsymbol{K}(t)\boldsymbol{y})\partial_w u^{no} + \boldsymbol{\Sigma_{FY}}\nabla_{\boldsymbol{y}}\partial_w u^{no}. \tag{3.29}$$

Then, we obtain the HJB equation for the candidate value function $u^{no}(t, \boldsymbol{y}, w)$,

$$\partial_t u^{no} + \mathcal{L}u^{no} + \max_{\boldsymbol{\pi}\in\mathcal{A}}\left\{\boldsymbol{\pi}^{\top}\boldsymbol{a}^{no}(t, \boldsymbol{y}, w) + \frac{\partial_{ww}u^{no}}{2}\boldsymbol{\pi}^{\top}\boldsymbol{\Sigma_F}\boldsymbol{\pi}\right\} = 0, \tag{3.30}$$

for $(t, \boldsymbol{y}, w) \in [0, T)\times\mathbb{R}^N\times\mathcal{D}$, where operator $\mathcal{L}$ is defined in (3.27). The terminal condition is

$$u^{no}(T, \boldsymbol{y}, w) = U(w) = -e^{-\gamma w}, \tag{3.31}$$

for $(\boldsymbol{y}, w) \in \mathbb{R}^N\times\mathcal{D}$.

Next, we present the solution to the HJB equation (3.30). To that end, we first define

$$\boldsymbol{\Sigma}^{no} = \boldsymbol{\Sigma_Y} - \boldsymbol{\Sigma}_{\boldsymbol{FY}}^{\top}\boldsymbol{\Sigma}_{\boldsymbol{F}}^{-1}\boldsymbol{\Sigma_{FY}}, \tag{3.32}$$

which is a $N\times N$ matrix.

Theorem 3. *1. The matrix Riccati differential equation below has a unique solution that is positive definite for all $t \in [0, T]$,*

$$\begin{aligned}\frac{d}{dt}\boldsymbol{H}^{no}(t) &= \left(\boldsymbol{K}(t) - \boldsymbol{K}(t)\boldsymbol{\Sigma}_{\boldsymbol{F}}^{-1}\boldsymbol{\Sigma}_{\boldsymbol{FY}}\right)\boldsymbol{H}^{no}(t) \\ &\quad + \boldsymbol{H}^{no}(t)\left(\boldsymbol{K}(t) - \boldsymbol{K}(t)\boldsymbol{\Sigma}_{\boldsymbol{F}}^{-1}\boldsymbol{\Sigma}_{\boldsymbol{FY}}\right)^{\top} \\ &\quad + \boldsymbol{H}^{no}(t)\boldsymbol{\Sigma}^{no}\boldsymbol{H}^{no}(t) - \boldsymbol{K}(t)^{\top}\boldsymbol{\Sigma}_{\boldsymbol{F}}^{-1}\boldsymbol{K}(t), \\ \boldsymbol{H}^{no}(T) &= \mathbf{0}_{N\times N},\end{aligned} \tag{3.33}$$

where $\mathbf{0}_{N\times N}$ denotes the zero matrix of dimension $N \times N$.

2. The solution of the HJB equation (3.30) is given by

$$u^{no}(t, \boldsymbol{y}, w) = U(w)\exp\left(-\frac{1}{2}\boldsymbol{y}^{\top}\boldsymbol{H}^{no}(t)\boldsymbol{y} + \boldsymbol{y}^{\top}\boldsymbol{g}^{no}(t) + f^{no}(t)\right), \tag{3.34}$$

for $(t, \boldsymbol{y}, w) \in [0, T] \times \mathbb{R}^N \times \mathbb{R}^+$, where $\boldsymbol{H}^{no}(t) \in \mathbb{R}^{N\times N}$ satisfies the matrix Riccati differential equation (3.33)*, $\boldsymbol{g}^{no}(t) \in \mathbb{R}^N$ satisfies the following ODE system,*

$$\begin{aligned}\frac{d}{dt}\boldsymbol{g}^{no}(t) &= \boldsymbol{K}(t)\boldsymbol{g}^{no}(t) + \boldsymbol{H}^{no}(t)\boldsymbol{m} + \left(\boldsymbol{H}^{no}(t)\boldsymbol{\Sigma}^{no} - \boldsymbol{K}(t)\boldsymbol{\Sigma}_{\boldsymbol{F}}^{-1}\boldsymbol{\Sigma}_{\boldsymbol{FY}}\right)\boldsymbol{g}^{no}(t) \\ &\quad - \left(\boldsymbol{K}(t) + \boldsymbol{H}^{no}(t)\boldsymbol{\Sigma}_{\boldsymbol{FY}}^{\top}\right)\boldsymbol{\Sigma}_{\boldsymbol{F}}^{-1}\boldsymbol{\theta}, \\ \boldsymbol{g}^{no}(T) &= \mathbf{0}_{N\times 1},\end{aligned} \tag{3.35}$$

and $f^{no}(t) \in \mathbb{R}$ follows the ODE,

$$\begin{aligned}\frac{d}{dt}f^{no}(t) &= -\boldsymbol{m}^{\top}\boldsymbol{g}^{no}(t) + \frac{1}{2}tr\left(\boldsymbol{\Sigma}_{\boldsymbol{Y}}\boldsymbol{H}^{no}(t)\right) - \frac{1}{2}\boldsymbol{g}^{no}(t)^{\top}\boldsymbol{\Sigma}_{\boldsymbol{Y}}\boldsymbol{g}^{no}(t) \\ &\quad + \frac{1}{2}\left(\boldsymbol{\theta} + \boldsymbol{\Sigma}_{\boldsymbol{FY}}\boldsymbol{g}^{no}(t)\right)^{\top}\boldsymbol{\Sigma}_{\boldsymbol{F}}^{-1}\left(\boldsymbol{\theta} + \boldsymbol{\Sigma}_{\boldsymbol{FY}}\boldsymbol{g}^{no}(t)\right), \\ f^{no}(T) &= 0.\end{aligned} \tag{3.36}$$

3. The optimal strategy is given by

$$\boldsymbol{\pi}^{*}(t, \boldsymbol{y}) = \frac{1}{\gamma}\boldsymbol{\Sigma}_{\boldsymbol{F}}^{-1}\left(\boldsymbol{\theta} - \boldsymbol{K}(t)\boldsymbol{y} + \boldsymbol{\Sigma}_{\boldsymbol{FY}}\left(\boldsymbol{g}^{no}(t) - \boldsymbol{H}^{no}(t)\boldsymbol{y}\right)\right). \tag{3.37}$$

Proof. A detailed proof is provided in Section 3.7.1. □

Futures portfolios often come with portfolio constraints, among which dollar neutrality or market neutrality are the most popular. Within the stochastic basis framework, we now give a rigorous definition of portfolio constraints, and introduce a general class of constraints that includes both dollar and market neutrality.

3.3.2 Constrained Futures Portfolio

We consider linear constraints, so the portfolio constraints can be written in the form:

$$\boldsymbol{\Gamma}^\top \boldsymbol{\pi} = \boldsymbol{c}, \tag{3.38}$$

where $\boldsymbol{\Gamma}$ is a $N \times d$ matrix, and $\boldsymbol{c} \in \mathbb{R}^d$ is a column vector. Furthermore, we assume these d constraints are linearly independent, i.e. $\text{rank}(\boldsymbol{\Gamma}) = d$. Otherwise, some constraints are either redundant or infeasible.

The admissible set $\mathcal{A}$ for constrained case is almost the same that in Definition 1, except that $\boldsymbol{H}^{no}$ and $\boldsymbol{g}^{no}$ in the auxiliary process $A^{\boldsymbol{\pi}}$ should be replaced by $\boldsymbol{H}$ and $\boldsymbol{g}$ (given in (3.46) and (3.48) below) respectively. With this, the investor seeks an admissible strategy $\boldsymbol{\pi} \in \{\boldsymbol{\pi} \in \mathcal{A} \,|\, \boldsymbol{\Gamma}^\top \boldsymbol{\pi}_t = \boldsymbol{c}, \quad \text{for } t \in [0, T]\}$ that maximizes the expected utility of wealth at T.

Therefore, the value function is defined as

$$V(t, \boldsymbol{y}, w) = \sup_{\boldsymbol{\pi} \in \mathcal{A}, \boldsymbol{\Gamma}^\top \boldsymbol{\pi} = \boldsymbol{c}} I\!E^{\mathbb{P}}[U(W_T^{\boldsymbol{\pi}}) | \boldsymbol{Y}_t = \boldsymbol{y}, W_t^{\boldsymbol{\pi}} = w]. \tag{3.39}$$

Next, we define the column-vector-valued function

$$\boldsymbol{a}(t, \boldsymbol{y}, w) = (\partial_w u)(\boldsymbol{\theta} - \boldsymbol{K}(t)\boldsymbol{y}) + \boldsymbol{\Sigma}_{\boldsymbol{FY}}(\partial_w \nabla_{\boldsymbol{y}} u). \tag{3.40}$$

Then, the corresponding HJB equation for the candidate value function $u(t, \boldsymbol{y}, w)$ follows

$$\partial_t u + \mathcal{L}\, u + \max_{\boldsymbol{\pi} \in \mathcal{A}, \boldsymbol{\Gamma}^\top \boldsymbol{\pi} = \boldsymbol{c}} \left\{ \boldsymbol{\pi}^\top \boldsymbol{a}(t, \boldsymbol{y}, w) + \frac{\partial_{ww} u}{2} \boldsymbol{\pi}^\top \boldsymbol{\Sigma}_{\boldsymbol{F}} \boldsymbol{\pi} \right\} = 0, \tag{3.41}$$

for $(t, \boldsymbol{y}, w) \in [0, T) \times \mathbb{R}^N \times \mathcal{D}$, where the set $\mathcal{D}$ contains all possible values for the wealth w. The terminal condition is

$$u(T, \boldsymbol{y}, w) = U(w), \tag{3.42}$$

for $(\boldsymbol{y}, w) \in \mathbb{R}^N \times \mathcal{D}$.

Now we present the solution to the HJB equation (3.41). To that end, we first define $\boldsymbol{D}_{\boldsymbol{\Gamma}} \in \mathbb{R}^{d\times d}$, $\boldsymbol{\Sigma}_{\boldsymbol{\Gamma}} \in \mathbb{R}^{N\times N}$ and $\boldsymbol{\Sigma} \in \mathbb{R}^{N\times N}$ as

$$\boldsymbol{D}_{\boldsymbol{\Gamma}} = \boldsymbol{\Gamma}^\top \boldsymbol{\Sigma}_{\boldsymbol{F}}^{-1} \boldsymbol{\Gamma}, \tag{3.43}$$

$$\boldsymbol{\Sigma}_{\boldsymbol{\Gamma}} = \boldsymbol{\Sigma}_{\boldsymbol{F}}^{-1} \boldsymbol{\Gamma} \boldsymbol{D}_{\boldsymbol{\Gamma}}^{-1} \boldsymbol{\Gamma}^\top \boldsymbol{\Sigma}_{\boldsymbol{F}}^{-1}, \tag{3.44}$$

$$\boldsymbol{\Sigma} = \boldsymbol{\Sigma}_{\boldsymbol{Y}} - \boldsymbol{\Sigma}_{\boldsymbol{FY}}^\top (\boldsymbol{\Sigma}_{\boldsymbol{F}}^{-1} - \boldsymbol{\Sigma}_{\boldsymbol{\Gamma}}) \boldsymbol{\Sigma}_{\boldsymbol{FY}}. \tag{3.45}$$

Note that $\boldsymbol{D}_{\boldsymbol{\Gamma}}$ is invertible due to the assumption that $\operatorname{rank}(\boldsymbol{\Gamma}) = d$.

Theorem 4. *Assume the investor's utility is given by* (3.21)*. Then, the following statements hold.*

1. *The matrix Riccati differential equation below has a unique solution that is positive definite for all $t \in [0, T]$,*

$$\begin{aligned} \boldsymbol{H}'(t) = &\left(\boldsymbol{K}(t) - \boldsymbol{K}(t)(\boldsymbol{\Sigma}_{\boldsymbol{F}}^{-1} - \boldsymbol{\Sigma}_{\boldsymbol{\Gamma}})\boldsymbol{\Sigma}_{\boldsymbol{FY}}\right) \boldsymbol{H}(t) \\ &+ \boldsymbol{H}(t) \left(\boldsymbol{K}(t) - \boldsymbol{K}(t)(\boldsymbol{\Sigma}_{\boldsymbol{F}}^{-1} - \boldsymbol{\Sigma}_{\boldsymbol{\Gamma}})\boldsymbol{\Sigma}_{\boldsymbol{FY}}\right)^\top \\ &+ \boldsymbol{H}(t)\boldsymbol{\Sigma}\boldsymbol{H}(t) - \boldsymbol{K}(t)(\boldsymbol{\Sigma}_{\boldsymbol{F}}^{-1} - \boldsymbol{\Sigma}_{\boldsymbol{\Gamma}})\boldsymbol{K}(t), \\ \boldsymbol{H}(T) = &\, \mathbf{0}_{N\times N}, \end{aligned} \tag{3.46}$$

   where $\mathbf{0}_{N\times N}$ denotes the zero matrix of dimension $N \times N$.

2. *The solution of the HJB equation (3.41) is given by*

$$u(t, \boldsymbol{y}, w) = U(w) \exp\left(-\frac{1}{2}\boldsymbol{y}^\top \boldsymbol{H}(t)\boldsymbol{y} + \boldsymbol{y}^\top \boldsymbol{g}(t) + f(t)\right), \tag{3.47}$$

for $(t, \boldsymbol{y}, w) \in [0,T] \times \mathbb{R}^N \times \mathbb{R}^+$, *where* $\boldsymbol{H}(t) \in \mathbb{R}^{N\times N}$ *satisfies the matrix Riccati differential equation* (3.46), $\boldsymbol{g}(t) \in \mathbb{R}^N$ *satisfies the following ODE system*

$$\begin{aligned}\boldsymbol{g}'(t) &= \left(\boldsymbol{K}(t) + \boldsymbol{H}(t)\boldsymbol{\Sigma} - \boldsymbol{K}(t)(\boldsymbol{\Sigma}_{\boldsymbol{F}}^{-1} - \boldsymbol{\Sigma}_{\boldsymbol{\Gamma}})\boldsymbol{\Sigma}_{\boldsymbol{FY}}\right)\boldsymbol{g}(t) + \boldsymbol{H}(t)\boldsymbol{m} \\ &\quad - \left(\boldsymbol{K}(t) + \boldsymbol{H}(t)\boldsymbol{\Sigma}_{\boldsymbol{FY}}^{\top}\right)\left((\boldsymbol{\Sigma}_{\boldsymbol{F}}^{-1} - \boldsymbol{\Sigma}_{\boldsymbol{\Gamma}})\boldsymbol{\theta} + \gamma\boldsymbol{\Sigma}_{\boldsymbol{F}}^{-1}\boldsymbol{\Gamma}\boldsymbol{D}_{\boldsymbol{\Gamma}}^{-1}\boldsymbol{c}\right), \qquad (3.48)\\ \boldsymbol{g}(T) &= \boldsymbol{0}_{N\times 1},\end{aligned}$$

and $f(t) \in \mathbb{R}$ *follows the ODE,*

$$\begin{aligned}f'(t) &= -\boldsymbol{m}^{\top}\boldsymbol{g}(t) + \frac{1}{2}Tr(\boldsymbol{\Sigma}_{\boldsymbol{Y}}\boldsymbol{H}(t)) - \frac{1}{2}\boldsymbol{g}(t)^{\top}\boldsymbol{\Sigma}_{\boldsymbol{Y}}\boldsymbol{g}(t) \\ &\quad + \frac{1}{2}\left(\boldsymbol{\theta} + \boldsymbol{\Sigma}_{\boldsymbol{FY}}\boldsymbol{g}(t)\right)^{\top}(\boldsymbol{\Sigma}_{\boldsymbol{F}}^{-1} - \boldsymbol{\Sigma}_{\boldsymbol{\Gamma}})\left(\boldsymbol{\theta} + \boldsymbol{\Sigma}_{\boldsymbol{FY}}\boldsymbol{g}(t)\right) \qquad (3.49)\\ &\quad + \gamma\left(\boldsymbol{\theta} + \boldsymbol{\Sigma}_{\boldsymbol{FY}}\boldsymbol{g}(t)\right)^{\top}\boldsymbol{\Sigma}_{\boldsymbol{F}}^{-1}\boldsymbol{\Gamma}\boldsymbol{D}_{\boldsymbol{\Gamma}}^{-1}\boldsymbol{c} - \frac{\gamma^2}{2}\boldsymbol{c}^{\top}\boldsymbol{D}_{\boldsymbol{\Gamma}}^{-1}\boldsymbol{c}, \\ f(T) &= 0.\end{aligned}$$

3. The optimal strategy is given by

$$\boldsymbol{\pi}^*(t,\boldsymbol{y}) = \boldsymbol{\Sigma}_{\boldsymbol{F}}^{-1}\boldsymbol{\Gamma}\boldsymbol{D}_{\boldsymbol{\Gamma}}^{-1}\boldsymbol{c} + \frac{1}{\gamma}(\boldsymbol{\Sigma}_{\boldsymbol{F}}^{-1} - \boldsymbol{\Sigma}_{\boldsymbol{\Gamma}})\Big(\boldsymbol{\theta} - \boldsymbol{K}(t)\boldsymbol{y} + \boldsymbol{\Sigma}_{\boldsymbol{FY}}\big(\boldsymbol{g}(t) - \boldsymbol{H}(t)\boldsymbol{y}\big)\Big). \quad (3.50)$$

Proof. See Section 3.7.2. □

Remark 4. *If instead inequality constraints of the form* $\boldsymbol{\Gamma}^{\top}\boldsymbol{\pi} \leq \boldsymbol{c}$ *are imposed in* (3.41)*, then one must maximize the Lagrangian function* (3.85) *with constraints* $\boldsymbol{\lambda}(t) \geq \boldsymbol{0}$*. There is no analytic solution to this constrained quadratic optimization problem, so numerical methods need to be developed for this extension, which is not discussed in this book.*

Let's look at the optimal strategies associated with some well-known portfolio constraints.

Example 3. *Dollar Neutral Strategy A dollar neutral strategy invests the same amount of money in long and short positions. The resulting portfolio is certainly not risk-free and end up positively or negatively correlated with the underlying assets. Mathematically, a portfolio is said to be dollar neutral if the corresponding strategy satisfies the single constraint:*

$$\boldsymbol{1}_{N\times 1}^{\top}\boldsymbol{\pi} = 0, \qquad (3.51)$$

where $\mathbf{1}_{N\times 1}$ *is a vector of* N *ones. This amounts to set* $\boldsymbol{c} = 0$ *(scalar) and* $\boldsymbol{\Gamma} = \mathbf{1}_{N\times 1}$ *in* (3.38)*. When* $N = 1$*, meaning that only one futures is traded, the strategy* $\boldsymbol{\pi}$ *has to be zero to satisfy the dollar neutral constraint.*

Then, according to Theorem 4, the optimal strategy for dollar neutral portfolio is given by

$$\boldsymbol{\pi}_t^* = \frac{1}{\gamma}(\boldsymbol{\Sigma}_{\boldsymbol{F}}^{-1} - \boldsymbol{\Sigma}_{\boldsymbol{\Gamma}})\Big(\boldsymbol{\theta} - \boldsymbol{K}(t)\boldsymbol{y} + \boldsymbol{\Sigma}_{\boldsymbol{FY}}\big(\boldsymbol{g}(t) - \boldsymbol{H}(t)\boldsymbol{y}\big)\Big). \tag{3.52}$$

Example 4. *Market Neutral Strategy A market neutral strategy is designed to eliminate the correlation between the portfolio and market (see [52, 59]). For futures portfolios, a trading strategy is said to be market neutral if the resulting portfolio wealth process* $W_t^{\boldsymbol{\pi}}$ *is uncorrelated with the underlying assets* $S_{i,t}$*, satisfying*

$$dW_t^{\boldsymbol{\pi}}\, dS_{i,t} = 0, \tag{3.53}$$

for $i \in \{1, \ldots, M\}$*. Hence, the market neutral constraints are described by the system of equations:*

$$(\widetilde{\boldsymbol{\Sigma}}_{\boldsymbol{FS}}\widetilde{\boldsymbol{\Sigma}}_{\boldsymbol{S}}^{\top})^{\top}\boldsymbol{\pi} = \mathbf{0}_{M\times 1}. \tag{3.54}$$

This amounts to setting $\boldsymbol{\Gamma} = \widetilde{\Sigma}_{\boldsymbol{FS}}\widetilde{\Sigma}_{\boldsymbol{S}}^{\top}$ *and* $\boldsymbol{c} = \mathbf{0}$ *in* (3.38)*. In particular, if* $\boldsymbol{\Gamma}$ *is an invertible matrix, then it follows that* $\boldsymbol{\pi}_t^* = \mathbf{0}_{N\times 1}$*, which means that the only feasible strategy is to not trade anything at all. This issue can be remedied by increasing the number of futures traded (see Figure 3.3 and its discussion below).*

Then according to Theorem 4, the optimal strategy for the market neutral portfolio is given by

$$\boldsymbol{\pi}_t^* = \frac{1}{\gamma}(\boldsymbol{\Sigma}_{\boldsymbol{F}}^{-1} - \boldsymbol{\Sigma}_{\boldsymbol{\Gamma}})\Big(\boldsymbol{\theta} - \boldsymbol{K}(t)\boldsymbol{y} + \boldsymbol{\Sigma}_{\boldsymbol{FY}}\big(\boldsymbol{g}(t) - \boldsymbol{H}(t)\boldsymbol{y}\big)\Big). \tag{3.55}$$

Since $\boldsymbol{\Sigma}_{\boldsymbol{\Gamma}}$, $\boldsymbol{H}(t)$ and $\boldsymbol{g}(t)$ depend on the choice of portfolio constraints, $\boldsymbol{\Gamma}$ and $\boldsymbol{c}$, the optimal strategy presented in two examples are different.

In order to unify the two special constraints above, we introduce a class of constraints that enforces neutrality with respect to any given constraint matrix Γ.

Definition 2 ($\boldsymbol{\Gamma}$-Neutral)**.** *A strategy $\boldsymbol{\pi}$ is said to be $\boldsymbol{\Gamma}$-neutral if it satisfies the constraints:*

$$\boldsymbol{\Gamma}^\top \boldsymbol{\pi} = \mathbf{0}. \tag{3.56}$$

Remark 5. *Recall that $\boldsymbol{\pi}$ stands for the amount money invested, but the $\boldsymbol{\Gamma}$-neutral condition also holds for portfolio weights.*

With the definition of $\boldsymbol{\Gamma}$-neutral strategy, we can now view the dollar neutral strategy as setting $\boldsymbol{\Gamma} = \mathbf{1}$ and the market neutral strategy as setting $\widetilde{\boldsymbol{\Sigma}}_{\boldsymbol{SF}}\widetilde{\boldsymbol{\Sigma}}_{\boldsymbol{S}}^\top$. Moreover, we can decompose the optimal strategies for general constraints $\boldsymbol{\Gamma}^\top\boldsymbol{\pi} = \boldsymbol{c}$ into two components, one of which is dominated by the $\boldsymbol{\Gamma}$-neutral case, and the remaining component reveals the hedging demand when $\boldsymbol{c} \neq 0$. To that end, we first decompose the coefficient functions $\boldsymbol{g}(t)$ and $f(t)$ as follows:

Lemma 1. *There exist $\boldsymbol{\Psi}(t)$, $\boldsymbol{\beta}(t)$, $\boldsymbol{\Lambda}(t)$, which are $N \times d, 1 \times d$ and $d \times d$ matrices, respectively, such that*

$$\begin{aligned} \boldsymbol{g}(t) &= \boldsymbol{g}_0(t) + \boldsymbol{\Psi}(t)\boldsymbol{c}, \\ f(t) &= f_0(t) + \boldsymbol{\beta}(t)\boldsymbol{c} + \boldsymbol{c}^\top\boldsymbol{\Lambda}(t)\boldsymbol{c}, \end{aligned} \tag{3.57}$$

where $\boldsymbol{g}_0(t)$ and $f_0(t)$ correspond to the solutions of ODEs (3.48) *and* (3.49) *under the Γ-neutral constraint $\boldsymbol{\Gamma}^\top\boldsymbol{\pi} = \mathbf{0}$. In addition, $\boldsymbol{\Lambda}(t)$ is positive semidefinite.*

Proof. The detailed proof is provided in Section 3.7.3. □

While $\boldsymbol{g}(t)$ and $f(t)$ are found from solving an ODE system and may not be fully explicit, the decomposition in Lemma 1 reveals some interesting structure in terms of the effects of $\boldsymbol{c}$. Since the functions $\boldsymbol{\Psi}(t)$, $\boldsymbol{\beta}(t)$, and $\boldsymbol{\Lambda}(t)$ are all independent of $\boldsymbol{c}$. Additionally, given that the ODEs for $\boldsymbol{H}(t)$ do not depend on $\boldsymbol{c}$, $\boldsymbol{H}(t)$ is the same as that in $\boldsymbol{\Gamma}$-neutral case. Hence, applying Lemma 1 and rearranging (3.50), we obtain the following decomposition for optimal strategy.

Proposition 4. *The optimal strategy in* (3.50) *can be decomposed into two components:*

$$\begin{aligned}\boldsymbol{\pi}^*(t,\boldsymbol{y}) &= \boldsymbol{\Sigma}_{\boldsymbol{F}}^{-1}\boldsymbol{\Gamma}\boldsymbol{D}_{\boldsymbol{\Gamma}}^{-1}\boldsymbol{c} + \frac{1}{\gamma}(\boldsymbol{\Sigma}_{\boldsymbol{F}}^{-1} - \boldsymbol{\Sigma}_{\boldsymbol{\Gamma}})\Big(\boldsymbol{\theta} - \boldsymbol{K}(t)\boldsymbol{y} + \boldsymbol{\Sigma}_{\boldsymbol{FY}}\big(\boldsymbol{g}(t) - \boldsymbol{H}(t)\boldsymbol{y}\big)\Big), \\ &= \underbrace{\frac{1}{\gamma}(\boldsymbol{\Sigma}_{\boldsymbol{F}}^{-1} - \boldsymbol{\Sigma}_{\boldsymbol{\Gamma}})\Big(\boldsymbol{\theta} - \boldsymbol{K}(t)\boldsymbol{y} + \boldsymbol{\Sigma}_{\boldsymbol{FY}}\big(\boldsymbol{g}_0(t) - \boldsymbol{H}(t)\boldsymbol{y}\big)\Big)}_{\boldsymbol{\Gamma}\text{-neutral holding position}} \\ &\quad + \underbrace{\left(\boldsymbol{\Sigma}_{\boldsymbol{F}}^{-1}\boldsymbol{\Gamma}\boldsymbol{D}_{\boldsymbol{\Gamma}}^{-1} + \frac{1}{\gamma}(\boldsymbol{\Sigma}_{\boldsymbol{F}}^{-1} - \boldsymbol{\Sigma}_{\boldsymbol{\Gamma}})\boldsymbol{\Sigma}_{\boldsymbol{FY}}\boldsymbol{\Phi}(t)\right)\boldsymbol{c}}_{\text{hedging demand for } \boldsymbol{c}}.\end{aligned} \tag{3.58}$$

The first component of the optimal strategy reflects the portion due to the $\boldsymbol{\Gamma}$-neutral constraint. The second component has linear dependence on $\boldsymbol{c}$, which is called the hedging demand as it represents extra positions required due to a non-zero constraint vector $\boldsymbol{c}$.

In general, any admissible strategy in the constrained portfolio case is also admissible in unconstrained case, so one expects the value function for the unconstrained portfolio to dominate that for the constrained one. Furthermore, by directly comparing (3.34) and (3.47), we can in fact find a direct link between the value functions by analyzing the associated HJB equations and solutions $u(t,\boldsymbol{y},w)$ and $u^{no}(t,\boldsymbol{y},w)$.

Proposition 5. *Define the auxiliary functions:*

$$\widetilde{\boldsymbol{H}}(t) = \boldsymbol{H}^{no}(t) - \boldsymbol{H}(t), \tag{3.59}$$

$$\widetilde{\boldsymbol{g}}(t) = \boldsymbol{g}^{no}(t) - \boldsymbol{g}(t), \tag{3.60}$$

$$\widetilde{f}(t) = f^{no}(t) - f(t). \tag{3.61}$$

Then, we have $u(t,\boldsymbol{y},w)$ *and* $u^{no}(t,\boldsymbol{y},w)$ *:*

$$u(t,\boldsymbol{y},w) = u^{no}(t,\boldsymbol{y},w)\exp\left(\frac{1}{2}\left(\boldsymbol{y}^\top,1\right)\begin{pmatrix}\widetilde{\boldsymbol{H}}(t), & -\widetilde{\boldsymbol{g}}(t)\\ -\widetilde{\boldsymbol{g}}(t)^\top, & -2\widetilde{f}(t)\end{pmatrix}\begin{pmatrix}\boldsymbol{y}\\ 1\end{pmatrix}\right). \tag{3.62}$$

In addition, the matrix $\begin{pmatrix}\widetilde{\boldsymbol{H}}(t), & -\widetilde{\boldsymbol{g}}(t)\\ -\widetilde{\boldsymbol{g}}(t)^\top, & -2\widetilde{f}(t)\end{pmatrix}$ *is positive semidefinite.*

Proof. See Section 3.7.4. □

Since the matrix $\begin{pmatrix} \widetilde{\boldsymbol{H}}(t), & -\widetilde{\boldsymbol{g}}(t) \\ -\widetilde{\boldsymbol{g}}(t)^\top, & -2\widetilde{f}(t) \end{pmatrix}$ is positive semidefinite by Proposition 5, the exponential term in (3.62) is greater than 1. Couple this with the fact that the value functions $u^{no}(t, \boldsymbol{y}, w)$ and $u(t, \boldsymbol{y}, w)$ are negative, we have the following result.

Corollary 1. *We have inequality*

$$u(t, \boldsymbol{y}, w) \leq u^{no}(t, \boldsymbol{y}, w). \tag{3.63}$$

Next, we verify that the value function (3.39) coincides with the solution of HJB equation (3.41) from Theorem 4. We also identify the optimal trading strategy.

Theorem 5 (Verification Theorem)**.** *1. The value function in* (3.23) *is equal to the function u^{no} given in Theorem 3. Furthermore, the optimal trading strategy is given by* (3.37)*.*

2. The value function in (3.39) *is equal to the function u given in Theorem 4. Furthermore, the optimal trading strategy is given by* (3.50)*.*

Proof. Since the unconstrained scenario is just a special constrained case where $\boldsymbol{\Gamma} = \boldsymbol{0}$ and $\boldsymbol{c} = \boldsymbol{0}$, it suffices to prove the second statement. See Section 3.7.5. □

3.4 Certainty Equivalent

In order to quantify the value of investing in a dynamic futures portfolio, we utilize the notion of certainty equivalent (CE). Certainty equivalent is the guaranteed cash amount that would yield the same utility as that from optimally and dynamically trading futures. This amounts to applying the inverse of the exponential utility function to the value function associated with the futures trading problem.

Since there are several cases with and without constraints, let us denote $CE(t, \boldsymbol{y}, w)$ to be the certainty equivalent value for the general constrained portfolio, and $CE^{no}(t, \boldsymbol{y}, w)$ for

the unconstrained case. They are defined as follows:

$$CE(t,\boldsymbol{y},w)=w+\frac{1}{\gamma}\left(\frac{1}{2}\boldsymbol{y}^{\top}\boldsymbol{H}(t)\boldsymbol{y}-\boldsymbol{y}^{\top}\boldsymbol{g}(t)-f(t)\right), \tag{3.64}$$

and

$$CE^{no}(t,\boldsymbol{y},w)=w+\frac{1}{\gamma}\left(\frac{1}{2}\boldsymbol{y}^{\top}\boldsymbol{H}^{no}(t)\boldsymbol{y}-\boldsymbol{y}^{\top}\boldsymbol{g}^{no}(t)-f^{no}(t)\right). \tag{3.65}$$

In particular, for the $\boldsymbol{\Gamma}-$neutral case, the certainty equivalent is defined by

$$CE_0(t,\boldsymbol{y},w)=w+\frac{1}{\gamma}\left(\frac{1}{2}\boldsymbol{y}^{\top}\boldsymbol{H}_0(t)\boldsymbol{y}-\boldsymbol{y}^{\top}\boldsymbol{g}_0(t)-f_0(t)\right), \tag{3.66}$$

where $f_0,\boldsymbol{g}_0$ are given in Lemma 1 and $H_0(t)=H(t)$.

In Theorem 5, we compare the unconstrained and constrained portfolio optimization problems through the corresponding value functions. We can now do the same using certainty equivalents.

Proposition 6. *We have the following equality between constrained and unconstrained case:*

$$CE(t,\boldsymbol{y},w)=CE^{no}(t,\boldsymbol{y},w)-\frac{1}{2\gamma}\left(\boldsymbol{y}^{\top},1\right)\begin{pmatrix}\widetilde{\boldsymbol{H}}(t), & -\widetilde{\boldsymbol{g}}(t)\\ -\widetilde{\boldsymbol{g}}(t)^{\top}, & -2\widetilde{f}(t)\end{pmatrix}\begin{pmatrix}\boldsymbol{y}\\ 1\end{pmatrix}. \tag{3.67}$$

In addition, $CE(t,\boldsymbol{y},w)\leq CE^{no}(t,\boldsymbol{y},w)$.

We can also connect the certain equivalent of a Γ-constrained portfolio with the Γ-neutral certainty equivalent.

Theorem 6. *The certainty equivalent admits the following decomposition:*

$$CE(t,\boldsymbol{y},w)=\underbrace{CE_0(t,\boldsymbol{y},w)}_{\boldsymbol{\Gamma}\text{-neutral CE}}-\underbrace{\frac{1}{\gamma}\left(\boldsymbol{y}^{\top}\boldsymbol{\Psi}(t)\boldsymbol{c}+\boldsymbol{\beta}(t)\boldsymbol{c}+\boldsymbol{c}^{\top}\boldsymbol{\Lambda}(t)\boldsymbol{c}\right)}_{\text{opportunity multiplier by }\boldsymbol{c}}, \tag{3.68}$$

as indicated in the equation, the first part in the certainty equivalent corresponds to $\boldsymbol{\Gamma}$*-neutral case, and the second part is a multiplier in quadratic form w.r.t* $\boldsymbol{c}$.

Proof. Substituting in the decomposition given in Lemma 1 for $\boldsymbol{g}$ and f, we obtain the decomposition for certainty equivalents as above. □

By Theorem 6, the second part is exponential of a quadratic form, whose convexity is guaranteed by positive semidefinite property of $\mathbf{\Lambda}(t)$. Therefore, the corresponding certainty equivalent $CE(t, \boldsymbol{y}, w)$ has a global maximum when optimized over the constraint vector $\boldsymbol{c}$. This leads us to define the optimal constraint vector $\boldsymbol{c}^*$

Definition 3. *The $\boldsymbol{c}$ for maximizing the certainty equivalent in exponential utility is denoted by*

$$\boldsymbol{c}^*(t, \boldsymbol{y}, w) = \arg\max_{\boldsymbol{c}\in\mathbb{R}^d} \; CE(t, \boldsymbol{y}, w), \tag{3.69}$$

moreover, if $\mathbf{\Lambda}(t)$ is strictly positive, then $\boldsymbol{c}^*(t, \boldsymbol{y}, w)$ is unique.

With Theorem 6, seeking the optimal $\boldsymbol{c}$ is equivalent to maximize the part with the opportunity multiplier generated by $\boldsymbol{c}$. And if $\mathbf{\Lambda}(t)$ is strictly positive, then $\boldsymbol{c}^*$ admits the formula

$$\boldsymbol{c}^*(t, \boldsymbol{y}, w) = -\mathbf{\Lambda}(t)^{-1}\left(\Psi(t)^\top \boldsymbol{y} + \boldsymbol{\beta}(t)^\top\right). \tag{3.70}$$

Remark 6.

1. *Like Γ, the constraint vector $\boldsymbol{c}$ is exogenously imposed on the portfolio, which means it is not a choice by the investor. The vector $\boldsymbol{c}^*$ serves as reference that allows the investor to observe the difference between $\boldsymbol{c}$ and $\boldsymbol{c}^*$ and compare the corresponding certainty equivalents. In other words, the investor can determine the value lost, measured by the reduction in certainty equivalent, due to using the constraint vector $\boldsymbol{c}$ instead of $\boldsymbol{c}^*$.*

2. *Note that $\boldsymbol{c}^*$ does not depend on wealth w. Moreover, it has linear dependence on the basis $\boldsymbol{y}$.*

3. *If $\mathbf{\Gamma} = \mathbf{1}_{N\times 1}$, $\boldsymbol{c} \equiv c$ (a scalar) represents the required net exposure of portfolio, with 1 meaning 100% exposure.*

We provide some numerical examples for certainty equivalents in Section 3.5.

3.5 Numerical Illustration

In this section, we simulate the asset's spot prices, futures prices and optimal strategies for our basis model. We also generate empirical wealth distribution at terminal time and certainty equivalents for different constraints and parameters. Primarily, we consider a market with two different assets S_1 and S_2 and three futures that $F_{1,1}$ is written on S_1, while $F_{2,1}$ and $F_{2,2}$ are written on S_2. Their maturities are $T_{1,1} = T_{2,1} = 2/12$ year and $T_{2,2} = 3/12$ year, respectively. Then, our trading horizon is set to be $T = 1/12$ year, strictly less than the futures maturities. We use 'months' or 'trading day' as the w axis in figures. For clarification, we assume there be 252 trading days in a year and 21 trading days for a month. Therefore, our trading horizon is 21 trading days in total. For other model parameters, we list them as follows.

$$\boldsymbol{\mu} = (0.1, 0.2)^\top, \quad \boldsymbol{m} = (0, 0, 0)^\top, \quad (\kappa_{1,1}, \kappa_{2,1}, \kappa_{2,2}) = (0.5, 0.5, 0.5), \tag{3.71}$$

$$\widetilde{\boldsymbol{\Sigma}}_{\boldsymbol{S}} = \begin{bmatrix} 0.5 & 0 \\ 0.3 & 0.4 \end{bmatrix}, \quad \widetilde{\boldsymbol{\Sigma}}_{\boldsymbol{YS}} = \begin{bmatrix} -0.25 & 0 \\ -0.15 & -0.2 \\ -0.15 & -0.2 \end{bmatrix}, \quad \widetilde{\boldsymbol{\Sigma}}_{\boldsymbol{Y}} = \begin{bmatrix} 0.1 & 0 & 0 \\ 0 & 0.1 & 0 \\ 0 & 0 & 0.1 \end{bmatrix}. \tag{3.72}$$

We obtain the values for $\boldsymbol{\theta}$, $\widetilde{\boldsymbol{\Sigma}}_{\boldsymbol{FS}}$ and $\widetilde{\boldsymbol{\Sigma}}_{\boldsymbol{F}}$ by equations (3.4), (3.7) and (3.8):

$$\boldsymbol{\theta} = \begin{bmatrix} 0.18625 \\ 0.27625 \\ 0.23625 \end{bmatrix}, \quad \widetilde{\boldsymbol{\Sigma}}_{\boldsymbol{FS}} = \begin{bmatrix} 0.25 & 0 \\ 0.15 & 0.2 \\ 0.15 & 0.2 \end{bmatrix}, \quad \widetilde{\boldsymbol{\Sigma}}_{\boldsymbol{F}} = \begin{bmatrix} 0.1 & 0 & 0 \\ 0 & 0.1 & 0 \\ 0 & 0 & 0.1 \end{bmatrix}. \tag{3.73}$$

In Figure 3.1, we simulate the sample paths for the underling asset price $\boldsymbol{S}_t$, futures price $\boldsymbol{F}_t$ and log-basis $\boldsymbol{Y}_t$. The top plot shows the price paths for asset S_1 and its 2-month futures $F_{1,1}$. The price paths for asset S_2 and its two futures $F_{2,1}$ and $F_{2,2}$ are presented in the middle plot. The bottom one shows the simulated paths for the three log-bases associated with the three futures $F_{1,1}$, $F_{2,1}$, and $F_{2,2}$. The initial prices for both assets are \$10. The log-basis vector $\boldsymbol{Y}_t$ is a multidimensional Brownian bridge that starts from $\boldsymbol{Y}_0 = (0.02, 0.02, 0.02)^\top$

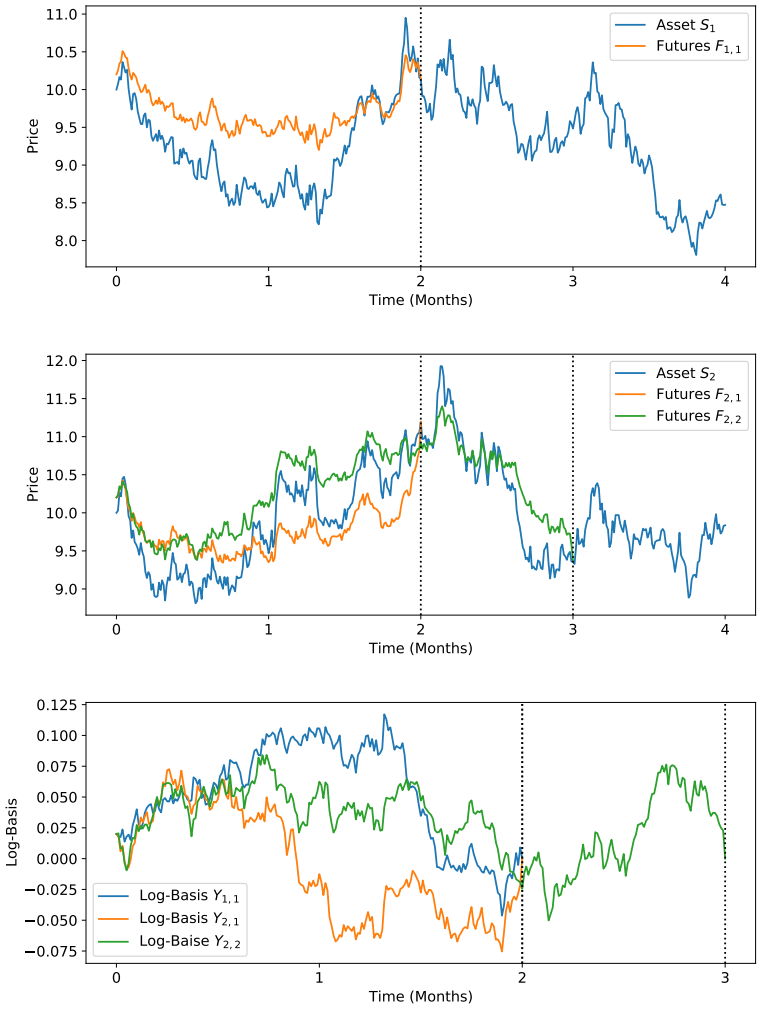

Figure 3.1: Simulated path for assets prices $\boldsymbol{S}_t$, futures prices $\boldsymbol{F}_t$ and log-bases $\boldsymbol{Y}_t$. Top: asset S_1 with its 2-month futures $F_{1,1}$. Middle: asset S_2 with its 2-month futures $F_{2,1}$ and 3-month futures $F_{2,2}$. Bottom: log-basis $\boldsymbol{Y}_t$. Initial value: $\boldsymbol{S}_0 = (10, 10)^\top$ and $\boldsymbol{Y}_0 = (0.02, 0.02, 0.02)^\top$.

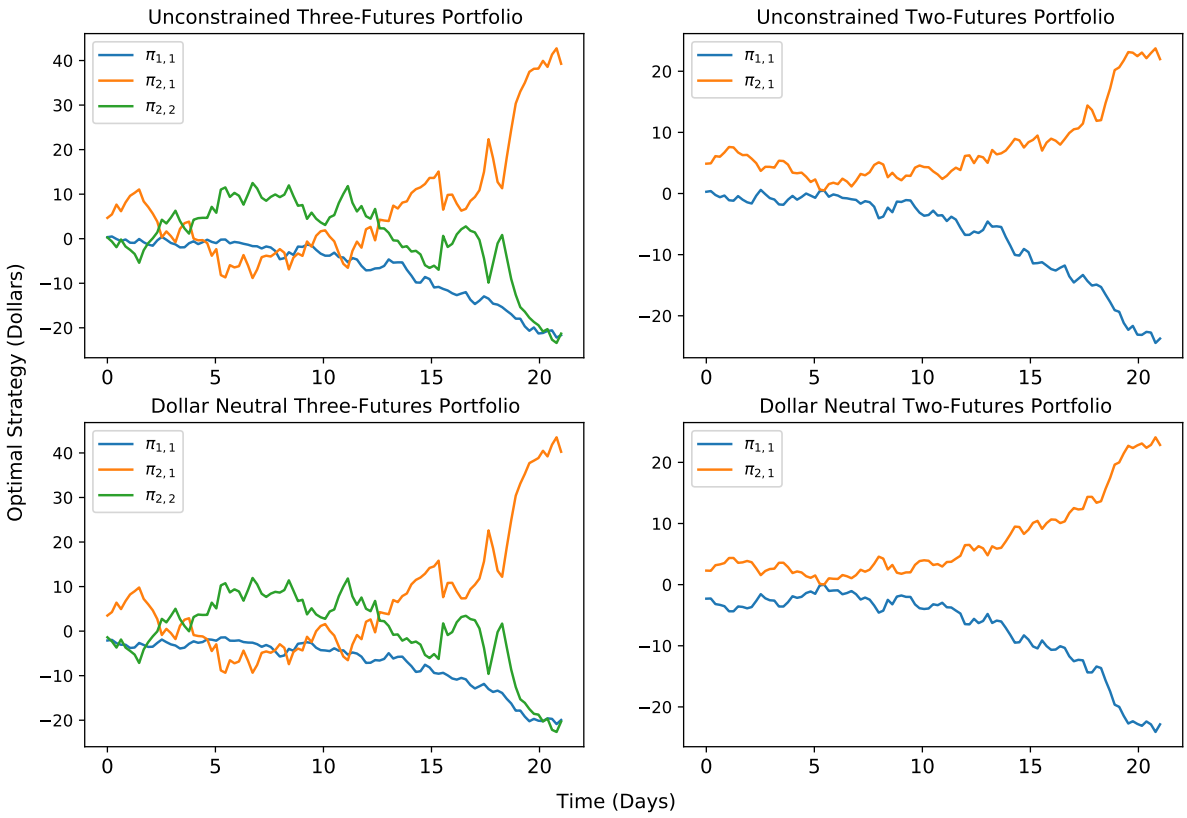

Figure 3.2: Optimal strategies. Top left: unconstrained three-futures portfolio. Top right: unconstrained two-futures portfolio. Bottom left: dollar neutral three-futures portfolio. Bottom right: dollar neutral two futures portfolio.

and converges to zero, which guarantees that each futures price is equal to corresponding asset price at maturity, which are $T_{1,1} = T_{2,1} = 2$ months and $T_{2,2} = 3$ months, respectively.

In Figure 3.2, we illustrate the path behaviors of the optimal strategies under different settings. In the top and bottom left plots, we illustrate optimal unconstrained strategy and optimal dollar neutral strategy for three-futures portfolio. For the dollar neutral strategy, the sum of positions for all futures must be equal to zero in order to satisfy the constraint. Interestinly, the two sets of strategies look similar, which means that the unconstrained optimal strategy is close to being dollar neutral. Also, we observe that in both cases the portfolio has a long-short combinations with opposite positions in two sets of futures, i.e. $F_{2,1}$ vs $F_{1,1}$ and $F_{2,2}$. The same phenomenon can be observed for the two-futures portfolios (right panel) as well. With two futures $F_{1,1}$ and $F_{2,1}$, the investor tends to long one and short the other whether the dollar neutral constraint is enforced or not. Lastly, in our model the optimal strategies depend crucially on the log-basis vector process $\boldsymbol{Y}_t$ over time. This is unlike the optimal strategies obtained by [43, 44], which are time-deterministic.

In Figure 3.3, we present the empirical distributions of terminal wealth associated with portfolios with different number of futures and constraints under different risk aversion parameters γ. From top to bottom, the wealth distributions are for (i) three-futures portfolio with $\gamma = 0.5$; (ii) two-futures portfolio with $\gamma = 0.5$; (iii) three-futures portfolio with $\gamma = 0.1$; (iv) two-futures portfolio with $\gamma = 0.1$. Like Figure 3.2, we use the combination of $F_{1,1}$ and $F_{2,1}$ as the two-futures portfolio. We note that for the two-futures portfolio, the market neutral constraint matrix

$$\boldsymbol{\Gamma} = \widetilde{\Sigma}_{\boldsymbol{FS}}[1,2;1,2]\widetilde{\Sigma}_{\boldsymbol{S}}^{\top} = \begin{bmatrix} 0.25 & 0 \\ 0.15 & 0.2 \end{bmatrix} \begin{bmatrix} 0.5 & 0.3 \\ 0 & 0.4 \end{bmatrix}, \tag{3.74}$$

is invertible. This implies $\boldsymbol{\pi}^* = \mathbf{0}$, meaning that the only feasible strategy is not to invest at all. Therefore, the market neutral strategy does not appear in the second and fourth charts.

Among the strategies, the market neutral strategy leads to a more narrow and centralized distribution of terminal wealth, while the unconstrained portfolio wealth has a wider distribution with the heaviest tails. This reflects that the unconstrained strategy has the highest

degree of freedom and the investor ends up bearing more risk when no constraint is imposed. On the other hand, risk aversion also plays a role in the terminal wealth distribution. If we compare the top two charts to the bottom two, the more risk averse investor ($\gamma = 0.5$), the distribution is more centralized than those for the less risk averse investor ($\gamma = 0.1$). Given that the optimal strategy π^* is inversely proportional to γ according to Theorem 4, the less risk averse investor is likely to hold larger net positions in futures and bear more risk as a result.

For the wealth distributions in Figure 3.3, we provide the summary statistics, including average one-month P&L, standard deviation, and quantiles, in Table 3.1. In addition, we report the average net exposure and maximum net exposure for each portfolio, which are defined as $\frac{1}{T}\int_0^T \mathbf{1}^\top \boldsymbol{\pi}_t dt$ and $\max_{0\le t\le T} |\mathbf{1}^\top \boldsymbol{\pi}_t|$, respectively. The statistics for the less risk averse investor ($\gamma = 0.1$) is shown in the upper table, while the other one ($\gamma = 0.5$) is shown in lower table. From the average one-month P&L, we see that the unconstrained strategy is most profitable and the market neutral strategy is the least when trading three futures in the portfolio with $\gamma = 0.1$. Also, in terms of standard deviation, the unconstrained portfolio is the riskiest and the market neutral strategy is the most conservative, which is consistent with Figure 3.3. Furthermore, comparing the top and bottom tables, we observe that the average one-month P&L, standard deviation and net exposure are inversely proportional to risk aversion for all three strategies. This phenomenon is expected from the optimal strategy formulas in (3.37) and (3.50).

In Figure 3.4, we plot the certainty equivalents for the dollar constraint portfolios, where the total amount invested $\mathbf{1}^\top \boldsymbol{\pi}$ is set to be a fixed parameter c. In other words, the dollar neutral constraint is a special case with $c = 0$.

The green and red curves represent the certainty equivalents for the three-futures portfolio and two-futures portfolio, respectively. Since, with respect to dollar constraint, the admissible strategy for two-futures portfolio is always the admissible strategy for three-futures portfolio, the three-futures portfolio's certainty equivalent must be higher than the two-futures portfolio's certainty equivalent for any c. Figure 3.4 confirms this. For comparison,

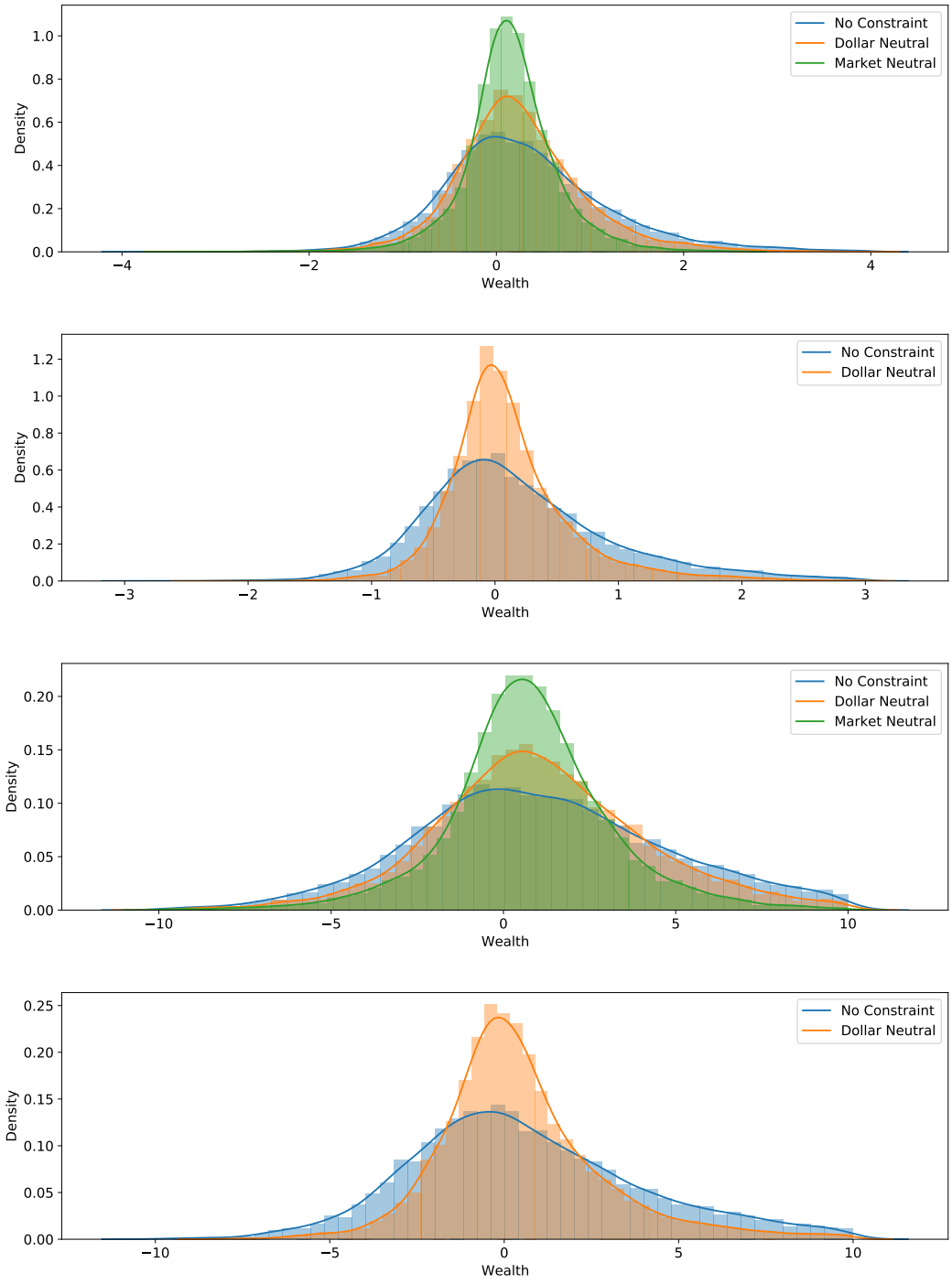

Figure 3.3: The distributions of terminal wealth for the unconstrained and constrained portfolios. From top to bottom: (i) three-futures portfolio with $\gamma = 0.5$; (ii) two-futures portfolio with $\gamma = 0.5$; (iii) three-futures portfolio with $\gamma = 0.1$; (iv) two-futures portfolio with $\gamma = 0.1$.

$\gamma = 0.1$	3 Futures			2 Futures	
	NC	DN	MN	NC	DN
Average One-Month P&L	1.68	1.27	0.77	1.10	0.58
Standard Deviation	4.67	3.50	2.52	4.18	2.61
Lower Quartile	-1.27	-0.84	-0.51	-1.56	-0.89
Median	1.11	0.96	0.69	0.35	0.18
Upper Quartile	3.97	3.07	2.02	2.97	1.57
Average Net Exposure	27.06	0	0	26.31	0
Maximum Net Exposure	61.11	0	0	66.92	0
$\gamma = 0.5$	3 Futures			2 Futures	
	NC	DN	MN	NC	DN
Average One-Month P&L	0.34	0.25	0.15	0.22	0.12
Standard Deviation	0.93	0.70	0.50	0.84	0.52
Lower Quartile	-0.25	-0.17	-0.10	-0.31	-0.18
Median	0.22	0.19	0.14	0.07	0.04
Upper Quartile	0.79	0.61	0.40	0.59	0.31
Average Net Exposure	5.41	0	0	5.26	0
Maximum Net Exposure	12.22	0	0	13.38	0

Table 3.1: Average one-month P&L, standard deviation and quantiles for the wealth distributions in Figure 3.3. 'NC', 'DN' and 'MN' stand for 'no constraint', 'dollar neutral' and 'market neutral', respectively. The top panel corresponds to a lower risk aversion ($\gamma = 0.1$) and the bottom panel corresponds to a higher risk aversion ($\gamma = 0.5$).

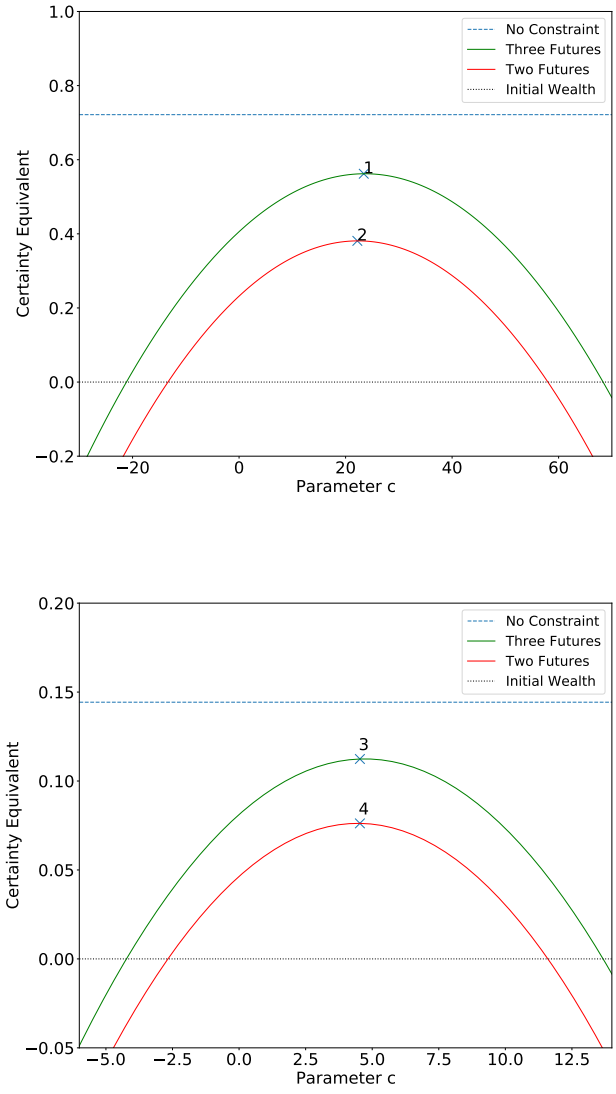

Figure 3.4: The certainty equivalent (CE) as the function of constraint parameter c. The top and bottom plots correspond to the cases with $\gamma = 0.1$ and $\gamma = 0.5$ respectively. In each plot, the blue dashed line shows the CE for unconstrained three-futures portfolio, which is independent of c. The green curve represents the CE for the constrained three-futures portfolio, and the red curve is the CE for the constrained two-futures portfolio. The black dashed line represents the initial wealth. Each cross marks the optimal parameter c^* (on the x-axis) and the corresponding maximum certainty equivalent $CE*$ (on the y-axis). Optimal parameters: $c_1^* = 23.4$, $c_2^* = 22.2$, $c_3^* = 4.54$ and $c_4^* = 4.53$, and maximum certainty equivalents: $CE_1^* = 0.562$, $CE_2^* = 0.381$, $CE_3^* = 0.112$ and $CE_4^* = 0.076$.

we use a blue dashed line to mark the certainty equivalent for the no constraint three-futures portfolio. As expected, it is higher than the certainty equivalent for the constrained portfolios. We also put a dark dashed line to show the initial wealth. If portfolio's certainty equivalent is lower than its initial wealth, then it is not worthwhile to trade.

For each portfolio, there is an optimal constraint parameter c^* (marked by a cross) that maximizes the certainty equivalent. For the less risk averse investor ($\gamma = 0.1$), the best parameters c^* for the three-futures and two-futures portfolios are $c_1^* = 23.4$ and $c_2^* = 22.2$, and the corresponding certainty equivalents are $CE_1^* = 0.562$ and $CE_2^* = 0.381$, respectively. In contrast, for the more risk averse investor ($\gamma = 0.5$), the highest certainty equivalents for two portfolios are lower with $CE_3^* = 0.112$ and $CE_4^* = 0.076$, and the corresponding constraint parameters are $c_3^* = 4.54$ and $c_4^* = 4.53$, respectively. Generally, the less risk averse investor can achieve a higher certainty equivalent than the more risk averse investor for each portfolio.

Lastly, we present in Figure 3.5 the certainty equivalent as a function of the constraint vector $\boldsymbol{c} = (c_1, c_2)$ for the market-constrained three-futures portfolios. For the market constraint, the strategy satisfies $(\widetilde{\boldsymbol{\Sigma}}_{\boldsymbol{FS}}\widetilde{\boldsymbol{\Sigma}}_{\boldsymbol{S}}^{\top})^{\top}\boldsymbol{\pi} = \boldsymbol{c}$ for some fixed $\boldsymbol{c} \in \mathbb{R}^{M\times 1}$, where $M = 2$ is the number of assets in our example. The dashed contours denote the certainty equivalent of value zero, same as the initial wealth $W_0 = 0$. For portfolios corresponding to the interior of the contour, the certainty equivalent is higher than the investor's initial wealth, which means it is worthwhile to trade. The contour region for less risk averse investor ($\gamma = 0.1$) is bigger than the contour region for more risk averse investor ($\gamma = 0.5$). Moreover, the less risk averse investor achieves a higher certainty equivalent with same portfolio. In both plots, the optimal constraint parameters $\boldsymbol{c}^*$ are marked by crosses, such that $\boldsymbol{c}_1^* = (1.71, 3.01)^{\top}$ and the corresponding certainty equivalent $CE_1^* = 0.39$ for $\gamma = 0.1$, and $\boldsymbol{c}_2^* = (0.34, 0.59)^{\top}$ and $CE_2^* = 0.08$ for $\gamma = 0.5$.

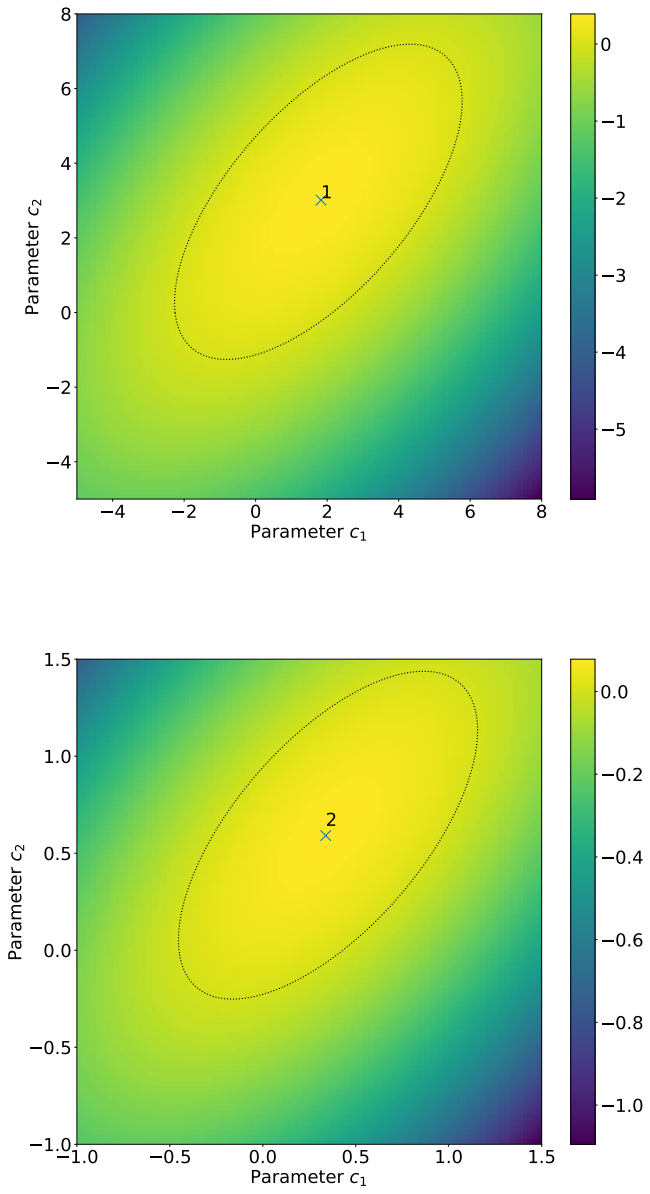

Figure 3.5: The certainty equivalent (CE) for the market-constrained three-futures portfolio with different risk aversion levels (top: $\gamma = 0.1$; bottom: $\gamma = 0.5$). The dashed contours denote the certainty equivalent with initial wealth $W_0 = 0$, and the optimal parameters $\boldsymbol{c}^*$ are marked by crosses. The optimized constraint vectors are $\boldsymbol{c}_1^* = (1.71, 3.01)^\top$ (top) and $\boldsymbol{c}_2^* = (0.34, 0.59)^\top$ (bottom), and the corresponding certainty equivalents are $CE_1^* = 0.39$ and $CE_2^* = 0.08$ respectively.

3.6 Conclusion

We have analyzed constrained dynamic futures portfolios in continuous time under a multidimensional stochastic basis model. One key element of our utility maximization problem is the incorporation of general portfolio constraints on the futures positions, which captures the dollar neutral and market neutral constraints. We have derived the optimal strategies in the unconstrained and constrained cases by solving the associated Hamilton-Jacobi-Bellman (HJB) equations, and presented a number of decomposition results for the corresponding optimal strategies and certainty equivalents.

Our model is related to a number of studies in finance involving Brownian bridges. Applications include modeling the flow of information in the market. For example, [11] use a Brownian bridge as the noise in the information about a future market event, and derived option pricing formulas based on this asset price dynamics and market information flow. For algorithmic trading, [16] utilize a randomized Brownian bridge (rBb) to model the mid-price of an asset with a random end-point perceived by an informed investor, and determined the optimal placements of market and limit orders. [40] also apply a similar rBb framework to derive the optimal timing strategies for options trading.

The random end point of a randomized Brownian bridge can be used to describe the non-convergence of futures. This is a common observation among several agricultural futures, where the futures prices may deviate from the spot price at expiry due to a number of factors, including storage costs. This non-convergence phenomenon has been illustrated in a few studies, including [32], [1], and [25]. We refer to [28] for a stochastic model for capturing this price behavior and pricing agricultural futures.

Apart from basis trading and utility maximization, there are a number of applications of futures. In practice, futures are commonly used as the sole or primary instruments in the design of many exchange-traded products. They are often advertised to provide tracking or exposure to certain commodity or index (see e.g. [38], and [42]). This should motivate future research on how to optimally and dynamically adjust futures positions so as to achieve the

best tracking or exposure control.

3.7 Proofs

3.7.1 Proof of Theorem 3

Before proving the Theorem 3, we begin with a lemma.

Lemma 2. $\boldsymbol{\Sigma}^{no}$ *is positive semidefinite.*

Proof. By (3.32), it suffices to show that $\boldsymbol{\Sigma_Y} - \boldsymbol{\Sigma}_{\boldsymbol{FY}}^{\top}\boldsymbol{\Sigma}_{\boldsymbol{F}}^{-1}\boldsymbol{\Sigma_{FY}}$ is positive semidefinite. Define $\boldsymbol{A_S} = \widetilde{\boldsymbol{\Sigma}}_{\boldsymbol{FS}}^{\top} - \widetilde{\boldsymbol{\Sigma}}_{\boldsymbol{YS}}^{\top}$. Then by (3.24), (3.25), (3.26) and $\widetilde{\boldsymbol{\Sigma}}_{\boldsymbol{F}} = \widetilde{\boldsymbol{\Sigma}}_{\boldsymbol{Y}}$, we have

$$\boldsymbol{\Sigma}_{\boldsymbol{FY}}^{\top}\boldsymbol{\Sigma}_{\boldsymbol{F}}^{-1}\boldsymbol{\Sigma_{FY}} = (\boldsymbol{\Sigma_F} - \widetilde{\boldsymbol{\Sigma}}_{\boldsymbol{FS}}\boldsymbol{A_S})^{\top}\boldsymbol{\Sigma}_{\boldsymbol{F}}^{-1}(\boldsymbol{\Sigma_F} - \widetilde{\boldsymbol{\Sigma}}_{\boldsymbol{FS}}\boldsymbol{A_S}). \tag{3.75}$$

Therefore, we obtain

$$\boldsymbol{\Sigma_Y} - \boldsymbol{\Sigma}_{\boldsymbol{FY}}^{\top}\boldsymbol{\Sigma}_{\boldsymbol{F}}^{-1}\boldsymbol{\Sigma_{FY}} = \boldsymbol{A}_{\boldsymbol{S}}^{\top}(\boldsymbol{I} - \widetilde{\boldsymbol{\Sigma}}_{\boldsymbol{FS}}^{\top}\boldsymbol{\Sigma}_{\boldsymbol{F}}^{-1}\widetilde{\boldsymbol{\Sigma}}_{\boldsymbol{FS}})\boldsymbol{A_S}. \tag{3.76}$$

Then, we only need to show $\boldsymbol{I} - \widetilde{\boldsymbol{\Sigma}}_{\boldsymbol{FS}}^{\top}\boldsymbol{\Sigma}_{\boldsymbol{F}}^{-1}\widetilde{\boldsymbol{\Sigma}}_{\boldsymbol{FS}}$ is the non-negative matrix. Therefore, it remains to show that the eigenvalues of $\widetilde{\boldsymbol{\Sigma}}_{\boldsymbol{FS}}^{\top}\boldsymbol{\Sigma}_{\boldsymbol{F}}^{-1}\widetilde{\boldsymbol{\Sigma}}_{\boldsymbol{FS}}$ are bounded between $[-1, 1]$. Suppose $\boldsymbol{v}$ is an eigenvector for $\widetilde{\boldsymbol{\Sigma}}_{\boldsymbol{FS}}^{\top}\boldsymbol{\Sigma}_{\boldsymbol{F}}^{-1}\widetilde{\boldsymbol{\Sigma}}_{\boldsymbol{FS}}$ such that

$$\widetilde{\boldsymbol{\Sigma}}_{\boldsymbol{FS}}^{\top}\boldsymbol{\Sigma}_{\boldsymbol{F}}^{-1}\widetilde{\boldsymbol{\Sigma}}_{\boldsymbol{FS}}\boldsymbol{v} = \lambda\boldsymbol{v}. \tag{3.77}$$

Then, we have

$$\begin{aligned}\lambda\boldsymbol{v}^{\top}\boldsymbol{v} &= \boldsymbol{v}^{\top}\widetilde{\boldsymbol{\Sigma}}_{\boldsymbol{FS}}^{\top}\boldsymbol{\Sigma}_{\boldsymbol{F}}^{-1}\widetilde{\boldsymbol{\Sigma}}_{\boldsymbol{FS}}\boldsymbol{v} = \boldsymbol{v}^{\top}\widetilde{\boldsymbol{\Sigma}}_{\boldsymbol{FS}}^{\top}\boldsymbol{\Sigma}_{\boldsymbol{F}}^{-1}\boldsymbol{\Sigma_F}\boldsymbol{\Sigma}_{\boldsymbol{F}}^{-1}\widetilde{\boldsymbol{\Sigma}}_{\boldsymbol{FS}}\boldsymbol{v} \\ &\geq \boldsymbol{v}^{\top}\widetilde{\boldsymbol{\Sigma}}_{\boldsymbol{FS}}^{\top}\boldsymbol{\Sigma}_{\boldsymbol{F}}^{-1}\widetilde{\boldsymbol{\Sigma}}_{\boldsymbol{FS}}\widetilde{\boldsymbol{\Sigma}}_{\boldsymbol{FS}}^{\top}\boldsymbol{\Sigma}_{\boldsymbol{F}}^{-1}\widetilde{\boldsymbol{\Sigma}}_{\boldsymbol{FS}}\boldsymbol{v} = \lambda^2\boldsymbol{v}^{\top}\boldsymbol{v}.\end{aligned} \tag{3.78}$$

Therefore, we obtain $\lambda \in [0, 1]$. □

Now, we give the proof for Theorem 3. According to Appendix A in [5], the Riccati equation (3.33) has a unique symmetric non-negative definite solution, since $\boldsymbol{\Sigma}_{\boldsymbol{F}}^{-1}$ and $\boldsymbol{\Sigma}^{no}$ are positive semidefinite.

Next, performing optimization in (3.30) and assuming that $\partial_{ww}u \leq 0$ (which will be verified later), we obtain the first-order condition for the optimal strategy $\boldsymbol{\pi}_t^*$,

$$\boldsymbol{a}^{no}(t,\boldsymbol{y},w) + (\partial_{ww}u)\boldsymbol{\Sigma_F}\boldsymbol{\pi}_t^* = 0. \tag{3.79}$$

Then, we obtain

$$\boldsymbol{\pi}_t^* = -\frac{\boldsymbol{\Sigma_F}^{-1}\boldsymbol{a}^{no}(t,\boldsymbol{y},w)}{\partial_{ww}u}. \tag{3.80}$$

Plugging (3.80) back to the HJB (3.30), we have

$$\partial_t u^{no} + \mathcal{L}u^{no} - \frac{1}{2\partial_{ww}u^{no}}\boldsymbol{a}^{no}(t,\boldsymbol{y},w)^\top\boldsymbol{\Sigma_F}^{-1}\boldsymbol{a}^{no}(t,\boldsymbol{y},w) = 0. \tag{3.81}$$

With the transformation $u^{no}(t,\boldsymbol{y},w) = U(w)\exp\left(-\frac{1}{2}\boldsymbol{y}^\top\boldsymbol{H}^{no}(t)\boldsymbol{y} + \boldsymbol{y}^\top\boldsymbol{g}^{no}(t) + f^{no}(t)\right)$, where $\boldsymbol{H}^{no}(t) \in \mathbb{R}^{N\times N}$ is a symmetric matrix and $\boldsymbol{g}^{no}(t) \in \mathbb{R}^N$, we obtain the matrix Riccati equation (3.33) for $\boldsymbol{H}^{no}(t)$, ODE system (3.35) for $\boldsymbol{g}^{no}(t)$ and ODE (3.36) for $f^{no}(t)$. In addition, $\partial_{ww}u = \gamma^2 u \leq 0$.

3.7.2 Proof of Theorem 4

Before proving Theorem 4, we first give two lemmas.

Lemma 3. *The matrix $\boldsymbol{\Sigma_F}^{-1} - \boldsymbol{\Sigma_\Gamma}$ is positive semidefinite.*

Proof. By (3.44), we have

$$\boldsymbol{\Sigma_F}^{-1} - \boldsymbol{\Sigma_\Gamma} = \boldsymbol{\Sigma_F}^{-1} - \boldsymbol{\Sigma_F}^{-1}\boldsymbol{\Gamma}\boldsymbol{D_\Gamma}^{-1}\boldsymbol{\Gamma}^\top\boldsymbol{\Sigma_F}^{-1}. \tag{3.82}$$

Since $\boldsymbol{\Sigma_F}$ is symmetric positive definite matrix, we define an auxiliary matrix $\boldsymbol{A} = \sqrt{\boldsymbol{\Sigma_F}^{-1}}\boldsymbol{\Gamma} \in \mathbb{R}^{N\times d}$. Thus, we obtain $\boldsymbol{D_\Gamma} = \boldsymbol{A}^\top\boldsymbol{A}$. Then, it suffices to show

$$\sqrt{\boldsymbol{\Sigma_F}}(\boldsymbol{\Sigma_F}^{-1} - \boldsymbol{\Sigma_F}^{-1}\boldsymbol{\Gamma}\boldsymbol{D_\Gamma}^{-1}\boldsymbol{\Gamma}^\top\boldsymbol{\Sigma_F}^{-1})\sqrt{\boldsymbol{\Sigma_F}} = \boldsymbol{I} - \boldsymbol{A}(\boldsymbol{A}^\top\boldsymbol{A})^{-1}\boldsymbol{A}^\top, \tag{3.83}$$

is non-negative definite. Since, $\boldsymbol{Av}$ is the eigenvector of $\boldsymbol{A}(\boldsymbol{A}^\top\boldsymbol{A})^{-1}\boldsymbol{A}^\top$, for any $\boldsymbol{v} \in \mathbb{R}^d$ and $\text{rank}(\boldsymbol{A}) = d$, the eigenvalues for $\boldsymbol{A}(\boldsymbol{A}^\top\boldsymbol{A})^{-1}\boldsymbol{A}^\top$ are 0 or 1. Therefore, $\boldsymbol{I} - \boldsymbol{A}(\boldsymbol{A}^\top\boldsymbol{A})^{-1}\boldsymbol{A}^\top$ is positive semidefinite. □

Lemma 4. *The matrix* $\mathbf{\Sigma}$ *is positive semidefinite.*

Proof. By (3.45), we can decompose $\mathbf{\Sigma}$ into two components, i.e.

$$\mathbf{\Sigma} = \mathbf{\Sigma}^{no} + \mathbf{\Sigma}_{\boldsymbol{FY}}^{\top} \mathbf{\Sigma}_{\mathbf{\Gamma}} \mathbf{\Sigma}_{\boldsymbol{FY}}. \tag{3.84}$$

According to Lemma 2, $\mathbf{\Sigma}^{no} \geq 0$. Besides, the second term is also positive semidefinite. Therefore, $\mathbf{\Sigma}$ is positive semidefinite. □

Now, we show the proof for Theorem 4. According to Appendix A in [5], To show that the Riccati Equation (3.46) has a unique symmetric positive semidefinite solution, it suffices to demonstrate that $\mathbf{\Sigma}_{\boldsymbol{F}}^{-1} - \mathbf{\Sigma}_{\mathbf{\Gamma}}$ and $\mathbf{\Sigma}$ being the coefficients of quadratic and constant terms are positive semidefinite, which are proved in Lemma 3 and Lemma 4.

Next, we turn to solve the HJB equation (3.41) by the method of Lagrange multiplier, similarly seen in [45]. Let $\boldsymbol{\lambda}(t) = (\lambda_1(t), \ldots, \lambda_d(t))^{\top}$ be the (vector) Lagrange multiplier, and we define the Lagrangian function for the constrained control model

$$L(t, \boldsymbol{\pi}, \boldsymbol{\lambda}) = \boldsymbol{\pi}^{\top} \boldsymbol{a}(t, \boldsymbol{y}, w) + \frac{\partial_{ww} u}{2} \boldsymbol{\pi}^{\top} \mathbf{\Sigma}_{\boldsymbol{F}} \boldsymbol{\pi} - \boldsymbol{\lambda}(t)^{\top} (\mathbf{\Gamma}^{\top} \boldsymbol{\pi} - \boldsymbol{c}). \tag{3.85}$$

Then, it suffices to solve

$$\begin{cases} \nabla_{\boldsymbol{\pi}} L = \boldsymbol{a}(t, \boldsymbol{y}, w) + (\partial_{ww} u) \mathbf{\Sigma}_{\boldsymbol{F}} \boldsymbol{\pi} - \mathbf{\Gamma} \boldsymbol{\lambda}(t) = 0, \\ \nabla_{\boldsymbol{\lambda}} L = \mathbf{\Gamma}^{\top} \boldsymbol{\pi} - \boldsymbol{c} = 0. \end{cases} \tag{3.86}$$

Therefore, we obtain

$$\boldsymbol{\pi}_t = -\mathbf{\Sigma}_{\boldsymbol{F}}^{-1} \frac{\boldsymbol{a}(t, \boldsymbol{y}, w) - \mathbf{\Gamma} \boldsymbol{\lambda}(t)}{\partial_{ww} u}, \tag{3.87}$$

and

$$\boldsymbol{\lambda}(t) = (\mathbf{\Gamma}^{\top} \mathbf{\Sigma}_{\boldsymbol{F}}^{-1} \mathbf{\Gamma})^{-1} (\mathbf{\Gamma}^{\top} \mathbf{\Sigma}_{\boldsymbol{F}}^{-1} \boldsymbol{a}(t, \boldsymbol{y}, w) + (\partial_{ww} u) \boldsymbol{c}). \tag{3.88}$$

Inserting $\boldsymbol{\lambda}$ back to formula (3.87), we have

$$\boldsymbol{\pi}_t = \mathbf{\Sigma}_{\boldsymbol{F}}^{-1} \mathbf{\Gamma} \boldsymbol{D}_{\mathbf{\Gamma}}^{-1} \boldsymbol{c} - \frac{(\mathbf{\Sigma}_{\boldsymbol{F}}^{-1} - \mathbf{\Sigma}_{\mathbf{\Gamma}}) \boldsymbol{a}(t, \boldsymbol{y}, w)}{\partial_{ww} u}, \tag{3.89}$$

where $\boldsymbol{D_\Gamma}$ and $\boldsymbol{\Sigma_\Gamma}$ are given by (3.43) and (3.44), respectively. We verify that the optimal strategy must satisfy the constraints

$$\boldsymbol{\Gamma}^\top \boldsymbol{\pi}_t = \boldsymbol{\Gamma}^\top \boldsymbol{\Sigma}_{\boldsymbol{F}}^{-1} \boldsymbol{\Gamma} \boldsymbol{D}_{\boldsymbol{\Gamma}}^{-1} \boldsymbol{c} - \frac{\boldsymbol{\Gamma}^\top (\boldsymbol{\Sigma}_{\boldsymbol{F}}^{-1} - \boldsymbol{\Sigma}_{\boldsymbol{\Gamma}}) \boldsymbol{a}(t, \boldsymbol{y}, w)}{\partial_{ww} u} = \boldsymbol{c}. \tag{3.90}$$

Putting the candidate $\boldsymbol{\pi}_t$ back to the HJB equation (3.41), we obtain

$$\begin{aligned} \partial_t u + \mathcal{L}\, u - \frac{\boldsymbol{a}(t, \boldsymbol{y}, w)^\top (\boldsymbol{\Sigma}_{\boldsymbol{F}}^{-1} - \boldsymbol{\Sigma}_{\boldsymbol{\Gamma}}) \boldsymbol{a}(t, \boldsymbol{y}, w)}{2 \partial_{ww} u} + \boldsymbol{c}^\top \boldsymbol{D}_{\boldsymbol{\Gamma}}^{-1} \boldsymbol{\Gamma}^\top \boldsymbol{\Sigma}_{\boldsymbol{F}}^{-1} \boldsymbol{a}(t, \boldsymbol{y}, w) \\ + \frac{\partial_{ww} u}{2} \boldsymbol{c}^\top \boldsymbol{D}_{\boldsymbol{\Gamma}}^{-1} \boldsymbol{c} = 0. \end{aligned} \tag{3.91}$$

With the ansatz $u(t, \boldsymbol{y}, w) = U(w) \exp\left(-\frac{1}{2} \boldsymbol{y}^\top \boldsymbol{H}(t) \boldsymbol{y} + \boldsymbol{y}^\top \boldsymbol{g}(t) + f(t)\right)$, where $\boldsymbol{H}(t) \in \mathbb{R}^{N \times N}$ is a symmetric matrix and $\boldsymbol{g}(t) \in \mathbb{R}^N$, we obtain the matrix Riccati equation (3.46) for $\boldsymbol{H}(t)$, ODE system (3.48) for $\boldsymbol{g}(t)$, and ODE (3.49) for $f(t)$. Lastly, putting $u(t, \boldsymbol{y}, w)$ into the (3.89), we obtain the formula of optimal strategy.

3.7.3 Proof of Lemma 1

First, a direct observation from matrix Riccati equation (3.46) shows that $\boldsymbol{H}(t)$ doesn't depend on $\boldsymbol{c}$. Then, substituting the decomposition (3.57) into the ODE system (3.48) and ODE (3.49), we obtain the ODE system for $\boldsymbol{g_0}(t) \in \mathbb{R}^N$ as follows:

$$\begin{aligned} \boldsymbol{g}_0'(t) &= \boldsymbol{K}(t) \boldsymbol{g}_0(t) + \boldsymbol{H}(t) \boldsymbol{m} + \left(\boldsymbol{H}(t) \boldsymbol{\Sigma} + \boldsymbol{K}(t) (\boldsymbol{\Sigma}_{\boldsymbol{F}}^{-1} - \boldsymbol{\Sigma}_{\boldsymbol{\Gamma}}) \boldsymbol{\Sigma}_{\boldsymbol{FY}}\right) \boldsymbol{g}_0(t) \\ &\quad + \left(\boldsymbol{K}(t) - \boldsymbol{H}(t) \boldsymbol{\Sigma}_{\boldsymbol{FY}}^\top\right) (\boldsymbol{\Sigma}_{\boldsymbol{F}}^{-1} - \boldsymbol{\Sigma}_{\boldsymbol{\Gamma}}) \boldsymbol{\mu}_{\boldsymbol{F}}, \\ \boldsymbol{g}_0(T) &= \boldsymbol{0}_{N \times 1}, \end{aligned} \tag{3.92}$$

and the ODE for $f_0(t)$:

$$\begin{aligned} f_0'(t) &= -\boldsymbol{m}^\top \boldsymbol{g}_0(t) + \frac{1}{2} tr\left(\boldsymbol{\Sigma}_{\boldsymbol{Y}} \boldsymbol{H}(t)\right) - \frac{1}{2} \boldsymbol{g}_0(t)^\top \boldsymbol{\Sigma}_{\boldsymbol{Y}} \boldsymbol{g}_0(t) \\ &\quad + \frac{1}{2} \left(\boldsymbol{\theta} + \boldsymbol{\Sigma}_{\boldsymbol{FY}} \boldsymbol{g}_0(t)\right)^\top (\boldsymbol{\Sigma}_{\boldsymbol{F}}^{-1} - \boldsymbol{\Sigma}_{\boldsymbol{\Gamma}}) \left(\boldsymbol{\theta} + \boldsymbol{\Sigma}_{\boldsymbol{FY}} \boldsymbol{g}_0(t)\right), \\ f_0(T) &= 0, \end{aligned} \tag{3.93}$$

along with the ODEs for $\boldsymbol{\Psi}(t), \boldsymbol{\beta}(t), \boldsymbol{\Lambda}(t)$,

$$\begin{aligned}
\boldsymbol{\Psi}'(t) &= \boldsymbol{K}(t)\boldsymbol{\Psi}(t) + \left(\boldsymbol{H}(t)\boldsymbol{\Sigma} + \boldsymbol{K}(t)(\boldsymbol{\Sigma}_{\boldsymbol{F}}^{-1} - \boldsymbol{\Sigma}_{\boldsymbol{\Gamma}})\boldsymbol{\Sigma}_{\boldsymbol{FY}}\right)\boldsymbol{\Psi}(t) \\
&\quad + \gamma\left(\boldsymbol{K}(t) - \boldsymbol{H}(t)\boldsymbol{\Sigma}_{\boldsymbol{FY}}^{\top}\right)\boldsymbol{\Sigma}_{\boldsymbol{F}}^{-1}\boldsymbol{\Gamma}\boldsymbol{D}_{\boldsymbol{\Gamma}}^{-1}, \qquad (3.94) \\
\boldsymbol{\beta}'(t) &= -\boldsymbol{m}^{\top}\boldsymbol{\Psi}(t) - \boldsymbol{g}_0(t)\boldsymbol{\Sigma}\boldsymbol{\Psi}(t) + \boldsymbol{\mu}_{\boldsymbol{F}}^{\top}(\boldsymbol{\Sigma}_{\boldsymbol{F}}^{-1} - \boldsymbol{\Sigma}_{\boldsymbol{\Gamma}})\boldsymbol{\Sigma}_{\boldsymbol{FY}} \\
&\quad + \gamma(\boldsymbol{\mu}_{\boldsymbol{F}} + \boldsymbol{g}_0(t)\boldsymbol{\Sigma}_{\boldsymbol{FY}})^{\top}\boldsymbol{\Sigma}_{\boldsymbol{F}}^{-1}\boldsymbol{\Gamma}\boldsymbol{D}_{\boldsymbol{\Gamma}}^{\top}, \qquad (3.95) \\
\boldsymbol{\Lambda}'(t) &= -\frac{1}{2}\boldsymbol{\Psi}(t)^{\top}\boldsymbol{\Sigma}\boldsymbol{\Psi}(t) + \frac{\gamma}{2}\boldsymbol{\Psi}(t)^{\top}\boldsymbol{\Sigma}_{\boldsymbol{FY}}^{\top}\boldsymbol{\Sigma}_{\boldsymbol{F}}^{-1}\boldsymbol{\Gamma}\boldsymbol{D}_{\boldsymbol{\Gamma}}^{-1} + \frac{\gamma}{2}\boldsymbol{D}_{\boldsymbol{\Gamma}}^{-1}\boldsymbol{\Gamma}^{\top}\boldsymbol{\Sigma}_{\boldsymbol{F}}^{-1}\boldsymbol{\Sigma}_{\boldsymbol{FY}}\boldsymbol{\Psi}(t) \\
&\quad - \frac{\gamma^2}{2}\boldsymbol{D}_{\boldsymbol{\Gamma}}^{-1}. \qquad (3.96)
\end{aligned}$$

Besides, we can check that $\boldsymbol{g}_0, f_0$ solve the corresponding ODEs for $\boldsymbol{\Gamma}$-neutral constraint.

As for matrix $\boldsymbol{\Lambda}(t)$, we have

$$\begin{aligned}
\boldsymbol{\Lambda}'(t) &= -\frac{1}{2}\boldsymbol{\Psi}(t)^{\top}\boldsymbol{\Sigma}\boldsymbol{\Psi}(t) + \frac{\gamma}{2}\boldsymbol{\Psi}(t)^{\top}\boldsymbol{\Sigma}_{\boldsymbol{FY}}\boldsymbol{\Sigma}_{\boldsymbol{F}}^{-1}\boldsymbol{\Gamma}\boldsymbol{D}_{\boldsymbol{\Gamma}}^{-1} \\
&\quad + \frac{\gamma}{2}\boldsymbol{D}_{\boldsymbol{\Gamma}}^{-1}\boldsymbol{\Gamma}^{\top}\boldsymbol{\Sigma}_{\boldsymbol{F}}^{-1}\boldsymbol{\Sigma}_{\boldsymbol{FY}}^{\top}\boldsymbol{\Psi}(t) - \frac{\gamma^2}{2}\boldsymbol{D}_{\boldsymbol{\Gamma}}^{-1} \\
&\leq -\frac{1}{2}\boldsymbol{\Psi}(t)^{\top}\boldsymbol{\Sigma}_{\boldsymbol{FY}}^{\top}\boldsymbol{\Sigma}_{\boldsymbol{\Gamma}}\boldsymbol{\Sigma}_{\boldsymbol{FY}}\boldsymbol{\Psi}(t) \qquad (3.97) \\
&\quad + \frac{\gamma}{2}\boldsymbol{\Psi}(t)^{\top}\boldsymbol{\Sigma}_{\boldsymbol{FY}}^{\top}\boldsymbol{\Sigma}_{\boldsymbol{F}}^{-1}\boldsymbol{\Gamma}\boldsymbol{D}_{\boldsymbol{\Gamma}}^{-1} + \frac{\gamma}{2}\boldsymbol{D}_{\boldsymbol{\Gamma}}^{-1}\boldsymbol{\Gamma}^{\top}\boldsymbol{\Sigma}_{\boldsymbol{F}}^{-1}\boldsymbol{\Sigma}_{\boldsymbol{FY}}\boldsymbol{\Psi}(t) - \frac{\gamma^2}{2}\boldsymbol{D}_{\boldsymbol{\Gamma}}^{-1} \\
&= -\frac{1}{2}\left(\boldsymbol{\Gamma}^{\top}\boldsymbol{\Sigma}_{\boldsymbol{F}}^{-1}\boldsymbol{\Sigma}_{\boldsymbol{FY}}\boldsymbol{\Psi}(t) + \gamma\right)^{\top}\boldsymbol{D}_{\boldsymbol{\Gamma}}^{-1}\left(\boldsymbol{\Gamma}^{\top}\boldsymbol{\Sigma}_{\boldsymbol{F}}^{-1}\boldsymbol{\Sigma}_{\boldsymbol{FY}}\boldsymbol{\Psi}(t) + \gamma\right),
\end{aligned}$$

where the first inequality comes from equation (3.45) that

$$\boldsymbol{\Sigma} = \boldsymbol{\Sigma}_{\boldsymbol{Y}} - \boldsymbol{\Sigma}_{\boldsymbol{FY}}^{\top}(\boldsymbol{\Sigma}_{\boldsymbol{F}}^{-1} - \boldsymbol{\Sigma}_{\boldsymbol{\Gamma}})\boldsymbol{\Sigma}_{\boldsymbol{FY}} \geq \boldsymbol{\Sigma}_{\boldsymbol{FY}}^{\top}\boldsymbol{\Sigma}_{\boldsymbol{\Gamma}}\boldsymbol{\Sigma}_{\boldsymbol{FY}}.$$

Hence, we have shown that $\boldsymbol{\Lambda}'(t)$ is negative semidefinite, so $\boldsymbol{\Lambda}(t)$ is positive semidefinite as $\boldsymbol{\Lambda}(T) = \boldsymbol{0}$.

3.7.4 Proof of Proposition 5

The ODEs for the auxiliary functions $\widetilde{\boldsymbol{H}}(t) = \boldsymbol{H}^{no}(t) - \boldsymbol{H}(t), \widetilde{\boldsymbol{g}}(t) = \boldsymbol{g}^{no}(t) - \boldsymbol{g}(t)$, and $\widetilde{f}(t) = f^{no}(t) - f(t)$ can be described in multiple ways. We opt to express them without

involving $\boldsymbol{H}^{no}(t), \boldsymbol{g}(t)$ or $f^{no}(t)$ as follows:

$$\begin{aligned}
\widetilde{\boldsymbol{H}}'(t) &= \left(\boldsymbol{K}(t) + \boldsymbol{K}(t)\boldsymbol{\Sigma}_{\boldsymbol{F}}^{-1}\boldsymbol{\Sigma}_{\boldsymbol{FY}} + \boldsymbol{H}(t)\boldsymbol{\Sigma}^{no}\right)\widetilde{\boldsymbol{H}}(t) \\
&\quad + \widetilde{\boldsymbol{H}}(t)\left(\boldsymbol{K}(t) + \boldsymbol{K}(t)\boldsymbol{\Sigma}_{\boldsymbol{F}}^{-1}\boldsymbol{\Sigma}_{\boldsymbol{FY}} + \boldsymbol{H}(t)\boldsymbol{\Sigma}^{no}\right)^{\top} \\
&\quad + \widetilde{\boldsymbol{H}}(t)\boldsymbol{\Sigma}^{no}\widetilde{\boldsymbol{H}}(t) - (\boldsymbol{H}(t)\boldsymbol{\Sigma}_{\boldsymbol{FY}}^{\top} - \boldsymbol{K}(t))\boldsymbol{\Sigma}_{\boldsymbol{\Gamma}}(\boldsymbol{\Sigma}_{\boldsymbol{FY}}\boldsymbol{H}(t) - \boldsymbol{K}(t)), \qquad (3.98) \\
\widetilde{\boldsymbol{g}}'(t) &= \boldsymbol{K}(t)\widetilde{\boldsymbol{g}}(t) + \widetilde{\boldsymbol{H}}(t)\boldsymbol{m} + \widetilde{\boldsymbol{H}}(t)\boldsymbol{\Sigma}^{no}\boldsymbol{g} + \widetilde{\boldsymbol{H}}\boldsymbol{\Sigma}^{no}\widetilde{\boldsymbol{g}} + \boldsymbol{H}\boldsymbol{\Sigma}^{no}\widetilde{\boldsymbol{g}} \\
&\quad + \boldsymbol{K}(t)\boldsymbol{\Sigma}_{\boldsymbol{F}}^{-1}\boldsymbol{\Sigma}_{\boldsymbol{FY}}\widetilde{\boldsymbol{g}} - \widetilde{\boldsymbol{H}}\boldsymbol{\Sigma}_{\boldsymbol{FY}}^{\top}\boldsymbol{\Sigma}_{\boldsymbol{F}}^{-1}\boldsymbol{\mu}_{\boldsymbol{F}} \\
&\quad - (\boldsymbol{H}(t)\boldsymbol{\Sigma}_{\boldsymbol{FY}}^{\top} - \boldsymbol{K}(t))\boldsymbol{\Sigma}_{\boldsymbol{\Gamma}}(\boldsymbol{\Sigma}_{\boldsymbol{FY}}\boldsymbol{g} + \boldsymbol{\mu}_{\boldsymbol{F}} - \gamma\boldsymbol{\Sigma}_{\boldsymbol{F}}\boldsymbol{\pi}), \\
\widetilde{f}'(t) &= -\boldsymbol{m}^{\top}\widetilde{\boldsymbol{g}}(t) + \frac{1}{2}tr\left(\boldsymbol{\Sigma}_{\boldsymbol{Y}}\widetilde{\boldsymbol{H}}(t)\right) - \frac{1}{2}\widetilde{\boldsymbol{g}}(t)^{\top}\boldsymbol{\Sigma}^{\boldsymbol{no}}\widetilde{\boldsymbol{g}}(t) - \boldsymbol{g}^{\top}\boldsymbol{\Sigma}^{\boldsymbol{no}}\widetilde{\boldsymbol{g}} + \boldsymbol{\mu}_{\boldsymbol{F}}^{\top}\boldsymbol{\Sigma}_{\boldsymbol{F}}^{-1}\boldsymbol{\Sigma}_{\boldsymbol{FY}}\widetilde{\boldsymbol{g}} \\
&\quad + \frac{1}{2}\left(\boldsymbol{\theta} + \boldsymbol{\Sigma}_{\boldsymbol{FY}}\boldsymbol{g}(t) + \gamma\boldsymbol{\Sigma}_{\boldsymbol{F}}\boldsymbol{\pi}\right)^{\top}\boldsymbol{\Sigma}_{\boldsymbol{\Gamma}}\left(\boldsymbol{\theta} + \boldsymbol{\Sigma}_{\boldsymbol{FY}}\boldsymbol{g}(t) + \gamma\boldsymbol{\Sigma}_{\boldsymbol{F}}\boldsymbol{\pi}\right), \\
\widetilde{\boldsymbol{H}}'(T) &= \boldsymbol{0}_{N\times N}, \\
\widetilde{\boldsymbol{g}}'(T) &= \boldsymbol{0}_{N\times 1}, \\
\widetilde{f}'(T) &= 0.
\end{aligned}$$

Now, we denote $\boldsymbol{M}(t) = \begin{pmatrix} \widetilde{\boldsymbol{H}}(t), & -\widetilde{\boldsymbol{g}}(t) \\ -\widetilde{\boldsymbol{g}}(t)^{\top}, & -2\widetilde{f}(t) \end{pmatrix}$, and show the matrix function satisfying some proper Riccati differential equation as following by direct calculation:

$$\begin{aligned}
\boldsymbol{M}'(t) &= \boldsymbol{M}(t)\begin{pmatrix} \boldsymbol{\Sigma}^{no}, & \boldsymbol{0} \\ \boldsymbol{0}, & 0 \end{pmatrix}\boldsymbol{M}(t) + \begin{pmatrix} \boldsymbol{K}(t) + \boldsymbol{H}\boldsymbol{\Sigma}^{no} + \boldsymbol{K}(t)\boldsymbol{\Sigma}_{\boldsymbol{F}}^{-1}\boldsymbol{\Sigma}_{\boldsymbol{FY}}, & \boldsymbol{0} \\ -\boldsymbol{m}^{\top} - \boldsymbol{g}^{\top}\boldsymbol{\Sigma}^{no} + \boldsymbol{\mu}_{\boldsymbol{F}}^{\top}\boldsymbol{\Sigma}_{\boldsymbol{F}}^{-1}\boldsymbol{\Sigma}_{\boldsymbol{FY}}, & 0 \end{pmatrix}\boldsymbol{M}(t) \\
&\quad + \boldsymbol{M}(t)\begin{pmatrix} \boldsymbol{K}(t) + \boldsymbol{H}\boldsymbol{\Sigma}^{no} + \boldsymbol{K}(t)\boldsymbol{\Sigma}_{\boldsymbol{F}}^{-1}\boldsymbol{\Sigma}_{\boldsymbol{FY}}, & \boldsymbol{0} \\ -\boldsymbol{m}^{\top} - \boldsymbol{g}^{\top}\boldsymbol{\Sigma}^{no} + \boldsymbol{\mu}_{\boldsymbol{F}}^{\top}\boldsymbol{\Sigma}_{\boldsymbol{F}}^{-1}\boldsymbol{\Sigma}_{\boldsymbol{FY}}, & 0 \end{pmatrix}^{\top} + \begin{pmatrix} Q_1, & Q_2 \\ Q_2^{\top}, & Q_4 \end{pmatrix},
\end{aligned} \qquad (3.99)$$

where

$$\begin{aligned}
Q_1 &= -(\boldsymbol{\Sigma}_{\boldsymbol{FY}}\boldsymbol{H}(t) - \boldsymbol{K}(t))^{\top}\boldsymbol{\Sigma}_{\boldsymbol{\Gamma}}(\boldsymbol{\Sigma}_{\boldsymbol{FY}}\boldsymbol{H}(t) - \boldsymbol{K}(t)), \\
Q_2 &= (\boldsymbol{H}(t)\boldsymbol{\Sigma}_{\boldsymbol{FY}}^{\top} - \boldsymbol{K}(t))\boldsymbol{\Sigma}_{\boldsymbol{\Gamma}}(\boldsymbol{\Sigma}_{\boldsymbol{FY}}\boldsymbol{g} + \boldsymbol{\mu}_{\boldsymbol{F}} - \gamma\boldsymbol{\Sigma}_{\boldsymbol{F}}\boldsymbol{\pi}), \\
Q_4 &= -tr(\boldsymbol{\Sigma}_{\boldsymbol{Y}}\widetilde{\boldsymbol{H}}) - \left(\boldsymbol{\theta} + \boldsymbol{\Sigma}_{\boldsymbol{FY}}\boldsymbol{g}(t) - \gamma\boldsymbol{\Sigma}_{\boldsymbol{F}}\boldsymbol{\pi}\right)^{\top}\boldsymbol{\Sigma}_{\boldsymbol{\Gamma}}\left(\boldsymbol{\theta} + \boldsymbol{\Sigma}_{\boldsymbol{FY}}\boldsymbol{g}(t) + \gamma\boldsymbol{\Sigma}_{\boldsymbol{F}}\boldsymbol{\pi}\right).
\end{aligned}$$

Moreover, the differential question (3.98) implies that $\widetilde{\boldsymbol{H}}$ is positive semidefinite. Therefore, there exists matrix B such that $\widetilde{\boldsymbol{H}} = B^\top B$, then $-tr(\boldsymbol{\Sigma_Y}\widetilde{\boldsymbol{H}}) = -tr(B\boldsymbol{\Sigma_Y}B^\top) \leq 0$. Combining $p < 0$, we know that

$$\begin{aligned}\begin{pmatrix} Q_1, & Q_2 \\ Q_2^\top, & Q_4 \end{pmatrix} = \begin{pmatrix} \mathbf{0}, & \mathbf{0} \\ \mathbf{0}, & -tr(\boldsymbol{\Sigma_Y}\widetilde{\boldsymbol{H}}) \end{pmatrix} - \\ \begin{pmatrix} \boldsymbol{K}(t) - \boldsymbol{H}(t)\boldsymbol{\Sigma}_{\boldsymbol{FY}}^\top \\ \boldsymbol{\theta}^\top + \boldsymbol{g}(t)^\top\boldsymbol{\Sigma}_{\boldsymbol{FY}}^\top - \gamma\boldsymbol{\pi}^\top\boldsymbol{\Sigma_F} \end{pmatrix} \boldsymbol{\Sigma_\Gamma} \begin{pmatrix} \boldsymbol{K}(t) - \boldsymbol{H}(t)\boldsymbol{\Sigma}_{\boldsymbol{FY}}^\top \\ \boldsymbol{\theta}^\top + \boldsymbol{g}(t)^\top\boldsymbol{\Sigma}_{\boldsymbol{FY}}^\top - \gamma\boldsymbol{\pi}^\top\boldsymbol{\Sigma_F} \end{pmatrix}^\top,\end{aligned} \tag{3.100}$$

is negative semidefinite. In addition, $\boldsymbol{\Sigma}^{no}$ is positive semidefinite. Therefore, $\boldsymbol{M}(t)$ is the corresponding unique positive semidefinite solution for the Riccati equation (3.99).

3.7.5 Proof of Theorem 5

Let u be the solution given in Theorem 4. We prove the following two assertions:

(a) With any admissible strategy $\boldsymbol{\pi} \in \mathcal{A}$, satisfying linear constraints $\boldsymbol{\Gamma}^\top\boldsymbol{\pi} = \boldsymbol{c}$, we have

$$u(t, \boldsymbol{y}, w) \geq I\!E^{\mathbb{P}}_{t,\boldsymbol{y},w}[U\left(W_T^{\boldsymbol{\pi}}\right)], \tag{3.101}$$

for all $(t, \boldsymbol{y}, w) \in [0, T] \times \mathbb{R}^N \times D$, where $I\!E^{\mathbb{P}}_{t,\boldsymbol{y},w}[\cdot]$ denotes the conditional expectation $I\!E^{\mathbb{P}}[\cdot|W_t^{\boldsymbol{\pi}} = w, \boldsymbol{Y}_t = \boldsymbol{y}]$ and $W_T^{\boldsymbol{\pi}}$ is the terminal wealth.

(b) There exists an admissible strategy $\boldsymbol{\pi}^* \in \mathcal{A}$, satisfying $\boldsymbol{\Gamma}^\top\boldsymbol{\pi}^* = \boldsymbol{c}$ such that

$$u(t, \boldsymbol{y}, w) = I\!E^{\mathbb{P}}_{t,\boldsymbol{y},w}[U\left(W_T^{\boldsymbol{\pi}^*}\right)], \tag{3.102}$$

for $(t, \boldsymbol{y}, w) \in [0, T] \times \mathbb{R}^N \times D$.

Combining the above two statements, (a) implies $u \geq V$, and (b) implies $u \leq V$, therefore, $u = V$ as desired.

Proof. (a) Given $\pi \in \mathcal{A}$, satisfying the constraint $\mathbf{\Gamma}^\top \pi = \boldsymbol{c}$, we apply Ito's formula to $u(t, \boldsymbol{y}, w)$, to get

$$\begin{aligned} du(t,\boldsymbol{Y}_t, W_t^{\boldsymbol{\pi}}) = \Big\{ & u_t + (\mathbf{m} - \boldsymbol{K}(t)\boldsymbol{Y}_t)\nabla_{\boldsymbol{y}} u + \frac{1}{2} tr(\mathbf{\Sigma}_{\boldsymbol{Y}} \nabla^2_{\mathbf{y}} u) \\ & + \boldsymbol{\pi}^\top (\boldsymbol{\mu}_{\mathbf{F}} + \boldsymbol{K}(t)\boldsymbol{Y}_t) u_w + \boldsymbol{\pi}^\top \mathbf{\Sigma}_{\boldsymbol{FY}} \nabla_{\boldsymbol{y}}(u_w) + \frac{1}{2} \boldsymbol{\pi}^\top \mathbf{\Sigma}_{\boldsymbol{F}} \boldsymbol{\pi} \partial_{ww} u \Big\} dt \\ & + (\nabla_{\boldsymbol{y}} u)^\top \left(\widetilde{\mathbf{\Sigma}}_{\boldsymbol{YS}} d\boldsymbol{Z}_{t,1} + \widetilde{\mathbf{\Sigma}}_{\boldsymbol{Y}} d\boldsymbol{Z}_{t,2} \right) + u_w \boldsymbol{\pi}^\top \left(\widetilde{\mathbf{\Sigma}}_{\mathbf{FS}} d\boldsymbol{Z}_{t,1} + \widetilde{\mathbf{\Sigma}}_{\mathbf{F}} d\boldsymbol{Z}_{t,2} \right). \end{aligned} \tag{3.103}$$

According to the HJB equation (3.41) for $u(t, \boldsymbol{y}, w)$, we have

$$\begin{aligned} du(t, \boldsymbol{Y}_t, W_t^{\boldsymbol{\pi}}) &\leq (\nabla_{\boldsymbol{y}} u)^\top \left(\widetilde{\mathbf{\Sigma}}_{\boldsymbol{YS}} d\boldsymbol{Z}_{t,1} + \widetilde{\mathbf{\Sigma}}_{\boldsymbol{Y}} d\boldsymbol{Z}_{t,2} \right) \qquad (3.104) \\ &\quad + u_w \boldsymbol{\pi}^\top \left(\widetilde{\mathbf{\Sigma}}_{\mathbf{FS}} d\boldsymbol{Z}_{t,1} + \widetilde{\mathbf{\Sigma}}_{\mathbf{F}} d\boldsymbol{Z}_{t,2} \right) \\ &= u(t, \boldsymbol{Y}_t, W_t^{\boldsymbol{\pi}}) \Big((\boldsymbol{g}(t) - \boldsymbol{H}(t)\boldsymbol{Y}_t)^\top \left(\widetilde{\mathbf{\Sigma}}_{\boldsymbol{YS}} d\boldsymbol{Z}_{t,1} + \widetilde{\mathbf{\Sigma}}_{\boldsymbol{Y}} d\boldsymbol{Z}_{t,2} \right) \\ &\quad - \gamma \boldsymbol{\pi}^\top \left(\widetilde{\mathbf{\Sigma}}_{\mathbf{FS}} d\boldsymbol{Z}_{t,1} + \widetilde{\mathbf{\Sigma}}_{\mathbf{F}} d\boldsymbol{Z}_{t,2} \right) \Big) \\ &= u(t, \boldsymbol{Y}_t, W_t^{\boldsymbol{\pi}}) dA_t^{\boldsymbol{\pi}}. \qquad (3.105) \end{aligned}$$

Therefore, we obtain

$$U\left(W_T^{\boldsymbol{\pi}}\right) \leq u(t, \boldsymbol{Y}_t, W_t^{\boldsymbol{\pi}}) \mathcal{E}\left(A_\cdot^{\boldsymbol{\pi}} - A_t^{\boldsymbol{\pi}}\right)_T . \tag{3.106}$$

Taking the conditional expectation for both sides completes the proof of assertion (a) above. Moreover, the equality holds when taking $\boldsymbol{\pi} = \boldsymbol{\pi}^*$.

(b) It suffices to show that $\boldsymbol{\pi}^*$ is admissible. We combine the integral form of $\boldsymbol{Y}_t$ according to Remark 3.5 in [5] and integration by parts technique to check that $\boldsymbol{Y}_t$ satisfies Benes condition below, thus, the corresponding integrand of $A^{\boldsymbol{\pi}^*}$ also satisfies Benes

condition. That is, there exists some constant K such that

$$\begin{aligned}
\|(-\boldsymbol{Y}_t^\top \boldsymbol{H}(t) + \boldsymbol{g}(t)^\top)\tilde{\boldsymbol{\Sigma}}_{\boldsymbol{YS}}\|_{L^1} &\leq K(1 + \max_{0\leq s\leq t} \|(\boldsymbol{Z}_{s,1}, \boldsymbol{Z}_{s,2})\|_{L^1}), \\
\|(-\boldsymbol{Y}_t^\top \boldsymbol{H}(t) + \boldsymbol{g}(t)^\top)\tilde{\boldsymbol{\Sigma}}_{\boldsymbol{Y}}\|_{L^1} &\leq K(1 + \max_{0\leq s\leq t} \|(\boldsymbol{Z}_{s,1}, \boldsymbol{Z}_{s,2})\|_{L^1}), \\
\|\boldsymbol{\pi}_t^{*\top} \tilde{\boldsymbol{\Sigma}}_{\boldsymbol{FS}}\|_{L^1} &\leq K(1 + \max_{0\leq s\leq t} \|(\boldsymbol{Z}_{s,1}, \boldsymbol{Z}_{s,2})\|_{L^1}), \\
\|\boldsymbol{\pi}_t^{*\top} \tilde{\boldsymbol{\Sigma}}_{\boldsymbol{F}}\|_{L^1} &\leq K(1 + \max_{0\leq s\leq t} \|(\boldsymbol{Z}_{s,1}, \boldsymbol{Z}_{s,2})\|_{L^1}),
\end{aligned} \tag{3.107}$$

where $\boldsymbol{\pi}^*$ is given by (3.50). See [7] or [34], which verifies the admissibility conditions.

□

BIBLIOGRAPHY

[1] Michael K Adjemian, P Garcia, S Irwin, and A Smith. Non-convergence in domestic commodity futures markets: Causes, consequences, and remedies. *US Department of Agriculture, Economic Research Service*, 115:155381, 2013.

[2] Abdullah Almansour. Convenience yield in commodity price modeling: a regime switching approach. *Energy Economics*, 53:238–247, 2016.

[3] B. Angoshtari. On the market-neutrality of optimal pairs-trading strategies. *ArXiv e-prints*, August 2016.

[4] Bahman Angoshtari and Tim Leung. Optimal dynamic basis trading. *Annals of Finance*, 15(3):307–335, 2019.

[5] Bahman Angoshtari and Tim Leung. Optimal trading of a basket of futures contracts. *Annals of Finance*, 16(2):253–280, 2020.

[6] George O. Aragon, Rajnish Mehra, and Sunil Wahal. Do properly anticipated prices fluctuate randomly? evidence from VIX futures markets. *The Journal of Portfolio Management*, 46(7):144–159, 2020.

[7] V. E. Beneš. Existence of optimal stochastic control laws. *SIAM Journal on Control*, 9(3):446–472, 1971.

[8] Fred Espen Benth and Kenneth Hvistendahl Karlsen. A note on Merton's portfolio selection problem for the Schwartz mean-reversion model. *Stochastic Analysis and Applications*, 23(4):687–704, 2005.

[9] Michael J Brennan and Eduardo S Schwartz. Optimal arbitrage strategies under basis variability. In M. Sarnat, editor, *Essays in Financial Economics*. North Holland, 1988.

[10] Michael J. Brennan and Eduardo S. Schwartz. Arbitrage in stock index futures. *Journal of Business*, 63(1):S7–S31, 1990.

[11] Dorje C Brody, Lane P Hughston, and Andrea Macrina. Information-based asset pricing. *International Journal of Theoretical and Applied Finance*, 11(01):107–142, 2008.

[12] Gerald W. Buetow and Brian J. Henderson. The VIX futures basis: Determinants and implications. *The Journal of Portfolio Management*, 42(2):119–130, 2016.

[13] J. Buffington and R. J. Elliott. American options with regime switching. *International Journal of Theoretical and Applied Finance*, 5:497–514, 2002.

[14] Rene Carmona and Michael Ludkovski. Spot convenience yield models for energy markets. *Contemporary Mathematics*, 351:65–80, 2004.

[15] Álvaro Cartea and Sebastian Jaimungal. Algorithmic trading of co-integrated assets. *International Journal of Theoretical and Applied Finance*, 19(06):1650038, 2016.

[16] Álvaro Cartea, Sebastian Jaimungal, and Damir Kinzebulatov. Algorithmic trading with learning. *International Journal of Theoretical and Applied Finance*, 19(04):1650028, 2016.

[17] K. Chen, M. Chiu, and H. Wong. Time-consistent mean-variance pairs-trading under regime-switching cointegration. *SIAM Journal on Financial Mathematics*, 10(2):632–665, 2019.

[18] Gonzalo Cortazar, Matias Lopez, and Lorenzo Naranjo. A multifactor stochastic volatility model of commodity prices. *Energy Economics*, 67:182–201, 2017.

[19] Gonzalo Cortazar and Lorenzo Naranjo. An N-factor Gaussian model of oil futures prices. *Journal of Futures Markets*, 26(3):243–268, 2006.

[20] Min Dai, Yifei Zhong, and Yue Kuen Kwok. Optimal arbitrage strategies on stock index futures under position limits. *Journal of Futures Markets*, 31(4):394–406, 2011.

[21] Jun Deng, Huifeng Pan, Shuyu Zhang, and Bin Zou. Minimum-variance hedging of bitcoin inverse futures. *Applied Economics*, 52(58):6320–6337, 2020.

[22] Gert Elaut, Peter Erdoss, and John Sjodin. An analysis of the risk-return characteristics of serially correlated managed futures. *Journal of Futures Markets*, 36(10):992–1013, 2016.

[23] R. J. Elliott, L. Chan, and T. K. Siu. Option pricing and esscher transform under regime switching. *Annals of Finance*, 1:423– 432, 2005.

[24] W. Fleming and H. Soner. *Controlled Markov Processes and Viscosity Solutions*. Springer, New York, 1993.

[25] Philip Garcia, Scott H Irwin, and Aaron Smith. Futures market failure? *American Journal of Agricultural Economics*, 97(1):40–64, 2015.

[26] Greg N. Gregoriou, Georges Hubner, and Maher Kooli. Performance and persistence of Commodity Trading Advisors: Further evidence. *Journal of Futures Markets*, 30(8):725–752, 2010.

[27] Jorge Guijarro-Ordonez. Stochastic control in high-dimensional statistical arbitrage under an Ornstein-Uhlenbeck process. *Applied Mathematical Finance*, 26(4):328–358, 01 2019.

[28] K. Guo and T. Leung. Understanding the non-convergence of agricultural futures via stochastic storage costs and timing options. *Journal of Commodity Markets*, 6:32–49, 2017.

[29] Kevin Guo, Tim Leung, and Brian Ward. How to mine gold without digging. *International Journal of Financial Engineering*, 2019. Forthcoming.

[30] J. Hamilton. A new approach to the economic analysis of nonstationary time series and the business cycle. *Econometrica*, 57:357–384, 1989.

[31] Brian Hurst, Yao Hua Ooi, and Lasse Heje Pedersen. Demystifying managed futures. *Journal of Investment Management*, 11(3):42–58, 2013.

[32] Scott H Irwin, Philip Garcia, Darrel L Good, and Eugene L Kunda. Spreads and non-convergence in Chicago board of trade corn, soybean, and wheat futures: Are index funds to blame? *Applied Economic Perspectives and Policy*, 33(1):116–142, 2011.

[33] Kenneth R. Jackson, Sebastian Jaimungal, and Vladimir Surkov. Fourier space time-stepping for option pricing with Lévy models. *Journal of Computational Finance*, 12(2):1–29, 2008.

[34] I. Karatzas and S.E. Shreve. *Brownian motion and stochastic calculus*. Springer-Verlag, 1991.

[35] Kazutaka Kuroda and Hideo Nagai. Risk-sensitive portfolio optimization on infinite time horizon. *Stochastics and Stochastics Reports*, 73:309–331, 2002.

[36] T. Leung. A Markov-modulated stochastic control problem with optimal stopping with application to finance. In *Proceedings of the 49th IEEE Conference on Decision and Control*, pages 559–566, 2010.

[37] T. Leung, J. Li, X. Li, and Z. Wang. Speculative futures trading under mean reversion. *Asia-Pacific Financial Markets*, 23(4):281–304, 2016.

[38] T. Leung and B. Ward. The golden target: Analyzing the tracking performance of leveraged gold ETFs. *Studies in Economics and Finance*, 32(3):278–297, 2015.

[39] T. Leung and Y. Zhou. Dynamic optimal futures portfolio in a regime-switching market framework. *Internation Journal of Financial Engineering*, 6(4):1950034, 2019.

[40] Tim Leung, Jiao Li, and Xin Li. Optimal timing to trade along a randomized Brownian bridge. *International Journal of Financial Studies*, 6(3):75, 2018.

[41] Tim Leung and Xin Li. *Optimal Mean Reversion Trading: Mathematical Analysis and Practical Applications*. Modern Trends in Financial Engineering. World Scientific Publishing Company, March 2016.

[42] Tim Leung and Brian Ward. Dynamic index tracking and risk exposure control using derivatives. *Applied Mathematical Finance*, 25(2):180–212, 2018.

[43] Tim Leung and Raphael Yan. Optimal dynamic pairs trading of futures under a two-factor mean-reverting model. *International Journal of Financial Engineering*, 5(3):1850027, 2018.

[44] Tim Leung and Raphael Yan. A stochastic control approach to managed futures portfolios. *International Journal of Financial Engineering*, 6(1):1950005, 2019.

[45] T. N. Li and Andrew Papanicolaou. Dynamic optimal portfolios for multiple cointegrated assets. *Working paper*, 08 2019.

[46] J. Liu and F. A. Longstaff. Losing money on arbitrage: Optimal dynamic portfolio choice in markets with arbitrage opportunities. *The Review of Financial Studies*, 17(3):611–641, 2004.

[47] J. Liu and A. Timmermann. Optimal convergence trade strategies. *Review of Financial Studies*, 26(4):1048–1086, 2013.

[48] Javier Mencia and Enrique Sentana. Valuation of VIX derivatives. *Journal of Financial Economics*, 108:367–391, 2013.

[49] Robert Merton. Optimum consumption and portfolio rules in a continuous time model. *Journal of Economic Theory*, 03:373–413, 1971.

[50] A. A. Novikov. On an identity for stochastic integrals. *Theory of Probability & Its Applications*, 17(4), 1972.

[51] Bernt Oksendal. *Stochastic Differential Equations: An Introduction with Applications*. Springer, 6 edition, 2014.

[52] Andrew J. Patton. Are "Market Neutral" Hedge Funds Really Market Neutral? *The Review of Financial Studies*, 22(7):2495–2530, 12 2008.

[53] Kevin Ross. *Stochastic Control in Continuous Time*. Lecture Notes on Continuous Time Stochastic Control, 2008.

[54] J. Sass and U. G. Haussmann. Optimizing the terminal wealth under partial information: The drift process as a continuous time markov chain. *Finance and Stochastics*, 8:553–577, 2004.

[55] E.S. Schwartz. The stochastic behavior of commodity prices: Implications for valuation and hedging. *The Journal of Finance*, 52(3):923–973, 1997.

[56] David P. Simon and Jim Campasano. The VIX futures basis: Evidence and trading strategies. *The Journal of Derivatives*, 21(3):54–69, 2014.

[57] Luz Roco Sotomayor and Abel Cadenillas. Explicit solutions of consumption-investment problems in financial markets with regime switching. *Mathematical Finance*, 19(2):251–279, 2009.

[58] Vladimir Surkov. *Option Pricing Using Fourier Space Time-Stepping Framework*. PhD thesis, University of Toronto, 2009.

[59] C.A. Valle and J.E. Beasley N. Meade. Market neutral portfolios. *Optimization Letters*, 8(7):1961–1984, 2014.

[60] Carlos Armando Meja Vega. Calibration of the exponential ornsteinuhlenbeck process when spot prices are visible through the maximum log-likelihood method: Example with gold prices. *Advances in Difference Equations*, 269, 2018.

[61] Z. Zhao and D. P. Palomar. Mean-reverting portfolio with budget constraint. *IEEE Transactions on Signal Processing*, 66(9):2342–2357, 2018.

[62] X. Zhou and G. Yin. Markowitz's mean-variance portfolio selection with regime switching: A continuous-time model. *SIAM Journal on Control and Optimization*, 42(4):1466–1482, 2003.